

MAX-PLANCK-INSTITUT FÜR PLASMAPHYSIK
GARCHING BEI MÜNCHEN

Computer program for the evaluation of ion beam
analysis energy spectra

P. Børgeesen, B.M.U. Scherzer, R. Behrisch⁺)

L.G. Svendsen, and S.S. Eskildsen⁺⁺⁾

IPP 9/42

July 1983

⁺) Max-Planck-Institut für Plasmaphysik,
EURATOM-Association, D-8046 Garching
Federal Republic of Germany

⁺⁺⁾ Institute of Physics
University of Aarhus
DK-8000 Aarhus D, Denmark

*Die nachstehende Arbeit wurde im Rahmen des Vertrages zwischen dem
Max-Planck-Institut für Plasmaphysik und der Europäischen Atomgemeinschaft über die
Zusammenarbeit auf dem Gebiete der Plasmaphysik durchgeführt.*

IPP 9/42

P. Børgesen
B.M.U. Scherzer
R. Behrisch
L.G. Svendsen
S.S. Eskildsen

Computer program for the evaluation
of ion beam analysis energy
spectra

June 1983
(in English)

ABSTRACT

The computer program "SQUEAKIE" for evaluation of ion beam analysis (RBS or nuclear reaction) energy spectra is listed and described. Given an experimental energy spectrum in which the signals from all target elements may be identified, this program directly yields the target stoichiometry versus depth from the surface. The program is based on solving an eigenvector problem by means of inverse iteration. The formalism, which has been derived in detail previously /1/, is briefly reviewed. Attempts to reduce computing time on small computers are discussed. On a large computer (Amdahl 470) typical CPU-times were ~ 3 seconds per spectrum, on a smaller computer (NORD-100) ~ 40 seconds.

CONTENTS

	page
1. Introduction	1
2. Principle	3
2.1 Experiment	3
2.2 Formalism	5
i) RBS	5
ii) Nuclear reaction analysis	8
2.3 Is this program really necessary?	10
3. Function	11
3.1 Stoichiometry vs. depth	11
3.2 Inverse iteration vs. depth	12
3.3 Integrated contents vs. depth	14
3.4 Details	16
a) Choice of depthstep	16
b) Interpolation between channels.	16
c) Results from previous spectra	17
d) Stop-criteria	18
4. Calculations	19
4.1 Scattering/reaction - cross section	19
4.2 Scattering/reaction - energies.	21
4.3 Stopping power.	22
4.4 Inverse iteration	25
i) Principle	25
ii) Algorithm	28
iii) Practical calculation	29
4.5 Optimizing program.	29
5. Program	31
5.1 Main-program "SQUEAKIE"	33
5.2 Subroutine "STEP"	33
5.3 Function "CRSEC"	33
5.4 Function "XK"	33
5.5 Function "STPA"	33
5.6 Subroutine "ITER"	33

	page
5.7 Listing	33
5.8 Alternative version	33
5.9 Aarhus-version.	33
5.10 List of symbols	41
6. How to use the program	44
6.1 Submit	45
6.2 Job control cards	46
6.3 Input	48
6.4 Output	55
6.5 Examples.	57
6.6 Warnings.	83
7. Tests	85
7.1 Test of programming	85
7.2 Test of program	87
8. Resumé	109
References	111

1. INTRODUCTION

The measurement of energy distributions of light ions emerging from a target during irradiation is widely used for microanalysis of solids /2-4/. The emerging ions result either from a nuclear reaction or from an elastic scattering process between an energetic light ion beam and the target atoms. The evaluation of sample composition versus depth from the energy spectra obtained from either process is formally very similar /5/.

Several procedures have been proposed for more or less automatic evaluation of such spectra, but most of them are not very good if more than 2 elements are present in the target.

One quite general formalism has been developed and described in detail /1/ which in principle may treat any number of target elements. In the final approach one must here distinguish between cases where

- a) for one of the target components the light ion yield is unknown,
- or
- b) the light ion yields from all target components may be distinguished.

The treatment of cases, where two or more signals are unknown is not possible without additional information. The procedure described for case a) has been modified to include the case of overlapping signals, i.e. two of the elemental signals are unknown, but their sum is measured /13, 14/.

The case b) is the more general one and very frequent in ion beam analysis experiments. A computer program, "SQUEAKIE", has been developed

for this case on the basis of the formalism of Reference 1. The program directly calculates the target composition vs. depth from experimental spectra. Together with Ref. 1 the present report provides a description and documentation of the program. Applications of "SQUEAKIE" have been published elsewhere /6-9, 14, 20/, and Chapter 7 includes a few more examples.

The type of experiment for which the program may be used is described in Chapter 2. The terminology of that Chapter is then used in the following. The program has presently been applied to RBS-spectra, whereas nuclear reaction energy spectra may pose some problems because of resolution effects. In a brief review of the formalism it is recalled how the target stoichiometry at a given depth may be calculated by solving an eigenvector problem.

Without consideration of the specific formalism, calculations, etc., Chapter 3 gives an overview of the function of the program. Even users who are not interested in the following chapters should at least look through this.

The calculation of the necessary physical quantities is discussed in Chapter 4. A simple description is given of the inverse iteration method for solving eigenvector problems (Sect. 4.4), and finally some general suggestions for optimizing the program are made.

The program itself is listed and described in Chapter 5. Extensively treated are the versions in Garching (Sects. 5.1-5.8). These Sections are not included in the present report, but reside on the Amdahl 470.

An updated listing of the sections may be obtained at any time directly from the authors. A version of "SQUEAKIE" modified for smaller computers (the NORD-100 in Aarhus) is discussed in Sect. 5.9.

The use of the program in Garching (including input and job control cards) is described in Chapter 6. It is recommended that all users study Sections 6.5 and 6.6 to avoid problems in interpreting results.

Users implementing versions of the program on other computers may benefit from the tests described in Section 7.1, when searching for programming errors. Together with Ref. 1 Section 7.2 describes tests of precision, stability, speed and applicability of the program as performed by the authors.

2. PRINCIPLE

The principles behind the program are primarily described for a Rutherford backscattering (RBS) measurement, but also the modifications necessary when nuclear reactions contribute are indicated.

2.1 Experiment

An RBS-experiment is illustrated in Fig. 1:

A beam of light ions with mass M_1 impinges on the surface of a solid target at an incident angle α to the surface normal (Fig. 1a).

Penetrating the target the ions lose energy and the average inward energy $E(x)$ depends on depth x . Let us consider ions scattered through the angle θ at depth x by collision with a target atom of type 'i'. The

Geometry :

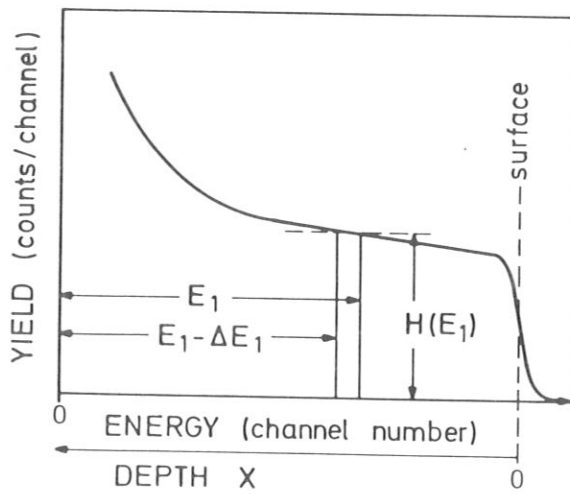
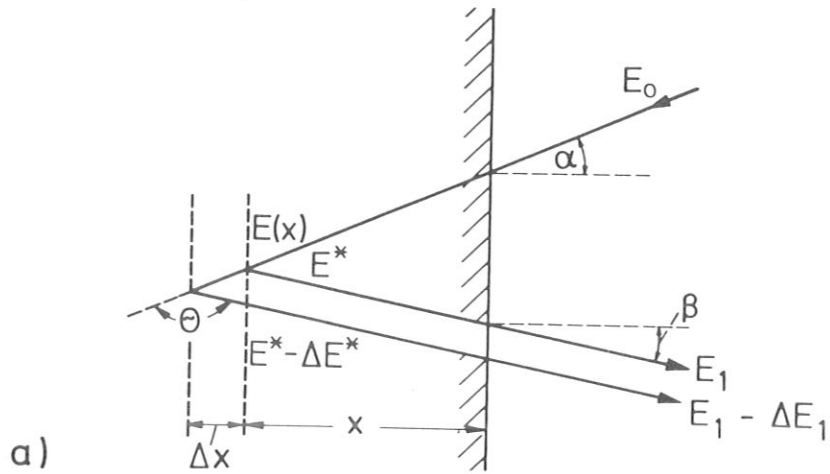


Fig. 1: Rutherford backscattering (RBS) measurement, see text.

a) Experimental geometry, b) Detected energy spectrum

energy $E_i^*(x)$ immediately after scattering depends on i and θ . Leaving the target at an angle β to the surface normal the ions lose energy on the way out and are finally detected with energy $E_{1,i}(x)$.

In the case of nuclear reaction, the detected particles may be of a different type than the projectiles.

The detected energy spectrum (Fig. 1b) now may be evaluated with respect to type, depth and concentration of the element 'i'. In the following it is assumed, that the individual signals from the target components are identified, and the spectrum resides on a multi-channel analyser. It is important to limit the number of elements which may be present in the target, before using the program: Clearly the program may not distinguish between RBS-signals from a light element near the surface and a heavy element at larger depth. A larger number of possible elements therefore at best limits the depth of evaluation.

2.2 Formalism

i) RBS

The formalism needed for the above experiment is quite simple. Let us assume that we have already determined the target composition versus depth up to some depth x . At this depth let the target be composed of m elements with relative atomic concentrations n_1, n_2, \dots, n_m , ($n_1 + n_2 + \dots + n_m = 1$), and atomic stopping powers S^1, S^2, \dots, S^m .

Let us now consider projectiles backscattered from element 'i' through the angle θ in the depth-interval $[x, x + \Delta x_i]$. Δx_i is chosen, so that it corresponds to the energy width ΔE_i of a channel in the experimental spectrum:

The average inward energy E varies between $E(x)$ and $E(x + \Delta x_i)$, and correspondingly the outward energy E_i^* immediately after scattering varies with depth. The precise functional relation between E_i^* and E (and i) is

described later. After escaping out through the target the scattered particles are finally detected with energies between $E_{1,i}(x)$ and $E_{1,i}(x) - \Delta E_1$. The energy $E_{1,i}(x)$ depends on element i and depth x , whereas the depth-interval Δx_i is related to i and the energy difference ΔE_1 through /3/

$$\Delta E_1 = \Delta x_i \cdot dE_{1,i}/dx \quad (2.1)$$

As ΔE_1 is a constant, Δx_i will in general vary with i . If this was not so, we could directly determine the relative concentrations n_i from the numbers H_i of detected particles in each channel:

$$H_i(E_{1,i}) = n_i(x) \cdot \left(\frac{d\sigma}{d\Omega}\right)_i \cdot N_{\text{prim}} \cdot \Delta\Omega \cdot \frac{\Delta x_i}{\cos\alpha} \quad (2.2)$$

where $\left(\frac{d\sigma}{d\Omega}\right)_i$ is the differential scattering cross section, N_{prim} is the primary beamdose (ions/cm²), and $\Delta\Omega$ is the detector acceptance solid angle.

As it is, the estimate

$$(n_1:n_2:\dots:n_m) \sim \frac{H_1}{\left(\frac{d\sigma}{d\Omega}\right)_1} : \frac{H_2}{\left(\frac{d\sigma}{d\Omega}\right)_2} : \dots : \frac{H_m}{\left(\frac{d\sigma}{d\Omega}\right)_m} \quad (2.3)$$

still provides a very good start 'guess' for our iteration (see later). We shall (later) see examples of the variation of Δx_i with i .

For now, we factorize the derivative $(dE_{1,i}/dx)$ of eq. (2.1) as

$$dE_{1,i}/dx = S_{c,i}(E) \cdot e_i(E_i^*, E_{1,i}, x) \quad (2.4)$$

where the general energy loss factor at depth x

$$S_{c,i}(E) = dE_i^*/dx \quad (2.5)$$

may be expressed as composed of contributions from the stopping before and after the collision

$$S_{c,i}(E) = \frac{\partial E_i^*}{\partial E} \frac{S(E)}{\cos \alpha} + \frac{S(E_i^*)}{\cos \beta} \quad (2.6)$$

Here $S(E')$ is the average total stopping power at energy E' and depth x.

The factor

$$e_i(E_i^*, E_{1,i}, x) = \frac{dE_{1,i}}{dE_i^*} (x) \quad (2.7)$$

enters because of the energy dependence of the stopping power: Two projectiles leaving the same depth x with an energy difference dE^* will reach the surface with an energy difference dE_1 , which is not exactly the same as dE^* . The factor is calculated in each depthstep.

Assuming linear additivity of the atomic stopping powers (Bragg's rule) we have

$$S(E) = \sum_{j=1}^m (n_j \cdot S^j(E)) \quad (2.8)$$

which inserted in eq. (2.6) gives

$$S_{c,i}(E) = \sum_{j=1}^m (n_j a_{ij}) \quad (2.9)$$

Here the coefficients a_{ij} are defined by

$$a_{ij} = \left(\frac{dE_i^*}{dE} \right) \cdot \frac{S^j(E)}{\cos \alpha} + \frac{S^j(E_i^*)}{\cos \beta} \quad (2.10)$$

From eqs. 2.1, 2.4 and 2.9 we thus get

$$\Delta x_i = \Delta E_1 / \left\{ e_i \cdot \sum_{j=1}^m (n_j a_{ij}) \right\} \quad (2.11)$$

and inserting this in eq. 2.2 and rewriting, we finally end up with the eigenvector problem /1/

$$\underline{D} \underline{n} = Q \underline{n} \quad (2.12)$$

where the matrix $\underline{D} \equiv (C_i a_{ij})$, the eigenvector $\underline{n} \equiv (n_1, n_2, \dots, n_m)$, the eigenvalue $Q \equiv N_{\text{prim}} \Delta \Omega$ and

$$C_i \equiv \frac{H_i \cdot \cos \alpha \cdot e_i}{\left(\frac{d\sigma}{d\Omega} \right)_i \Delta E_1} \quad (2.13)$$

Thus, the matrix \underline{D} is easily calculated from known quantities.

ii) Nuclear reaction analysis

The evaluation of the energy spectra obtained from nuclear reactions is formally very similar to the above /5/. The major difference is that the detected particles may be of a different type than the projectiles. In the above formalism this simply means that we must distinguish bet-

ween the atomic stopping powers S_p^j for the projectiles, and those (S_d^j) for the detected particles. It is then sufficient to modify eq. 2.10 to

$$a_{ij} = \left(\frac{\partial E_i^*}{\partial E} \right) \cdot \left(\frac{S_p^j(E)}{\cos \alpha} \right) + \frac{S_d^j(E_i^*)}{\cos \beta} \quad (2.10')$$

Of course, in the actual program this requires a few more changes.

Thus the factor $(\partial E_i^*/\partial E)$ now becomes somewhat more complicated /5/, and an analytical expression for the reaction cross section must be known $(d\sigma/d\Omega)_i$.

The typical application of the present method for nuclear reaction analysis would actually involve signals from both backscattering and nuclear reaction. It is not easy to design a program for general use in such experiments, as a variety of other considerations may play in, notably the quite different depth resolutions for RBS and nuclear reaction analysis. Quite often one might also wish to exploit some previous knowledge of the target composition: When nuclear reaction analysis is employed to determine the depth distribution of a light implant, we usually know the stoichiometry of the substrate before implantation! The description below should enable the reader to modify the program for his own purpose.

2.3 Is this program really necessary?

As mentioned above, the simple estimate (eq. 2.3) would be sufficient, if only Δx_i (eq. 2.2) did not depend on the element 'i'. It is therefore quite reasonable to ask whether Δx_i really does vary so much with i, that it justifies all the present work. Let us look briefly into this:

Comparing eqs. 2.1 and 2.4 we see that the element dependence of Δx_i is caused primarily by the corresponding variation of $S_{c,i}(E)$ with i. From eq. 2.6 we see that $S_{c,i}(E)$ depends on i in two ways - directly via the factor $(\partial E_i^*/\partial E)$ and indirectly because $S(E_i^*)$ varies with E_i^* . For a given set of target elements we shall therefore expect the strongest dependence in the energy region where the stopping varies fastest with energy. For RBS-experiments we thus find a significant effect for 1-2 MeV $^4\text{He}^+$ -beams.

For the somewhat special case of 1.5 MeV $^4\text{He}^+$ -ions backscattered from a thin Pt-film on BeO, we find a Δx_{Pt} which is almost twice as large as Δx_{Be} . The study of CuO_x -films on BN-substrates, however, has been of considerable interest in corrosion studies /7/, and here Δx_{B} and Δx_{O} would be of the order of 70 % and 80 % of Δx_{Cu} , only.

For experiments involving nuclear reactions considerably larger variations of Δx_i are possible.

Now, whether the present program is really necessary thus depends on the desired accuracy. Experience shows that for most applications until now /6-9, 14, 20/, the use of eq. 2.3 alone would typically lead to errors of 25 % or more in the estimate of relative concentrations $(n_i:n_j)$, even without the influence of statistical effects. In contrast, inverse iteration following such an initial estimate would effectively eliminate these errors.

3.0 FUNCTION

Let us first consider the structure of the program in general, the application of the inverse iteration, and the principles behind the two independent estimates of the total content of each element. A few details are discussed in Section 3.4, notably the choice of depth step and stop criteria, whereas the actual calculations are described in Chapter 4.

3.1 Stoichiometry vs. depth

1. The program starts with identifying the surface signals from the m_e possible target elements. Some of these may be zero or negligible, indicating that the corresponding elements are not present at the surface. A pointer is introduced, indicating only those elements yielding a significant contribution (estimated $> 10^{-3}$) in the order given by the element list in the input. From the non-zero signals the surface composition of the target is evaluated (by inverse iteration).
2. A depth step Δx_0 is chosen, within which the target composition is assumed to remain constant. This step is chosen to correspond approximately to the width of a channel in the last of the non-zero signals (indicated by the pointer, above). It will thus usually correspond to somewhat more or less than a channel in the other elemental signals (see Section 3.4).

3. From the 'known' composition (evaluated above) the energy losses within this depth step are calculated, and the elemental signals from depth Δx_0 are identified. Simultaneously the factors $e_i(\Delta x_0)$ of eq. 2.7 are estimated numerically. From the non-zero signals the composition of the target is evaluated at depth Δx_0 (compare above).

4. The next depth step Δx_1 is chosen so that it corresponds approximately to the width of a channel in the last of the non-zero signals from depth Δx_0 (indicated by the pointer). We note that this signal may originate from another element than the one used for choosing Δx_0 above. The target composition just derived for depth Δx_0 is assumed to remain constant in the interval $[\Delta x_0, \Delta x_0 + \Delta x_1]$.

5. From the 'known' compositions of both depth steps the necessary energy losses are calculated, and the elemental signals from depth $\Delta x_0 + \Delta x_1$ are identified. Simultaneously the factors $e_i(\Delta x_0 + \Delta x_1)$ are estimated. From the non-zero signals the composition of the target is evaluated at depth $\Delta x_0 + \Delta x_1$,
and so forth ...

3.2 Inverse iteration vs. depth

1. In each depth step the local stoichiometry is evaluated from the corresponding experimental yields by inverse iteration. The formalism does not allow for non-contributing elements (yield $H_i \simeq 0$). This was the reason for introducing the pointer

(Sect. 3.1) selecting only those elements yielding a significant contribution.

2. The inverse iteration requires an 'initial guess' of both eigenvector \underline{n} and eigenvalue Q . Here \underline{n} is estimated by means of eq. 2.3, i.e. an estimate which may be quite imprecise at larger depths (see Sect. 2.3). However, as demonstrated in Sect. 7.2 even very crude estimates of \underline{n} are more than sufficient for a very fast iteration.

Correspondingly, Q_0 is estimated from the 'initial guess' (eq. 2.3): Inserting eq. 2.2 in eq. 2.9, taking all depth-intervals Δx_i to be equal, substituting eq. 2.1 and finally eq. 2.4, we get the factor

$$D_{ef} \equiv \sum_j \{e_i \cdot a_{ij} H_j / (\frac{d\sigma}{d\Omega})_j\} \approx Q \cdot \Delta E_1 / \cos \alpha \quad (3.0)$$

As D_{ef} may in principle be determined, we have then an estimate for $Q \equiv N_{prim} \Delta \Omega$.

3. Along with an iterated eigenvector \underline{n} , the inverse iteration also yields an improved estimate of Q in each depth step. This value is tabulated together with the stoichiometry vs. depth for various purposes (see Sects. 3.3, 5.9 and 7.2).

3.3 Integrated contents vs. depth

For a given depth x , the integrated content $\text{Int}(i,x)$ of an element i is the total areal density (atoms/cm²) of the element between the surface and the depth x .

The program has facilities to print two independent estimates of $\text{Int}(i,x)$ vs. x for all i . None of these are particularly related to the formalism of Ref. 1. For further details see below and Sect. 7.2.

1. Assume that we have already calculated the stoichiometry vs. depth up to a given depth x . We then have a list of depth steps containing for the individual step ' j ' the length Δx_j (in atoms/cm²) and the relative contribution n_j for each element i . It is thus straightforward to add up these contributions from the surface up to the depth x :

$$\text{Int}(i,x) = \sum_{j=0}^k n_j \cdot \Delta x_j \quad (3.1)$$

We recall that $\sum_{i=1}^m n_i = 1$ (Sect. 2.2), and of course $\sum_{j=0}^k \Delta x_j = x$.

2. A quite independent approach is particularly suited for thin layers, e.g. contaminations on a surface, etc. In the so-called 'Thin Film Approximation' the total scattering yield from a thin film of thickness d_i (atoms/cm²) is given by /3/

$$A_i = N_{\text{prim}} \Delta \Omega \left(\frac{d\sigma}{d\Omega} \right)_i \cdot d_i / \cos \alpha \quad (3.2)$$

where the scattering cross-section $(d\sigma/d\Omega)_i$ is evaluated for the beamenergy. The approximation breaks down for film thicknesses

so large, that the inward energy loss in passing d_i causes a significant variation in $(d\sigma/d\Omega)_i$. In the present program the approximation is extended to slightly larger d_i by evaluating $(d\sigma/d\Omega)_i$ for the average energy between the primary E_0 and the energy $E(d_i)$ after passage of d_i .

While stepping in through the target, calculating stoichiometry vs. depth (above), the program calculates also the values of A_i for each depth step: Since the elemental signals corresponding to each step are identified anyway, it is simple to simultaneously add up the signals originating between the surface and the present depth, for each element. Clearly, this does not work if part of the target composition was already evaluated from a previous spectrum (see below).

A particular problem is the question of resolution effects /1/. Due to the finite experimental resolution, part of the signals are usually smeared so that they extend to channels above the 'ideal surfacechannels'. For very thin films up to half of the resulting peak may appear to originate from 'negative depths'. In summing up the total yield it is therefore necessary to specify how many channels above the surfacechannels are to be included. In the present program this is done by giving the FWHM of the experimental resolution at the surface (in number of channels) in the input.

In each depthstep the quantity

$$d_i \cdot N_{\text{prim}} \Delta\Omega = A_i \cos \alpha / \left(\frac{d\sigma}{d\Omega} \right)_i \quad (3.3)$$

is calculated, and this is the quantity listed vs depth later. It remains for the user to decide whether he will then take the factor $N_{\text{prim}} \Delta\Omega$ from the listed eigenvalues Q (above) or determine it otherwise experimentally.

3.4 Details

a) Choice_of_depthstep

The results are quite insensitive to the length of the depthstep, as long as it does not correspond to several channels in some signals. For normal use there is nothing gained by choosing steplengths corresponding to less than a channel in all the signals (see also b. Interpolation between channels). The program chooses a steplength Δx_s corresponding approximately to one channel (i.e. to the detected energy interval ΔE_1) in one of the signals:

For the signal from scattering on element i we calculate the corresponding general energy loss factor $S_{c,i}(E(x))$ of eq. 2.6. This is a crude approximation of the derivative $dE_{1,i}/dx$ (see eq. 2.4), so we may use the estimate

$$\Delta x_s = \Delta E_1 / S_{c,i}(E(x)) \quad (3.4)$$

for this depthstep.

b) Interpolation between channels

In general the ideal signals arising from a given depth do not correspond to an integral channel number for all elements. However, the discreteness induced by collecting a continuous energy spectrum in a finite number of channels is physically meaningless, and we introduce no additional error by interpolating linearly between channels.

c) Results from previous spectra

The optimum experimental parameters for determining depth distributions depend on the depths to be analysed. Thus, for a given target we may wish to improve the depth resolution at the surface by tilting the target (perhaps to $\alpha \sim 80^\circ / 10^\circ$), but this would be detrimental to signals arising from 'large' depths. One might then try to combine the results from two or more spectra obtained with various angles of incidence. Or we may need several different measurements in order to separate the elemental signals from various depths. Therefore the program allows a table to be read in from a file, listing target composition vs. depth as calculated from a previous spectrum. This list is now taken as specifying a number of depthsteps of 'known' composition, up to the maximum listed depth x_m .

Before evaluating the present spectrum, the program now calculates the corresponding inward beam energy $E(x_m)$, and then proceeds as above:

The next depthstep Δx_j is chosen, and the target composition taken as constant between x_m and $x_m + \Delta x_j$. From this the energy losses in this depthstep are calculated. From the above list furthermore the outward energy losses are calculated, stepping out through the target. Thus the elemental signals from depth $x_m + \Delta x_j$ are identified in the present spectrum, and so forth ...

d) Stop-criteria

A weakness of the original version (Sects. 5.1-5.7) is the difficulty in defining a reasonable 'stop-criterium'. We must somehow specify when the evaluation of a spectrum should be terminated, so that elemental signals are still distinguished: If the program proceeds to sufficiently large depths, it may eventually encounter again the surface signals originating from a light element, and now interpret this as the signal from a heavier element at large depth (see Sect. 2.1).

This problem is automatically avoided in the alternative version (Sect. 5.8) and in the Aarhus-version (Sect. 5.9) by the use of element 'markers', which however limits the applicability for some purposes.

In the original version the stop-criteria are problematic: One either specifies the minimum inward beam-energy 'EMIN', or the lowest channelnumber 'NCHMIN' to be evaluated (Sect. 5.1). The program progresses stepwise from the target surface towards larger depths x , calculating the stoichiometry (Sect. 3.1). In each step the inward beamenergy $E(x)$ is calculated, and the corresponding channels in the detected energy spectrum are identified. The evaluation of the spectrum is terminated, when either i) $E(x) < E_{MIN}$, or ii) a channelnumber below NCHMIN is to be evaluated.

These options are obviously not very good, except perhaps in routine evaluation of many similar spectra. One may often have to evaluate a spectrum twice, or evaluate it up to too large depths. A study of the printed output (Sect. 6.4) is usually necessary (see also Sect. 6.6).

4. CALCULATIONS

Below the calculation of the various quantities entering the formalism is discussed. A simple description is given of the inverse iteration method, sufficient for understanding the quite simple calculations used in the present program, whereas more sophisticated versions are available in the literature. Finally, in Section 4.5 a few general suggestions are made for optimizing the program. Such optimizations are discussed for an actual program version in Section 5.9.

4.1 Scattering/reaction - cross section

i) RBS

Rutherford Backscattering Spectrometry /3/ is based on the Rutherford scattering cross section for projectiles of mass M_1 incident on target atoms of mass M_i :

$$\frac{d\sigma}{d\Omega} R = \frac{Z_1^2 Z_i^2}{E^2} \frac{e^4}{16} f(\theta) \quad (4.1)$$

where

$$f(\theta) = \frac{4}{\sin^4 \theta} \frac{\{\cos \theta + g(\theta)\}^2}{g(\theta)} \quad (4.2)$$

and

$$g(\theta) = \sqrt{1 - M_1^2 \sin^2 \theta / M_i^2} \quad (4.3)$$

Andersen et al. /15/ present a thorough discussion of the Rutherford scattering cross section and various analytical screening corrections for the energies and angles of interest here, and conclude that the factor

$$\frac{d\sigma_s}{d\sigma_R} = \left\{ \frac{1 + \frac{1}{2} \frac{V_1}{E_{cm}}}{1 + \frac{V_1}{E_{cm}} + \left(\frac{1}{2} \frac{V_1}{E_{cm}} \frac{1}{\sin^2 \frac{\theta}{2}} \right)^2} \right\}^2 \quad (4.4)$$

can be used to describe backscattering results within 1 %. E_{cm} is the center-of-mass energy, and we approximate $V_1 \simeq 49 \cdot Z_1 \cdot Z_2^{4/3}$ eV (static screening?). At MeV-energies where $V_1/E_{cm} \ll 1$ we can then estimate

$$\frac{d\sigma_s}{d\sigma_R} \simeq \left\{ \frac{1 + 24.5 \frac{Z_1 Z_2^{4/3}}{E}}{1 + 49 \frac{Z_1 Z_2^{4/3}}{E}} \right\}^2 \quad (4.5)$$

for light ions. Finally we note, that if E is expressed in eV, then

$$\frac{d\sigma_R}{d\Omega} = \frac{Z_1^2 Z_i^2}{E^2} f(\theta) \cdot 1.296 \cdot 10^{-15}, \text{ in cm}^2 \quad (4.6)$$

ii) Nuclear reaction

For nuclear reaction analysis the differential cross section is usually not known as well as for RBS. In view of the remarks of Section 2.3 the present formalism is often only superior to a simple estimate (eq. 2.3) if the absolute cross section ($d\sigma/d\Omega$) is known to better than ~ 25 %. For the ${}^3\text{He}(d,p){}^4\text{He}$ -reaction, for instance, such an accuracy has only been obtained quite recently /16/.

4.2 Scattering/reaction - energies

i) RBS

For elastic scattering of projectiles of mass M_1 on atoms of mass M_i , conservation of energy and momentum give

$$E_i^* = K_i \cdot E \quad (4.7)$$

where the kinematic recoil factor /3/

$$K_i = \left\{ \frac{M_1 \cos \theta}{M_1 + M_i} + \left[\left(\frac{M_1}{M_1 + M_i} \cos \theta \right)^2 + \frac{M_i - M_1}{M_1 + M_i} \right]^{1/2} \right\}^2 \quad (4.8)$$

θ is the scattering angle.

In this case, furthermore, the derivative

$$\partial E_i^* / \partial E = K_i \quad (4.9)$$

so this is a useful constant to calculate once and for all.

We note for later use (Function XK) that a negative argument under the square-root corresponds to a scattering angle θ which is not possible for the given projectile-target combination. This is for instance encountered if the program attempts backscattering of ^4He -ions from H-atoms in the target!

ii) Nuclear reaction

If the projectiles (mass M_1) undergo some nuclear reaction (energy release \tilde{Q}) with a target atom of mass M_i resulting in a detected particle (mass M_3) and another particle (mass M_4) the energy E_i^* of the detected particle immediately after reaction is instead /5/

$$E_i^* = \frac{M_4}{M_3+M_4} \tilde{Q} + \frac{E}{(M_3+M_4)^2} f(M_j, \theta, E, \tilde{Q}), \quad j = 1, 3, 4 \quad (4.10a)$$

where

$$f = 2M_1M_3 \cos^2\theta + (M_3+M_4)(M_4-M_1) + 2\cos\theta g^{1/2}(M_j, \theta, E, \tilde{Q}) \quad (4.10b)$$

and

$$g = M_1^2 M_3^2 \cos^2\theta + M_1M_3(M_3+M_4)(M_4-M_1) + M_1M_3M_4(M_3+M_4) \frac{\tilde{Q}}{E} \quad (4.10c)$$

In this case the derivative $\partial E_i^*/\partial E$ is also a function of energy E:

$$\partial E_i^*/\partial E = \frac{f}{(M_3+M_4)^2} - \frac{M_1M_3M_4}{M_3+M_4} \frac{\tilde{Q}}{E} \cdot g^{-1/2} \cos\theta \quad (4.11)$$

4.3 Stopping power

i) In the original program the stopping power is calculated using the formula

$$S(E) = \frac{S_{High} \cdot S_{low}}{S_{High} + S_{low}} \quad (4.12a)$$

where

$$S_{low} = \epsilon_1 \cdot E^{\epsilon_2} \quad (4.12b)$$

and

$$S_{High} = (\epsilon_3/E) \ln [1 + \frac{\epsilon_4}{E} + \epsilon_5 \cdot E] \quad (4.12c)$$

E is the energy in keV.

This formula is meant to use the coefficients of the semi-empirical stopping powers of Ziegler /11/ and Andersen and Ziegler /12/ for He- and hydrogen ions. A few modifications are necessary, though:

For He-projectiles E should be replaced by $E/1000$ in S_{High} .

For ^3He -ions or deuterons $S(E)$ is evaluated as the stopping power of ^4He -ions or protons, respectively, at the same velocity. This is remedied by defining the energy scaling factor FE as 1.0 for protons and ^4He -ions, $4/3$ for ^3He -ions and 0.5 for deuterons. Then the stopping power for any of the isotopes at energy E equals $S(FE \ E)$.

ii) The expression (4.12) is quite complicated and time-consuming to calculate, especially on a smaller computer. For the version used on the NORD-100 in Aarhus computertime was reduced using an existing stopping power subroutine /17/ based on the expression

$$S(E) = \epsilon_a \cdot \sqrt{E} / (1 + \epsilon_b \sqrt{E} + \epsilon_c E) \quad (4.13)$$

The constants ϵ_a , ϵ_b and ϵ_c have been determined from a least squares fit to the semiempirical helium stopping power of Ziegler /11/ in the energy range 0 to 4 MeV.

This expression is considerably faster to calculate than (4.12), particularly on small computers (see Section 4.6). The goodness of the least squares fit and the accuracy of the stopping power expression (4.13) can be judged by a comparison to the Ziegler values /11/. Figure 2 shows typical examples of such a comparison: For energies higher than ~ 200 keV

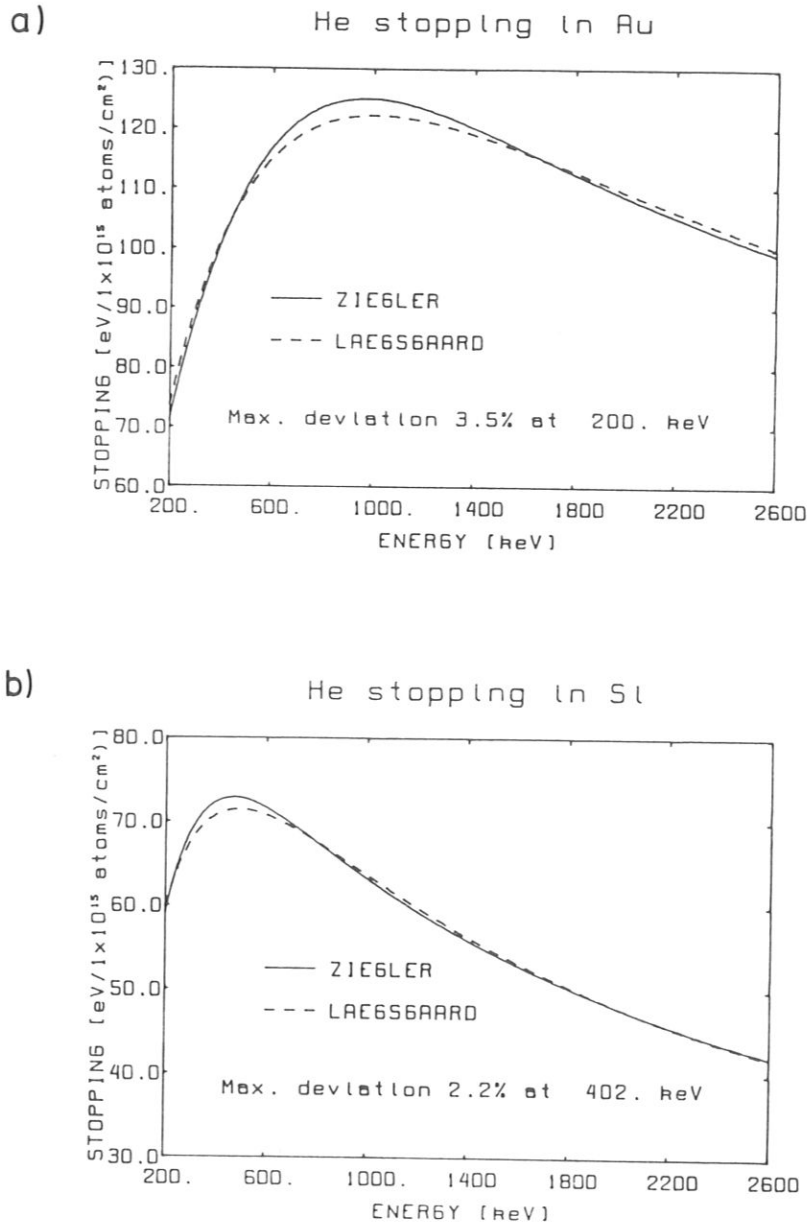


Fig. 2: Comparison of ^4He -stopping power expressions. Solid line semiempirical expression (Eq. 4.12) from Ref. 11; broken line—fit to this expression (eq. 4.13). Note suppressed zero on axis.

a) ^4He stopping power in Au, 200–2600 keV.

b) ^4He stopping power in Si, 200–2600 keV.

the expression (4.13) reproduces stopping power values very well, and the overall accuracy is clearly within the experimental uncertainties /11/. The accuracy is generally worst at the low energy end (see Fig. 2a).

4.4 Inverse Iteration

Inverse iteration is a powerful and accurate technique for the computation of the eigenvector \underline{s}_r corresponding to a given eigenvalue Q_r . The method is usually very economical, and yields, as a byproduct, also an improved value for Q_r . A detailed account is given in Ref. 18, but we have found it appropriate to include at least a simplified description here also.

i) Principle

We are given the (mxm)-matrix \underline{D} , which has the eigenvectors \underline{s}_j and the eigenvalues Q_j , where $j = 1, 2, \dots, m$. We want the eigenvector \underline{s}_r corresponding to some eigenvalue Q_r :

$$\underline{D} \cdot \underline{s}_r = Q_r \cdot \underline{s}_r \quad (4.14)$$

The vector \underline{s}_r is totally unknown, and only a very rough guess of Q_r is available.

We need to assume that

- a) the eigenvectors \underline{s}_j form a basis in C^m (all the eigenvalues are different from each other), and
- b) our initial guess, Q_0 , is closer to Q_r than to any other eigenvalue, but $Q_0 \neq Q_r$.

In reality we have always yet found these assumptions to hold (see below).

Then inverse iteration yields the eigenvector \underline{s}_r and a better estimate of Q_r :

\underline{s}_r is a solution to the singular system of equations (4.14)

$$\underline{B} \underline{s}_r = \underline{0} \quad (4.15)$$

where

$$\underline{B} = (\underline{D} - Q_r \underline{I}) \quad (4.16)$$

and \underline{I} is the unit matrix. From assumption b above, then, the matrix

$$\underline{B}_0 = (\underline{D} - Q_0 \underline{I}) \quad (4.17)$$

is regular, so the equation

$$\underline{B}_0 \underline{y}_k = \underline{y}_{k-1} \quad (4.18)$$

has precisely one solution for a given \underline{y}_{k-1} , namely the vector

$$\underline{y}_k = \underline{B}_0^{-1} \underline{y}_{k-1} \quad (4.19)$$

This is then used to define an iteration process, starting with some non-zero vector \underline{y}_0 ($k = 1$), and we may show this to converge towards the direction of \underline{s}_r .

For this purpose we note first, that for any eigenvector \underline{s}_i

$$\begin{aligned} \underline{D} \underline{s}_i &= Q_i \underline{s}_i = > (\underline{D} - Q_0 \underline{I}) \underline{s}_i = (Q_i - Q_0) \underline{s}_i \\ &= > \underline{B}_0^{-1} \underline{s}_i = (Q_i - Q_0)^{-1} \underline{s}_i \end{aligned} \quad (4.20)$$

Now, from assumption a we know that any vector \underline{y}_0 may be written as a sum

$$\underline{y}_0 = d_1 \underline{s}_1 + d_2 \underline{s}_2 + \dots + d_m \underline{s}_m \quad (4.21)$$

and we may easily choose a start vector, \underline{y}_0 , with a component along the basis (eigen) vector \underline{s}_r ($d_r \neq 0$) - for instance $\underline{y}_0 = (1, 1, \dots, 1)$.

Inserting eq. (4.21) in (4.19) we get first

$$\underline{y}_1 = \sum_{l=1}^m d_l \underline{B}_0^{-1} \underline{s}_l \quad (4.22)$$

and thus, from (4.20)

$$\underline{y}_1 = \sum_{l=1}^m \frac{d_l}{(Q_1 - Q_0)} \underline{s}_l \quad (4.23)$$

Repeated use of (4.19) then leads to

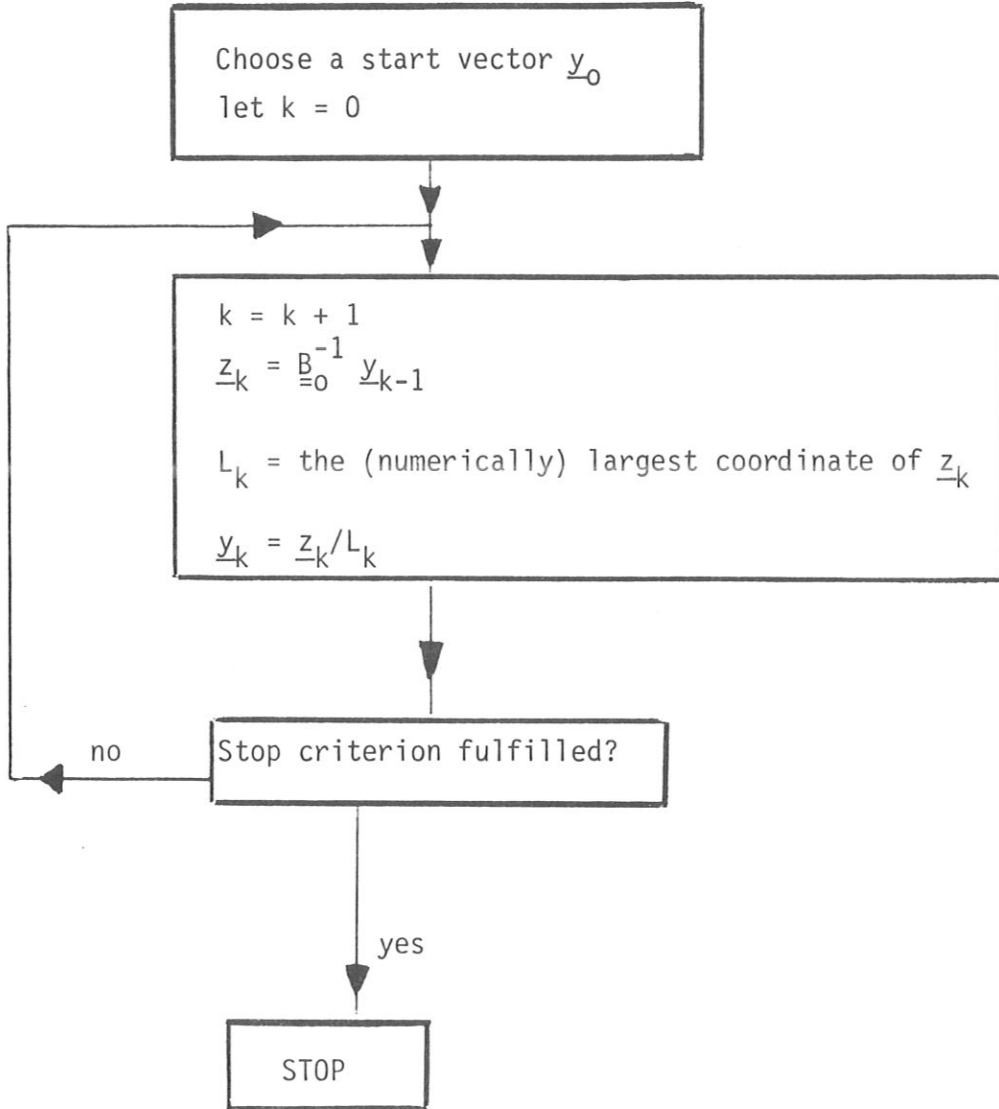
$$\underline{y}_k = \sum_{l=1}^m \frac{d_l}{(Q_1 - Q_0)^k} \underline{s}_l = (Q_r - Q_0)^{-k} \left\{ d_r \underline{s}_r + \sum_{l \neq r} d_l \left(\frac{Q_r - Q_0}{Q_1 - Q_0} \right)^k \underline{s}_l \right\} \quad (4.24)$$

From assumption b above $\frac{Q_r - Q_0}{Q_1 - Q_0} < 1$, so

$$\underline{y}_k \rightarrow \frac{d_r}{(Q_r - Q_0)^k} \underline{s}_r, \text{ and } \frac{|\underline{y}_k|}{|\underline{y}_{k-1}|} \rightarrow \frac{1}{(Q_r - Q_0)},$$

i.e. the iteration leads towards the direction of \underline{s}_r and the value of Q_r . In order to avoid overflow, \underline{y}_k is normalised in each step.

ii) Algorithm.



We note that in this algorithm

$$\left. \begin{aligned} L_k &\rightarrow \frac{1}{Q_r - Q_0} \\ \underline{y}_k &\rightarrow t \cdot \underline{s}_r \end{aligned} \right\} \text{ for } k \rightarrow \infty$$

where the value of the scalar t is unimportant, as we are only concerned with relative concentrations.

This means that we may also determine the 'true' eigenvalue Q_r from $Q_0 + 1/L_k \rightarrow Q_r$ for $k \rightarrow \infty$.

iii) Practical calculation

In every step of the iteration process we calculate $\underline{z}_k = \underline{B}_0^{-1} \underline{y}_{k-1}$ (see algorithm), or actually we solve the equation

$$\underline{B}_0 \underline{z}_k = \underline{y}_{k-1} \quad (4.25)$$

for \underline{z}_k . This is done by means of Gauss's elimination method (reducing \underline{B}_0 to triangular form) and should really be accompanied by partial pivoting [19]. Fortunately experience has shown that pivoting is unimportant in our case, so that it is simple to 'remember' how the elimination procedure is performed.

'Remembering' the elimination procedure is useful, because \underline{B}_0 is the same in every step of a given iteration, so that we may save time by reducing \underline{B}_0 to triangular form once at the beginning of the iteration, and then only apply the procedure to \underline{y}_{k-1} in the k'th step. Of course this could also be done including pivoting.

After thus rewriting eq. (4.25) we easily solve for \underline{z}_k by back-substitution.

4.5 Optimizing program

The listed versions (Chapter 5) have not been optimized with respect to time and space requirements. This is so partly because of the size and speed of the Amdahl 470, partly because these versions were intended for several different users and a variety of applications.

Users with a narrower range of applications, or with a smaller computer, may however wish to optimize their version correspondingly. An example is described in Section 5.9. Actually we suggest, that one might design a version of SQUEAKIE to run on a small personal computer (!) by tailoring it closely to a particular type of application.

Quite generally one may save computertime by using a simpler analytical expression for the stopping power (Sect. 4.3). Using eq. 4.12, the stopping power calculations take almost 70 % of the CPU-time! In contrast, the expression 4.13 is more than 3 times as fast to calculate, both on the NORD-100 and on the Amdahl 470. — on an ABC 80 personal computer it is ~ 7 times as fast as eq. 4.12.

In as far as space requirements are concerned we note, that the listed versions use an excessive number, and size, of arrays. If necessary, most users could easily limit the interesting part of their spectrum to much less than 1024 channels. Also, one does only rarely consider signals from more than 4 elements at a time, when measuring depthdistributions (the present version allows up to 6 elements). Omitting the calculation of 'integrated contents' (Sect. 3.3) also saves you an array. Finally the present version allows up to 500 depthsteps, whereas ~ 50 usually suffice.

Transferring all major arrays (particularly 'SPCT') to COMMON blocks is certain to save space, and the array 'DESCR' is specific for use in Garching. Also the use of double precision constants and variables is usually unnecessary.

For further discussion of program optimization the reader is referred to Sect. 5.9.

5. PROGRAM

1. The versions listed and described most extensively below both reside on the Amdahl 470 at the Max-Planck-Institut für Plasmaphysik (IPP) in Garching. This computer is so large and fast that little effort was devoted to saving time or space in these versions (see Sect. 4.5).

The necessary core storage is ~ 110 K bytes, plus several K bytes for the operating system and buffers. Requesting space in portions of 60 K we occupy a total of 180 K, which is low enough to give the program a high priority in the job-queue.

The total CPU-time varies faster than linearly with both the number of target elements, m_e , and the number of depthsteps, i.e. with the maximum depth evaluated. Typical CPU-times are ~ 3 seconds for a target containing 4 elements evaluated in 30 depthsteps.

2. It may often be desirable to use the program on much smaller computers, so a version residing presently on the NORD-100 computer at the University of Aarhus is also briefly described. This version is somewhat more specific for the computer, so it is not listed here, but the optimization relative to the Garching-versions is discussed. Computing time was reduced as suggested in Sect. 4.5, so that the evaluation of a target containing 4 elements in 30 depthsteps typically takes ~ 17 seconds.

3. The listed versions are specific for Rutherford Backscattering (RBS) spectra, but along with the description of the program, the few changes necessary for nuclear reaction energy spectra are indicated:

It is here assumed, that m_e possible target elements are specified in the input (see below), and that the experimental spectrum is composed of RBS-signals from some of the m_e-1 first elements and nuclear reaction signals from element number m_e . Usually, though, the resolution is much poorer for the nuclear reaction signals than for RBS, so one should consider also the possible problems concerning the comparison of such quite differently smeared signals (see also Sect. 7.2).

4. The purpose of the following description is to enable users to understand existing versions of the program, or possibly implement new versions on their own computer. The latter is perhaps a rather optimistic aim, as experience proves it quite difficult to make the necessary modifications in a program written by somebody else. In an attempt to overcome this, the present program is not only listed, but also explained in extreme detail - almost down to every single statement. This should also be helpful to those who prefer to design their own (superior?) program.

The statements of a given segment are identified by the numbers to the very left in the listing below.

If you are implementing the listed code on your computer, Section 7.1 may help you to catch programming errors, etc.

5.1 - 5.8

These sections all reside separately on the Amdahl 470. Both listings and descriptions are continuously updated as the program is being improved during use. The latest version may at any time be requested from the authors.

5.9 Aarhus-version

As an example of an alternative version of SQUEAKIE, the version residing presently on the NORD-100 computer in Aarhus is briefly described and commented upon below. The NORD-100 is considerably smaller than the Amdahl 470. It is equipped with a 64 kbyte 16 bit memory, and a real constant or variable occupies 3 bytes (words).

After optimization with respect to time and space (see below) the program code takes up 20.7 kbytes and the COMMON blocks 19.3 kbytes of memory, so the program is easily handled by the NORD-100 with respect to memory requirements. The optimized program has even been extended somewhat compared to the Garching versions.

A listing of the Aarhus-version may be requested from the authors at any time. In the following the reader is expected to be familiar with the descriptions of the IPP-versions (see previous sections).

i) Changes

Only minor modifications of the IPP-versions were absolutely necessary for making the program run on the NORD-100. These changes are nearly

all in the SQUEAKIE main program (compare Sect. 5.1) and concern the input/output statements.

Such a modified version, however, was found to be quite slow on the smaller computer. As discussed in Sects. 4.3 and 4.5 the CPU-time was considerably reduced by using instead the expression (4.13) for the stopping powers. The function STPA (Sect. 5.5) was therefore replaced by calls to existing subroutines /17/.

ii) Extensions

a) A preliminary subroutine has been included for the purpose of plotting the results. This is naturally a very machine dependent part of the program: The plotting is based on the two arrays (in subroutine STEP) 'CMP' and 'XINT', holding the calculated composition and the depth step lengths, respectively. These two arrays are moved to a common block for easier transfer to the plotting subroutine.

b) A new tool in the Aarhus version is the inclusion of limitations for each element: A lower and an upper channel number is specified for each element, defining the interval within which signals from this element may occur. This is a very useful feature, since the program may not always distinguish between signals from light elements at the surface or heavier elements at larger depths (see also Section 5.8).

In practice a statement has been included in STEP, checking in each depthstep whether the channel number considered for a given element lies within the specified interval. If this is not the case, the elemental signal from this depthstep is ignored.

ii) The element limitations should be used with care only. They require a certain pre-knowledge of the target/spectrum, but in many cases such a knowledge is present or can be acquired by a visual inspection of the spectrum.

c) The specification of the element limits is done in a subroutine also used for subtracting background signals. This subroutine is used in connection with a standard, interactive fitting program on the NORD-100, and is written for the specific purpose of supplying a background subtracted spectrum as input to SQUEAKIE. The background is fitted separately for each elemental signal, and the limits of the interval, within which the background is actually subtracted, are used afterwards as the element limits mentioned above. The nature of such a background subtraction necessitates a certain experience and knowledge of both the fitting procedure and the nature of the spectrum.

iii) Optimization

The program was optimized in various ways relative to the IPP-versions (see also Sect. 4.5):

a) All major arrays were transferred to the common area. The program then takes up less space, when it is saved on disk, and the transfer of parameters to subroutines is made easier.

b) The IPP-versions use double precision constants and variables, but this has been found to be unnecessary and is changed to single precision in the Aarhus version. Besides from a small reduction in size, the program becomes 8 % faster, since some time consuming routines for converting from double to single precision are no longer needed.

b) Since the NORD-100 is considerably slower than the Amdahl 470 some efforts have been made to speed up the program execution. For this purpose the CPU time-consumption in the various parts of the program were analyzed using a standard CPU measurement facility in the NORD system. The analysis shows that nearly 90 % of the CPU-time is used in the 'DO 140'-loop (Sect. 5.7) of STEP, and especially in the herein nested 402 and 403-loops. The time here mainly goes to calculating the stopping powers. The use of a stopping power expression which is 3 times faster than the Ziegler expression used in Garching (Sect. 4.3), made the whole program about 2.3 times faster.

The CPU-time was further reduced by 8 % by doing some calculations once instead of 3 times, again in the 402 and 403-loops: In these statements the appropriate parts ($CMP(NE,NI) * 1.E-15$ and $XINT(NI)/CBET*1.E-3$) are replaced by variables, which are calculated only once for each pass through the loop.

c) After the above optimizations a typical CPU-time measurement shows the following distribution of time consumption:

subroutine STEP		17 %
subroutines ITER, CRSEC, XK	total	1 %
subroutine STOPP(the stopping power expression)		44 %
subroutine HELI4 (selects the 3 constants for STOPP)		6 %
various system and FORTRAN routines for transfer of parameters, subroutine calls, etc.		32 %

Actually, in the calculation of the stopping power a certain time is also needed for parameter transfer etc., so that in the final program nearly 70 % of the CPU-time is devoted to stopping power calculations.

The total CPU-time for a given job is highly dependent on the number of elements, m_e , and the number of steps into the target, m_s . In the time consuming 'DO 140'-loop (see above) the total number of calls to subroutine STOPP is found to be

$$m_e^2 \cdot 3 \frac{(m_s-1)(m_s-2)}{2} + m_e$$

which is roughly proportional to $m_e^2 \cdot m_s^2$. This is in fine agreement with the empirical finding, that the total CPU-time is proportional to $(m_e \cdot m_s)^{1.7}$.

iv) Example

For an illustration of the use of the Aarhus-version a simple RBS-spectrum (Fig. 3a) is chosen. This is a spectrum of an Al-Co-Au alloy which has been prepared by a vacuum co-evaporation of the 3 elements on a carbon substrate. It is normally used for energy calibration because the 3 elements (all present at the surface) yield 3 distinct high-energy edges in the spectrum. A closer inspection of the low-energy signals (Fig. 3b) shows that a little native oxide was present on the carbon substrate before evaporation. Furthermore one finds carbon and oxygen as contaminants on top of the alloy, and since these signals only appear after months of use they are ascribed to respectively cracking of diffusion pump oil and oxidation of the sample.

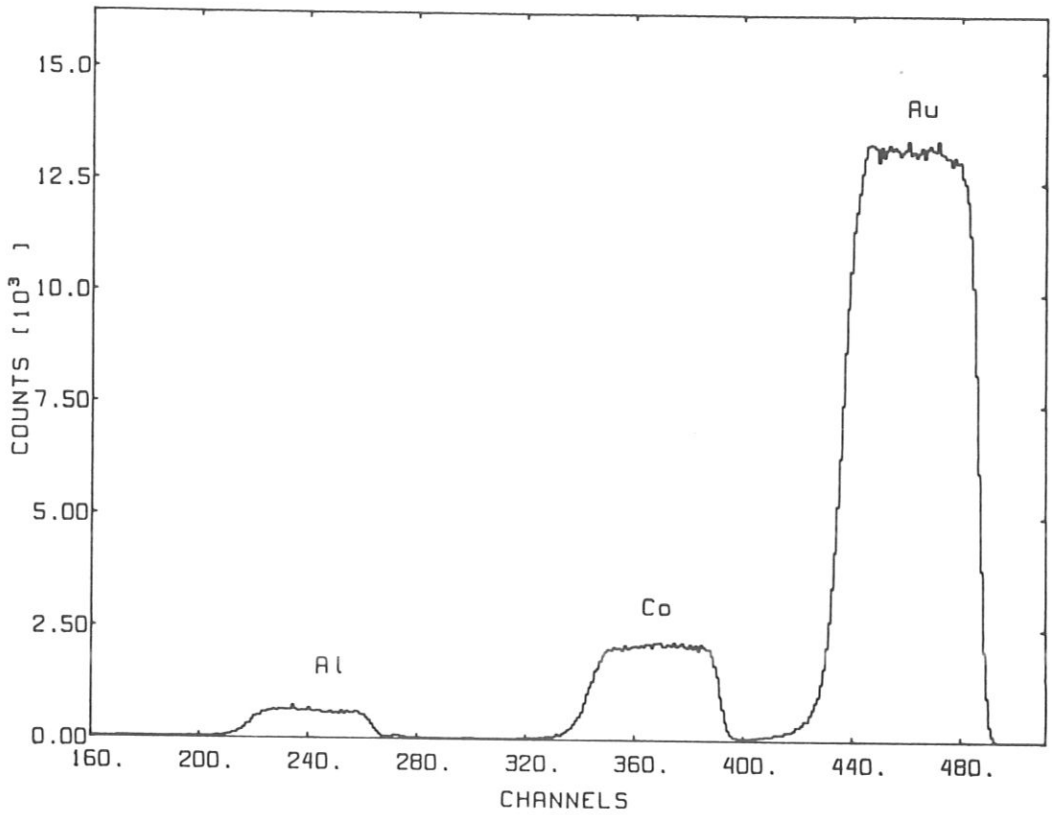


Fig. 3a: RBS-spectrum of Al-Co-Au alloy on a carbon substrate. High-energy signals

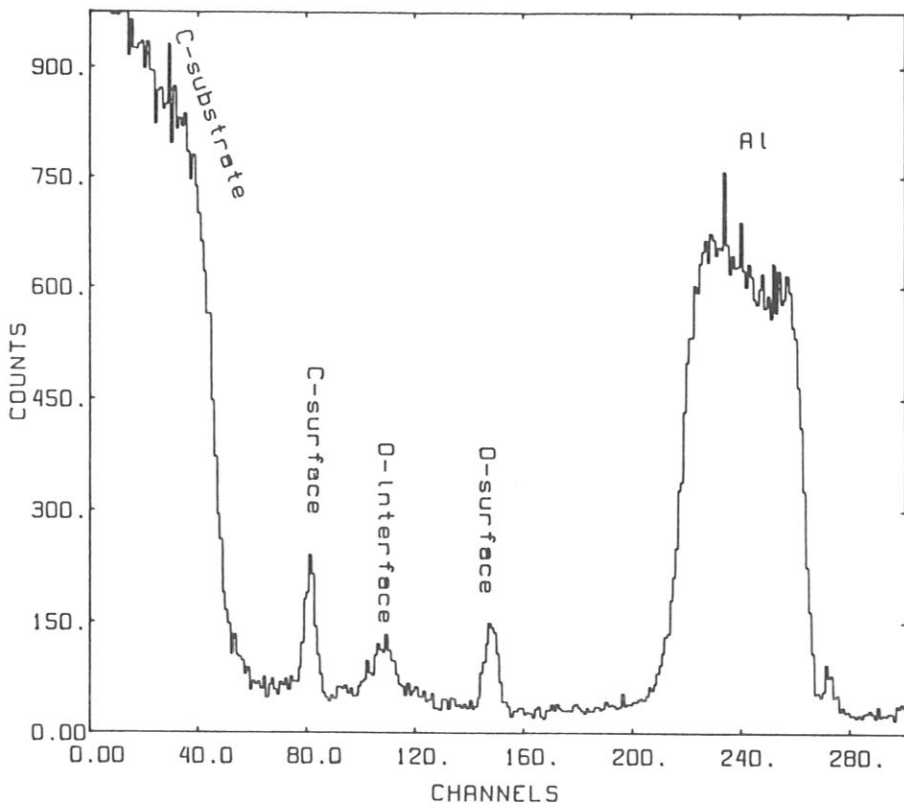


Fig. 3b: Low-energy signals (note change of scale)

The need for both background subtraction and element limits, as discussed above, is clearly seen in Fig. 3b. (In Garching background subtraction must be performed by an independent program.) The background was here fitted by a straight line through channels 88-96 and 157-165 (see Fig. 3c), and then subtracted in the whole region between the channels 88 and 165 to yield the oxygen signals. The channels 88 and 165 are then used as 'element limits' for oxygen.

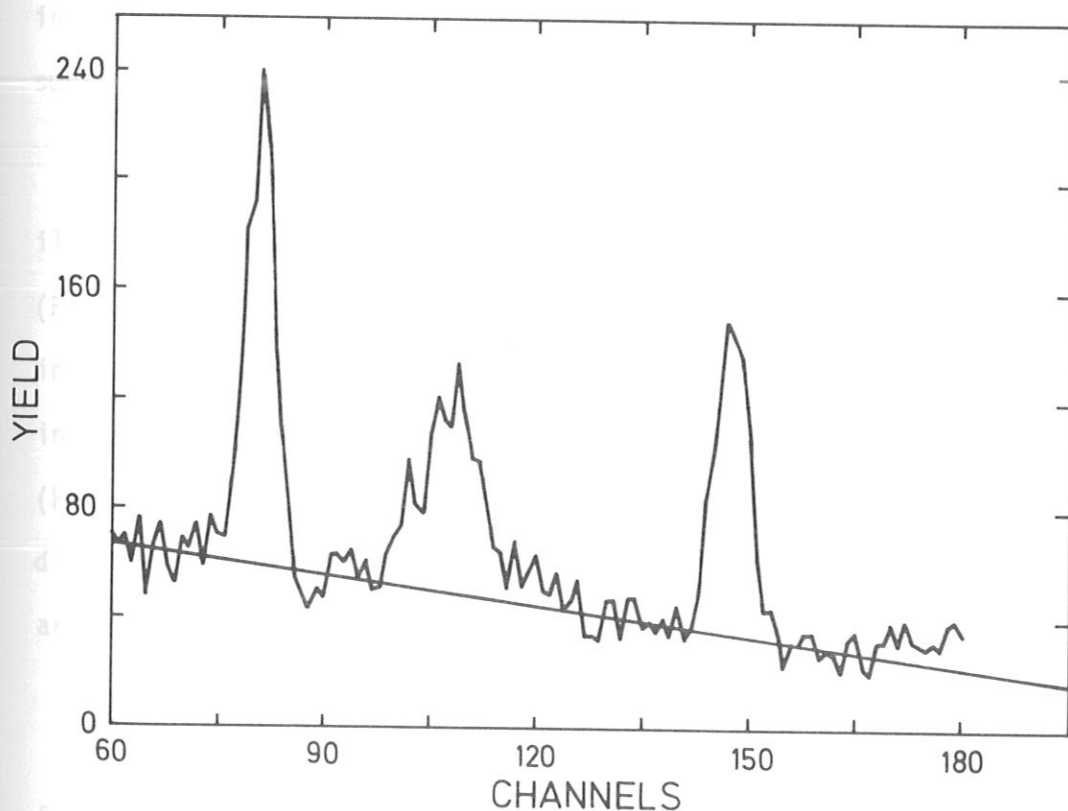


Fig. 3c: Part of spectrum expanded: Signals from C at the surface, and O at surface and interface. Straight line — background to be subtracted from signals

After all the elemental signals have been corrected for background and supplied with element limits, a run of SQUEAKIE yields the results of Fig. 4a. The depth distribution shows the expected thin layer of carbon and oxygen on the surface of a nearly homogeneous Al-Co-Au alloy. The Q-value ($N_{\text{prim}} \Delta \Omega$, Sect. 2.2) is estimated in each step, and for the present case it is plotted as a function of depth in Fig. 4b.

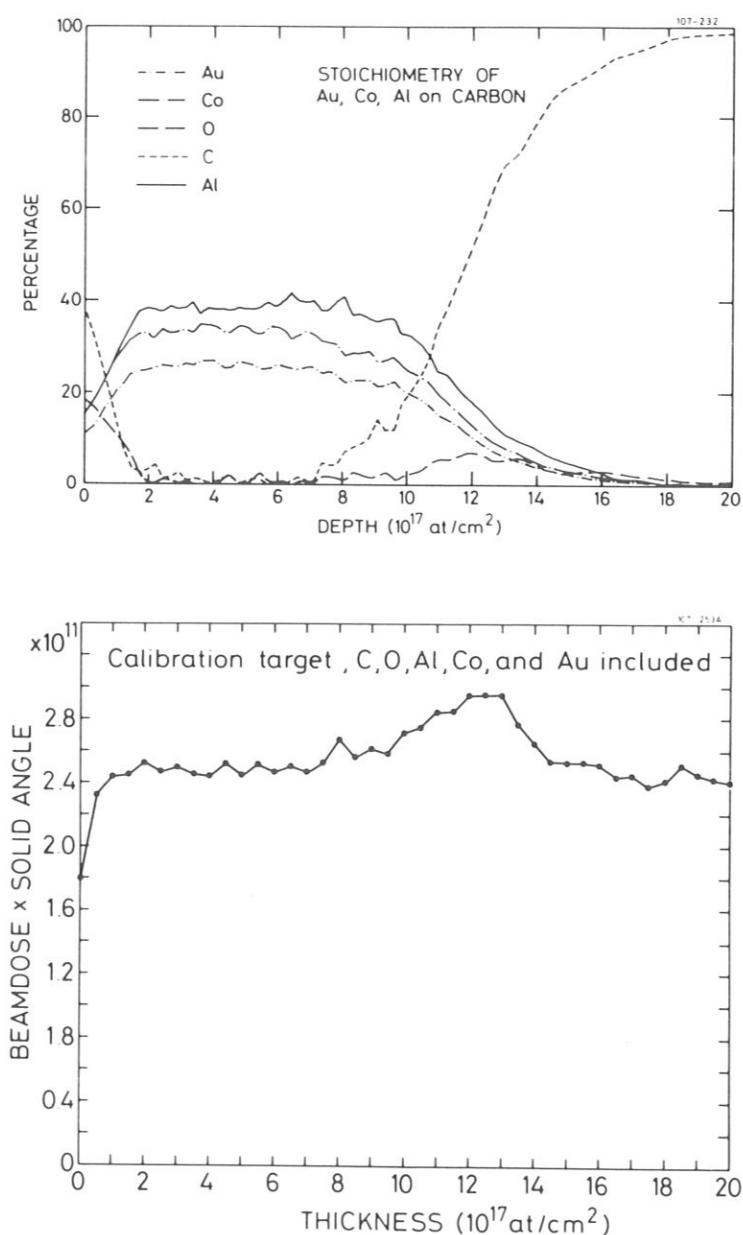


Fig. 4: Results obtained from spectrum in Fig. 3 by means of SQUEAKIE
a) Relative elemental concentrations vs. depth
b) Eigenvalue Q vs. depth. Note different depth scales!

This value can in a way be taken as a measure of the validity of the calculations:

The Q-value is actually a physical constant for a given spectrum, so for a correct calculation it should remain independent of depth. This argument, however, is somewhat obstructed by the possibility of 'cancellation of errors' /1/, where a correct stoichiometry may result from the relative signal heights while the absolute error is absorbed in Q. In Fig. 4b the Q-value is constant ($2.5 \cdot 10^{11}$) except at the surface and at the interface, where resolution effects, and possibly insufficient background subtraction, obscure the signals.

The behaviour of Q vs. depth in the case of errors is further illustrated by an alternative SQUEAKIE calculation on the same spectrum (Fig. 5). This time the carbon and oxygen signals are ignored, resulting in somewhat different results at larger depths (no signals), as seen in Fig. 5a. This "lack of signal" is reflected in the low Q-values (Fig. 5b), especially beyond $1.2 \cdot 10^{18}$ atoms/cm², where the depth distribution becomes clearly unrealistic. However, the elemental ratios are nicely reproduced at those depths, where Q remains constant.

5.10 List of symbols

Unfortunately it has not always been practical to use the same symbol for a variable or constant in the program and in the present text.

The following list should help avoid confusion.

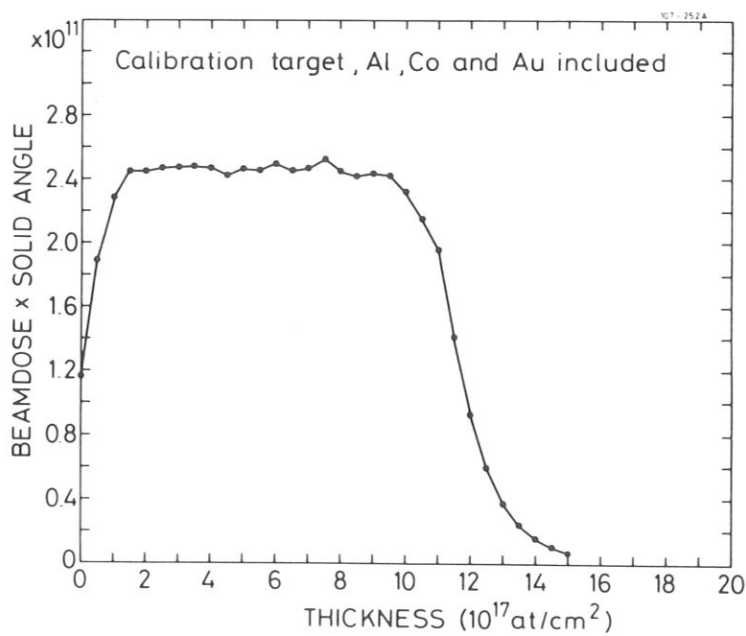
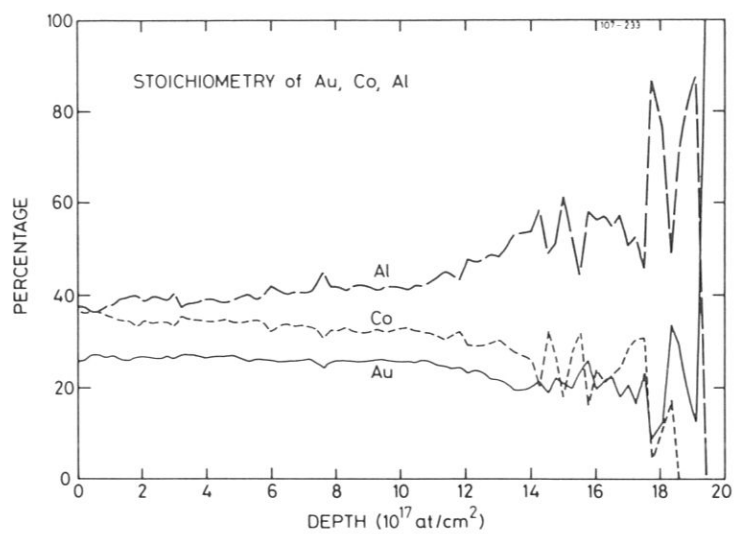


Fig. 5: As Fig. 4, but ignoring signals from C and O.

<u>Text</u>	<u>Program</u>	<u>Meaning</u>
m_e	NTOT	Total number of elements possibly present in target
m	N	Dimension of \underline{D} at given depth = number of elements at this depth
Q_0	Q0	Initial 'guess' of eigenvalue at given depth
\underline{D}	AM	Matrix \underline{D} of eigenvector problem (eq. 2.12)
$C_i a_{ij}$		element of \underline{D}
Q_r		True eigenvalue at given depth (the one we want)
\underline{s}_r		True eigenvector at given depth (the one we want)
\underline{s}_j		Some true eigenvector at given depth (not necessarily the one we want)
\underline{B}		$= \underline{D} - Q_m \underline{I}$
\underline{B}_0	A (in ITER)	$= \underline{D} - Q_0 \underline{I}$
M_i	A (in XK, STPA)	Masses of target elements
b_{ij}^0		element of \underline{B}_0
M_1	A1	projectile mass
E_0	E0	primary beam energy at target surface
α	ALFA	incident angle
n_i		relative atomic concentration of element 'i' at depth x

x	X	depth below target surface
S_{pj}^i		stopping power for particle 'pj' in targetelement 'i'
S^i		stopping power for projectile in targetelement 'i' (RBS-exp.)
Z_1	IZ1	projectile atomic number
ch1(i)	IH1(i)	lowest channel in signal from 'i'
ch2(i)	IH2(i)	highest channel in signal from 'i'

6. HOW TO USE THE PROGRAM

Below is described how to run the 2 existing versions of SQUEAKIE on the Amdahl 470 in Garching.

The first "problem" is to choose the appropriate version. This is best done by studying Sect. 6.5: For most purposes the alternative version (submitted as "SQU", Sect. 6.1) is the simpler one to use.

Section 6.1 demonstrates how to submit both versions for execution. This is followed by a short note (Sect. 6.2) on the job control cards. Note that these differ, depending on whether or not results from a previous run are included (see also Sect. 3.4).

The necessary input, and its format, is then described (Sect. 6.3), followed by an explanation of the output expected on various output-devices (Sect. 6.4).

The last two sections may also be of some interest for users elsewhere: A few examples of input and output are given in order to illustrate the preceding sections. Finally follows an assortment of warnings which may prove vital to any user.

Note: In case the system is changed, corrections to this Chapter will be listed together with Sections 5.1 - 5.8 on the Amdahl 470.

6.1 Submit

- a) The original version (Sects.5.1-5.7) employs the stop-criteria described in Section 3.4.

This version is chosen by submitting the AMOS-segment PRB: A.SQ. The necessary modifications of this segment are described in the following section.

For most applications the program may be submitted with the command XS PRB: A.SQ.

- b) The alternative version (Sect. 5.8) employs elemental 'markers' instead of the stop-criteria of Section 3.4.

This version is chosen by submitting PRB: A.SQU, usually with XS.

- c) For frequent use, please create your own control cards, input- and output-segments.

6.2 Job control cards

On the Amdahl 470 the program is preceded by a set of job control cards. This also links the various segments of the program (Sects. 5.1-5.6) together. Output is routed to the remote station RMT 10 (PWW).

a) Two examples of the use of the original version (SQ) are shown below, one for the case where previous runs are ignored, one for the case where results of a previous run are included. The input parameters (Sect.6.3) are found on the segment PRB:C.EUSDT.

1. example: This is the most common situation. The experimental spectrum is found on the segment BOM:BMSD4.SEG57. The output segment is PRB:B.EUS55.

No previous runs are included.

```
/*ROUTE PRINT RMT10
/*JOBPARM SYSAFF=S870
/** PRB:A.SQUEAKIE
// EXEC FORTRAN
//C.SYSPRINT DD SYSOUT=Z
//C.SYSIN DD *
$$ PRB:A.SQUEAKIE
$$ PRB:A.CRSEC
$$ PRB:A.XK
$$ PRB:A.STPA
$$ PRB:A.STEP
$$ PRB:A.ITER
//G.SYSLOUT DD DUMMY
//G.FT31F001 DD DSN='AMOS-PRB:B.EUS55,W',
$$ SYS:DD.FB0
//G.SYSIN DD *
$$ PRB:C.EUSDT
$$ BOM:BMSD4.SEG57
```

2. example: As mentioned in Section 3.4 and illustrated in Section 6.5 one may wish to include the results of a previous run. In example 1 (above) the results were tabulated on the segment PRB:B.EUS55. If we now want to include these results in an evaluation of the spectrum BOM:BMSD4.SEG55 obtained from the same target, we modify the job control cards as follows:

The segment PRB:B.EUS55 is linked to the data in the input stream, and a new output segment (PRB:B.EU355) is specified.

```
/*ROUTE PRINT RMT10
/*JOBPARM SYSAFF=S870
/** PRB:A.SQUEAKIE
// EXEC FORTRAN
//C.SYSPRINT DD SYSOUT=Z
//C.SYSIN DD *
$$ PRB:A.SQUEAKIE
$$ PRB:A.CRSEC
$$ PRB:A.XK
$$ PRB:A.STPA
$$ PRB:A.STEP
$$ PRB:A.ITER
//G.SYSLOUT DD DUMMY
//G.FT31F001 DD DSN='AMOS-PRB:B.EU355,W',
$$ SYS:DD.F80
//G.SYSIN DD *
$$ PRB:C.EUSDT
$$ BOM:BMSD4.SEG55
$$ PRB:B.EUS55
```

b) For the alternative version the job control cards are identical, except for replacing the segments A.SQUEAKIE and A.STEP by the segment A.ALTER.

This is actually only a formal replacement, as the latter segment uses both the others. Both A.SQUEAKIE and A.STEP must therefore also exist, when the alternative version is used.

```
/*ROUTE PRINT RMT10
/*JOBPARM SYSAFF=S870
/** PRB:A.SQUEAKIE
// EXEC FORTRAN
//C.SYSPRINT DD SYSOUT=Z
//C.SYSIN DD *
$$ PRB:A.ALTER
$$ PRB:A.CRSEC
$$ PRB:A.XK
$$ PRB:A.STPA
$$ PRB:A.ITER
//G.SYSLOUT DD DUMMY
//G.FT31F001 DD DSN='AMOS-PRB:B.EU355,W',
$$ SYS:DD.F80
//G.SYSIN DD *
$$ PRB:C.EUSDT
$$ BOM:BMSD4.SEG57
```

6.3 Input

a) Original version (Sects. 5.1-5.7), "SQ".

The amount of input parameters and data depends somewhat on the problem, but the first set of records is always needed:

Record # 1

Columns 1- 7 (F7.1): Scattering angle θ , in degrees.
" 11-17 (F7.1): Incident angle α , in degrees.
" 21-27 (F7.1): Detector angle β , in degrees.

Record # 2

Columns 1- 7 (F7.0): Incident energy E_0 , in keV
" 11-18 (F8.3): Energy per channel ΔE_1 , in the spectrum, in keV
" 21-28 (F8.3): Energy offset in calibration (energy of channel no. 0), in keV

Record # 3

Columns 1- 7 (F7.0): Minimum inward beamenergy $E(x)$ of interest (determines max. depth x), in keV
" 11-13 (I3): Lowest channelnumber of interest
" 17 (I1): Flag. Integrated contents vs. depth tabulated for flag > 0 .
" 19 (I1): FWHM of the exp. resolution at the surface (only used for integrating contents), in number of channels
" 21 (I1): Flag. Targetcomposition derived previously is read in, if flag > 0 . In that case only one experimental spectrum is allowed (see Record # 5).

Record # 4

Columns 1-2 (I2): Number m_e of possible target elements to look for.

Record # 5

Columns 1-2 (I2): Number of experimental spectra to be evaluated with this set of input parameters (see Record # 3, Col. 21)

" 6-9 (I4): Number of points in each experimental spectrum.

Record # 6

Columns 1-10 (F10.3): The projectile mass M_1 , in a.m.u.

" 16-17 (I2): The atomic number Z_1 of the projectile

" 21-30 (F10.3): The energy-scaling factor "FE" used in the function "STPA" for calculating the stopping power of isotopes. Equals 1.0 for ^4He and ^1H .

The following datapack must contain 2 records for each of the m_e target elements (see Record # 4 above). The first record specifies the element, the second the corresponding stopping power coefficients:

Record # 7

Columns 1-10 (F10.3): The mass M_i of the first element, in a.m.u.

" 15-17 (I3): The atomic number Z_i

" 20-21 (A2): The chemical name of the element.

Record # 8, for use of He-projectiles

Columns	1-13 (E13.4):	Stopping coefficient	A1 /11/
"	15-27 (E13.4):	"	A2 /11/
"	29-41 (E13.4):	"	A3 /11/
"	43-55 (E13.4):	"	A4 /11/
"	57-69 (E13.4):	"	A5 /11/

for the first element.

Record # 8, for use of H-projectiles

Columns	1-13 (E13.4):	Stopping coefficient	A2 /12/
"	15-27 (E13.4):	The number $\emptyset.45 D\emptyset$	
"	29-41 (E13.4):	Stopping coefficient	A3 /12/
"	43-55 (E13.4):	"	A4 /12/
"	57-69 (E13.4):	"	A5 /12/

Record # 9

Columns	1-1 \emptyset (F1 \emptyset .3):	The mass M_i of the second element, in a.m.u.
"	15-17 (I3):	

and so forth ---

The final datapack must now contain one or two sets of data for each experimental spectrum (Rec. # 5, Cols. 1-2), depending on the flag in Col. 21 of Rec. # 3.

In any case the pack must of course include the experimental spectrum, on the form automatically created in AMOS:

- i. The spectrum is preceded by a 'descriptor' - 10 lines (records) containing optional alphanumeric text in columns 1-72. This is printed again on all output for identification.
- ii. This is followed by a listing of the spectrum itself, 10 channels per line (record) in the columns 1-7, 8-14, 15-21, 22-28, 29-35, 36-42, 43-49, 50-56, 57-63, and 64-70. Format F 7. \emptyset .

If more data are to follow, it is essential that the number of points in the spectrum were correctly given in columns 6-9 of Record # 5. This is for instance the case if the flag in column 21 of Record # 3 was positive. In that case the present datapack must also include a table listing target composition vs. depth, with the elements in the same order as in the datapack above:

iii. Also this table is preceded by a 10 line descriptor, on the same form as for the spectra. This is not printed on output!

iv. The table itself consists of an optional number of lines, each giving in

Columns 11-20 (E10.3):	The depth x , in atoms/cm ²
" 26-30 (F5.3):	The relative concentration n_1 of the first element
" 34-38 (F5.3):	The relative concentration n_2 of the second element
" 42-46 (F5.3):	n_3
" 50-54 (F5.3):	n_4
" 58-62 (F5.3):	n_5
" 66-70 (F5.3):	n_6

We note that this table is on the same form as the output to be printed on a data file (below). We may thus directly use the output from a previous run of the program.

b) Alternative version (Sect. 5.8), "SQU".

The input parameters are almost the same as for the original version:

Record # 1

Columns 1- 7 (F7.1):	Scattering angle θ , in degrees.
" 11-17 (F7.1):	Incident angle α , in degrees
" 21-27 (F7.1):	Detector angle β , in degrees

Record # 2

Columns 1- 7 (F7.0):	Incident energy E_0 , in keV
" 11-18 (F8.3):	Energy per channel ΔE_1 in the spectrum, in keV
" 21-28 (F8.3):	Energy offset in calibration (energy of channel no. 0), in keV

Record # 3

- Column 17 (I1): Flag. Integrated contents vs depth tabulated for flag > 0.
- " 19 (I1): FWHM of the exp. resolution at the surface, in number of channels
- " 21 (I1): Flag. Target composition derived previously is read in, if flag > 0.

Record # 4

- Columns 1-2 (I2): Number m_e of possible target elements to look for.

Record # 5

- Columns 1-2 (I2): Number of experimental spectra to be evaluated with this set of input parameters. (Must equal 1 if flag > 0 in Record # 3, Col. 21).
- " 6-9 (I4): Number of points in each experimental spectrum

Record # 6

- Columns 1-10 (F10.3): The projectile mass M_1 , in a.m.u.
- " 16-17 (I2): The atomic number Z_1 of the projectile
- " 21-30 (F10.3): The energy-scaling factor "FE" used in the function "STPA" for calculating the stopping power of isotopes. Equals 1.0 for ^4He and ^1H , 4/3 for ^3He and 0.5 for deuterons.

The following datapack must contain 2 records for each of the m_e target-elements (see Record # 4 above). The first record specifies the element, and the element limits, the second the corresponding stopping power coefficients:

Record # 7

Columns	1-10 (F10.3):	The mass M_i of the first element, in a.m.u.
"	15-17 (I3):	The atomic number Z_i
"	20-21 (A2):	The chemical name of the element
"	30-33 (I4):	The lowest channel in which to find signals from this element.
"	40-43 (I4):	The highest channel in which to find signals from this element.

Signals from this element will be set equal to 0 if they do not fall between these limits.

Record # 8, for use of He-projectiles

Columns	1-13 (E13.4):	Stopping coefficient	A1 /11/
"	15-27 (E13.4):	"	A2 /11/
"	29-41 (E13.4):	"	A3 /11/
"	43-55 (E13.4):	"	A4 /11/
"	57-69 (E13.4):	"	A5 /11/

for the first element.

Record # 8, for use of H-projectiles

Columns	1-13 (E13.4):	Stopping coefficient	A2 /12/
"	15-27 (E13.4):	The number $0.45 D0$	
"	29-41 (E13.4):	Stopping coefficient	A3 /12/
"	43-55 (E13.4):	"	A4 /12/
"	57-69 (E13.4):	"	A5 /12/

Record # 9

Columns	1-10 (I0.3):	The mass M_i of the second element, in a.m.u.
"	15-17 (I3):	The atomic

and so forth (as Record # 7) ...

If the flag in Rec. # 3, Column 21 equals \emptyset , the final datapack contains the experimental spectra on the form automatically created in AMOS:

- i. The spectrum is preceded by a 'descriptor' - 10 lines (records) containing optional alphanumeric text in columns 1-72. This is printed again on all output for identification.
- ii. The spectrum itself is listed with 10 channels per line (record), in the columns 1-7, 8-14, 15-21, 22-28, 29-35, 36-42, 43-49, 50-56, 57-63, and 64-70. Format F7. \emptyset .

If the flag in Rec. # 3, Column 21 is positive, only one experimental spectrum is allowed. This is given on the form above, and followed by a table listing target composition vs. depth:

- iii. Also this table is preceded by a 10 line descriptor, on the same form as for the spectra. This is not printed on the output.

- iv. The table itself consists of an optional number of lines (records), each giving in

Columns 11-20 (E1 \emptyset .3):	The depth x , in atoms/cm ² .
" 26-30 (F5.3):	The relative concentration n_1 of the first element.
" 34-38 (F5.3):	The relative concentration n_2 of the second element.
" 42-46 (F5.3):	n_3
" 50-54 (F5.3):	n_4
" 58-62 (F5.3):	n_5
" 66-70 (F5.3):	n_6

This table is on the same form as the output printed on a datafile (Sect. 6.4). We may thus directly use the output from a previous run of the program.

6.4 Output

Output is partly printed, partly listed on an output segment specified in the control cards (see Sect. 6.2).

Printed output

The output begins with a list of the input parameters used (compare previous section):

Scattering angle (θ), incident angle (α), and exit-angle (β), as read in from Record # 1.

Incident energy (E_0), energy per channel (ΔE_1), and energy of channel no. 0, as read in from Record # 2. Minimum inward energy below which to stop evaluation, and lowest channel number, as read in from Record # 3. Number of spectra to be evaluated with this input, as read in from Record # 5.

Projectile mass (M_1) and atomic number (Z_1), as read in from Record # 6.

The energy-scaling factor (FE), as read in from Record # 6.

For each of the m_e possible target elements then the chemical name, the mass (M_i), the atomic number (Z_i), and the 5 stopping coefficients.

After the input parameters follows a listing of the experimental spectra, for later control and identification.

Finally, after each spectrum follows the calculated target-composition vs. depth:

Tabulated are the relative stoichiometric coefficients vs. depth. The depth is in units of atoms/cm², and the coefficients normalized so that the sum over all m_e elements equals unity. Along with each coefficient is given the statistical uncertainty as estimated from eq. 2.3.

Furthermore the table shows the approximate channels in which the elemental signals from each depth are found (the channel numbers are listed in the format F5.0, i.e. the actual numbers used usually deviate from these with fractions of a channel).

Finally the table includes the improved eigenvalue Q calculated in each depthstep (Sect. 4.4). This value should be compared to the product $N_{\text{prim}} \Delta\Omega$ of beamdose and detector solid angle, if this is known. Variations in Q may indicate resolution effects or direct errors /1, 9/, but the interpretation is not always obvious. Thus large variations in Q near the surface frequently indicate a partial 'cancellation of errors' (see Section 7.2 and Ref. 1).

Following the calculated target composition vs. depth the output may include a tabulation of integral contents vs. depth. As described in Sect. 3.3 the integral content of an element may be calculated in two independent ways. Correspondingly, the table consists of two parallel lists of results:

1. The total number of atoms/cm² of an element found between the surface and the depth x may be directly calculated from the target composition vs. depth listed above (Eq. 3.1). The results are thus based on relative scattering yields and the energy losses of the projectile, and are listed under the heading "FROM ENERGYLOSS". This approach is best for reasonably large depths x .
2. The total number of atoms/cm² of an element in a target may be independently calculated from the total scattering yield (Eq. 3.2). This approach is best for thin layers. Relating the numbers to a

depthscale of course implicitly involves the knowledge of the targetcomposition, but for many applications such a relation is really unnecessary. Listed are the integral contents times beamdose N_{prim} times detector solid angle $\Delta\Omega$ (Eq. 3.3). One obtains the total content of an element in number of atoms/cm² by dividing the listed quantity by $N_{\text{prim}} \Delta\Omega$ (taken from the table above, or determined independently).

6.5 Examples

Below are shown a few examples of use of the program. The program itself has no facilities to plot spectra or output, but we include figures here for the sake of illustration. The first examples are for the original version ("SQ"), the last example for the alternative version ("SQU").

1. The first example demonstrates the simplest application of the program:

It was attempted to produce an EuS-film (constant stoichiometry) of thickness 1110 Å on a Si-substrate. Ion beam spectrometry only yields filmthicknesses in terms of areal densities (e.g. atoms/cm²), but assuming 'bulk density' of the film the nominal value should be $\sim 2.1 \cdot 10^{17}$ EuS/cm².

A Rutherford backscattering spectrum was obtained using 2 MeV ⁴He⁺-ions and a scattering angle $\theta = 170^\circ$ (see Fig. 6). The target was tilted an angle $\alpha = 60^\circ$ in order to improve the depth resolution, resulting in a detectorangle $\beta = 60.5^\circ$. The energy calibration used was

EU-S/SI ANALYSE

BMSD4.SEG57

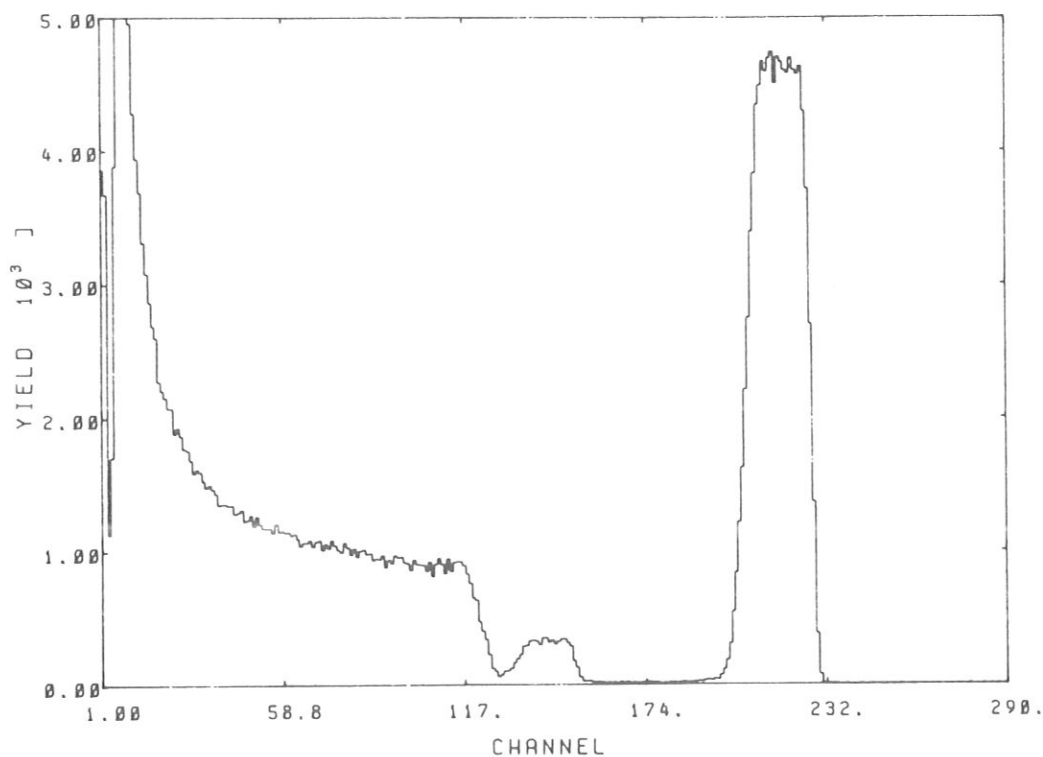


Fig. 6: RBS-spectrum of 2 MeV $^4\text{He}^+$ -ions scattered from 1110 \AA EuS on Si. $\theta = 170^\circ$, $\alpha = 60^\circ$, $\beta = 60.5^\circ$.

$$E_{\text{det}} = \text{ch} \times 7.683 + 55.0$$

where 'ch' is the channelnumber, and E_{det} is the corresponding energy in keV.

Of primary concern was the ratio of Eu- to S-contents in the film, so only these two elements were considered. For a beginning we make sure to evaluate the spectrum to sufficient depths - until the S-signal falls in a channel below 125. The necessary input was:

```

170.0      60.0      60.5
2000.      7.6830   +55.0000
1500.0     125    1 2 1
  2
  1
4.0016    289
  2    1.0
32.06     16    S
1.402     E+0 6.791 E-1 5.898 E+1 3.528 E+0 3.211 E+0
152.0     63    EU
1.402     E+1 3.63 E-1 2.284 E+2 7.024 E+0 1.016 E+0
  290  4401  4690  1104  6000  1
AMOS-FI-SG: BMSD4.SEG57 EXPERIMENT: EU-S/SI ANALYSE
NAME.....: BOR/SCHER DATE/TIME.: 27: 7:82 / 16:28:21
IMPL.IONS.: IMPL.ENERG:
IMPL.FLNCE.: ANALYSIS...: RBS
ANAL.IONS.: 4HE ALPHA.....: 60DEG
ANAL.DOSE.: 1.25E-7 C ANAL.ENERG: 2 MEV
THETA.....: 170 DEG MATERIAL...: 1110 A EUS/SI
TARGETPOS.: 29 MM LOGBOOK...: BMS 11/23
NOTE1.....: 500 CH./10 V NOTE2.....: HV 256X
3859 3673 1130 1700 3891 6028 6000 6354 5533 4955
4201 3937 3685 3311 3077 2865 2685 2597 2273 2203
2151 2070 2072 1881 1927 1863 1767 1755 1679 1584
1615 1594 1525 1475 1499 1464 1430 1345 1354 1354
1343 1344 1280 1293 1310 1224 1235 1270 1191 1261
1223 1171 1171 1177 1142 1205 1146 1156 1142 1146
1110 1131 1095 1043 1068 1068 1004 1037 1077 1004
1012 0600 1025 1003 1044 1011 992 1069 1029 976
1000 959 1005 1016 981 986 932 945 940 970
0800 939 910 849 956 959 916 905 860 939
0800 897 894 849 921 812 907 949 904 831
947 848 920 923 926 894 827 759 652 634
4700 4000 340 228 125 1000 64 81 106 112
108 173 202 231 295 297 331 338 300 303
356 355 321 336 305 330 346 347 314 289
1000 134 59 28 28 34 24 21 22 21
  5 21 15 18 13 24 15 22 13 19
 14 17 19 17 23 20 21 17 13 15
 16 21 21 17 19 26 19 18 19 29
 28 30 35 41 32 44 42 76 121 188
 309 550 842 1219 1630 2216 2749 3398 3832 4348
4495 4676 4598 4699 4740 4505 4707 4668 4606 4586
4696 4605 4577 4636 4299 3715 2698 1364 379 77
  8 8 4 7 6 0 2 5 2 3
  4 1 5 3 1 1 5 2 2 1
  2 0 1 0 2 3 0 1 3 3
  0 1 3 1 3 2 4 2 0 1
  1 2 0 2 2 2 2 1 0 1
  2 2 0 2 1 1 1 0 0 1

```

On the output we find first a list of the input used, for control purposes and identification. Then follows a table of the stoichiometric coefficients vs. depth. Along with each coefficient is given the estimated statistical uncertainty, and furthermore are listed the corresponding channel numbers in the experimental spectrum. Also included in the table are the improved estimates of the eigenvalue Q (Section 4.4). Finally is printed a table of 'integrated contents' vs. depth.

The target composition was evaluated up to a depth of $6.87 \cdot 10^{17}$ atoms/cm², corresponding to channels no. ~ 125 for S and ~ 199 for Eu, but a comparison with the spectrum shows this to be too far: Since the substrate (Si) was ignored, it is unreasonable to evaluate the spectrum up to depths where both the S- and the Eu-signals have essentially disappeared.

However, for the purpose of determining the filmthickness we need the integrated peaks from both elements, so here all the evaluated channels count: From the tabulation of the 'integrated contents' vs. depth we now obtain the values (eq. 3.3) $d_S \cdot N_{\text{prim}}^{\Delta\Omega} = 0.991 \cdot 10^{28}$ and $d_{\text{Eu}} \cdot N_{\text{prim}}^{\Delta\Omega} = 0.894 \cdot 10^{28}$. The product $N_{\text{prim}}^{\Delta\Omega}$ was determined roughly as $4 \cdot 10^{10}$, but may be estimated better from the heights of the back-scattering peaks. We see that the eigenvalue Q varies significantly within the first channels/depth steps, reflecting the effect of experimental resolution. However, for the channels corresponding to the peak-plateaus the eigenvalue remains almost constant around $3.65 \cdot 10^{10}$. Using this value for $N_{\text{prim}}^{\Delta\Omega}$ we thus have $\sim 2.72 \cdot 10^{17}$ S/cm² and $2.45 \cdot 10^{17}$ Eu/cm² in the target, i.e. a total of $\sim 5.17 \cdot 10^{17}$ atoms/cm².

Going back to the targetcomposition vs. depth we then ignore depths larger than $5.1 \cdot 10^{17}$ atoms/cm², and end up with the result shown in Fig. 7.

The program also provides a list of the results on an output-segment specified in the job control cards (Sect. 6.2). This segment (discussed and used further in the next example) may be used as input for our plotting programs.

2. The next example demonstrates the use of a particular facility:

The inclusion of results from previous runs.

a) First a qualitative investigation done without the program. The target was supposed to consist of 3 layers: 1080 Å of EuS on top of a 680 Å SrS-film, all on a Si-substrate. In Rutherford backscattering analysis reasonable depth resolution could be obtained using 2 MeV $^4\text{He}^+$ -ions and tilting the target. Unfortunately, signals from Si near the surface would be superposed on the S-signal from larger depths.

There is not supposed to be any Si near the surface, but in order to check this, a spectrum was first measured with 2.5 MeV $^4\text{He}^+$ -ions at an incident angle $\alpha = 15^\circ$ (Fig. 8). In this spectrum the depth resolution was poor, but it was clearly seen that there is no Si near the surface. Instead a small peak was found, indicating 5-10 % Sr at the surface.

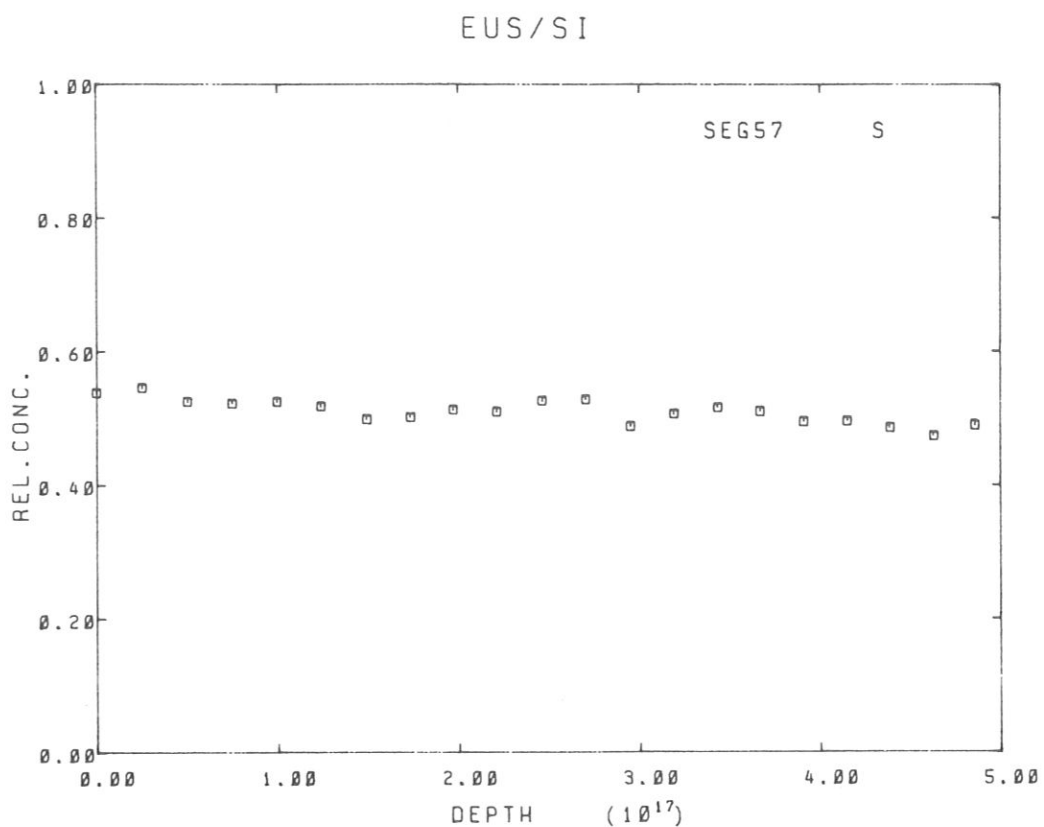


Fig. 7a: Plot of SQUEAKIE - output resulting from evaluation of spectrum in Fig.6. Original SQUEAKIE-version. Relative concentration vs. depth of S.

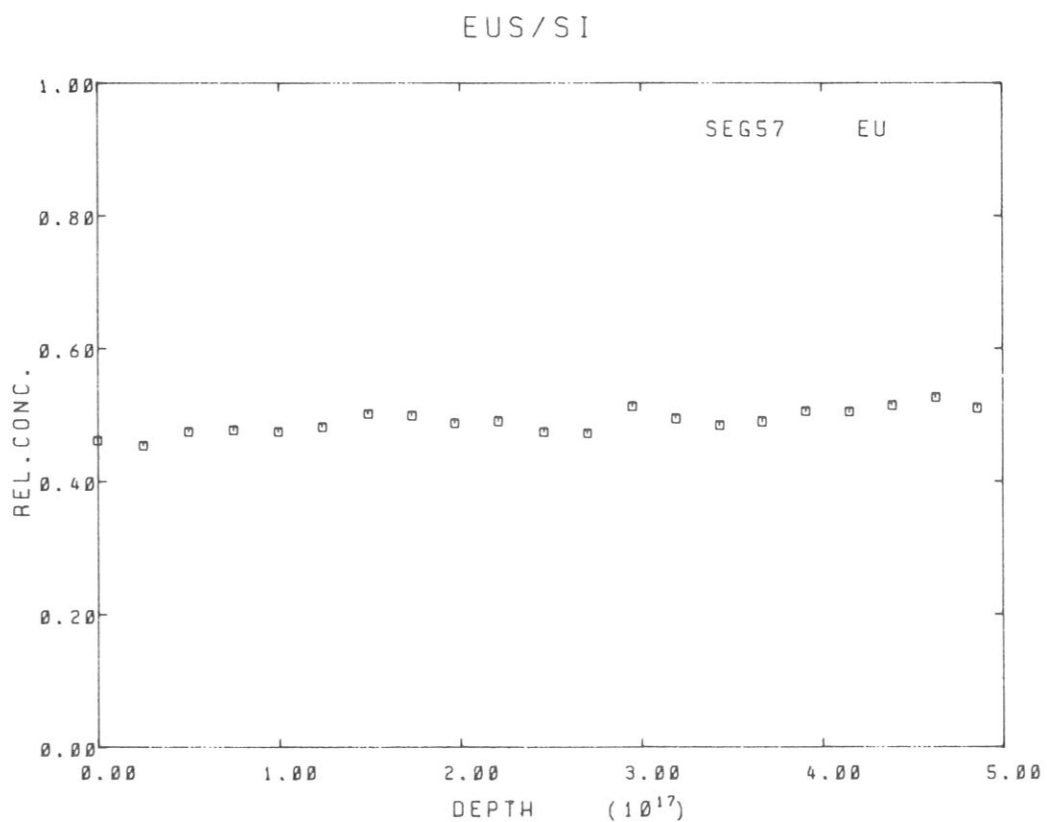


Fig. 7b: Relative concentration vs. depth of Eu

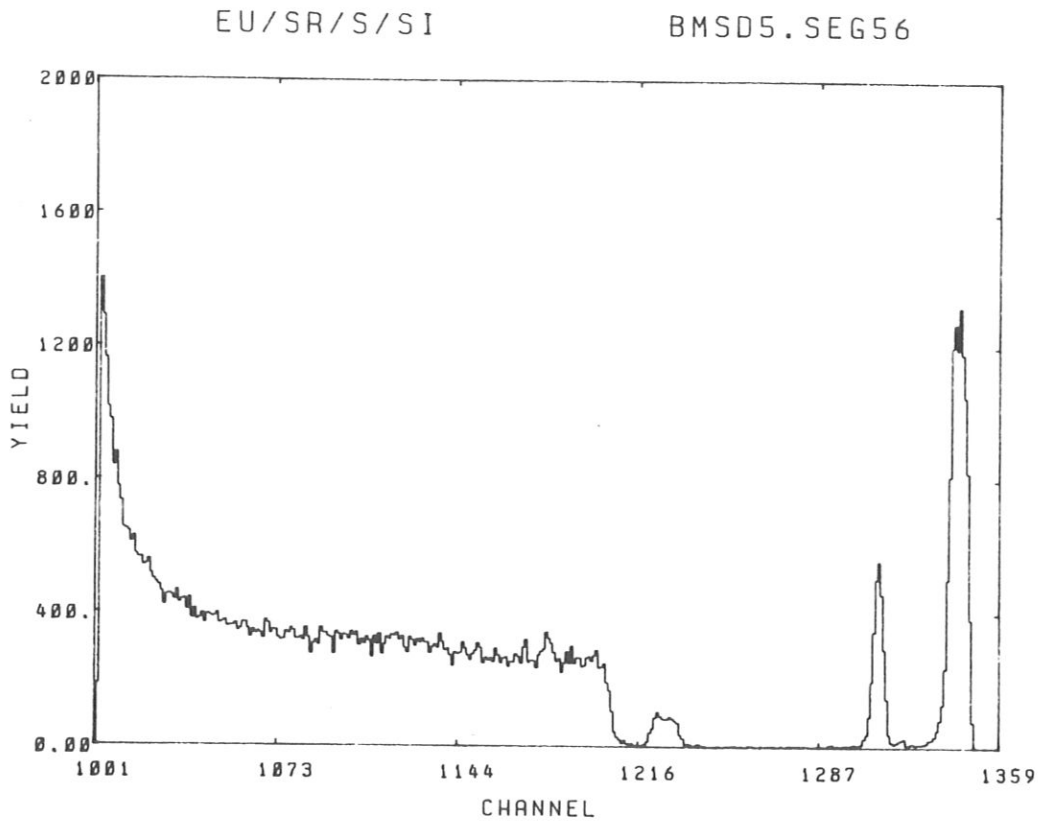


Fig. 8: RBS-spectrum for 2.5 MeV ^4He -ions scattered from 1080 Å EuS / 680 Å SrS/Si.

- b) An experimental spectrum was now obtained using 2 MeV $^4\text{He}^+$ -ions and a (laboratory) scattering angle θ of 165° (Fig. 9). The target was tilted an angle $\alpha = 15^\circ$ perpendicular to the scattering plane, giving the detector angle $\beta \approx 21.1^\circ$.

EU/SR/S/SI

BMSD5.SEG55

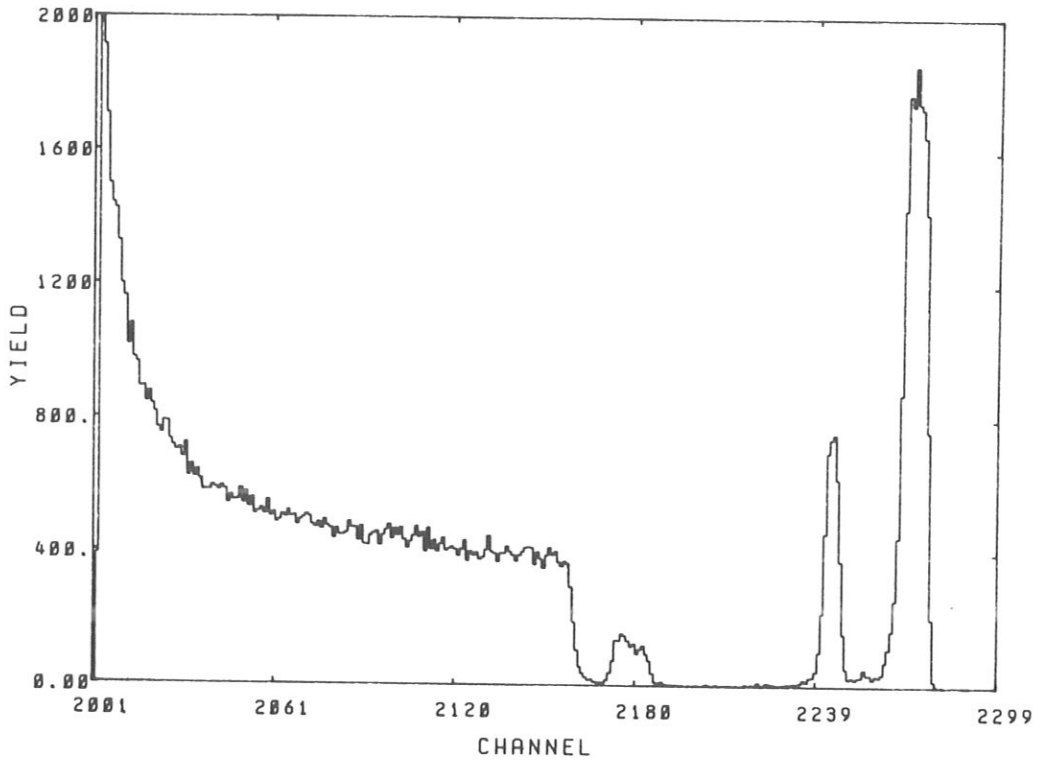


Fig. 9: RBS-spectrum for 2 MeV ^4He -ions scattered from 1080 Å EuS / 680 Å SrS/Si
 $\theta = 165^\circ$, $\alpha = 15^\circ$, $\beta = 21.1^\circ$

The energy calibration used was

$$E_{\text{det}} = \text{ch} \times 6.3909 + 41.172$$

where 'ch' is the channelnumber, and E_{det} is the corresponding energy in keV.

As noted above, signals from Si near the surface would be superposed on the S-signal from larger depths. We know that there is no Si-signal superposed on the S-signal, but the program is not capable of distinguishing this. In the Aarhus-version this is handled by defining appropriate markers

(see Sect. 5.9), here we first analyze the near-surface layer, looking only for the other three elements:

In the listed input-example (below) the calculations are to be terminated at the depth x, where the inward beam energy becomes less than 1000.0 keV, or from which one of the experimental signals falls in a channel below 181. In the present case this happens when the S-signal corresponds to a channel slightly below 181 (see output).

In the present calculations, the integrated contents are not of interest.

We expect to find three different target elements at the present depths: S, Eu, and Sr.

Only one experimental spectrum, containing 299 channels, is to be evaluated in this run.

For each of the three possible target elements the appropriate ⁴He-stopping power coefficients are taken from Ref. 11.

Input:

```

165.#      15.#      21.1
2000.#     6.39#9   +41.172
10000.#    181     # 2 #
3
1          299
4.0016    2          1.#
32.06     16        S
1.402     E+# 6.791  E-1 5.898   E+1 3.528   E+# 3.211   E+#
152.#     63        EU
1.422     E+1 3.63   E-1 2.284   E+2 7.024   E+# 1.016   E+#
87.63     38        SR
7.126     E+# 4.804  E-1 1.193   E+2 5.784   E+# 2.454   E+#

299 2001 2299 17 2102 # # # 1
AMOS-F1-SG: BMSD5.SEG55 EXPERIMENT: EU/SR/S/SI
NAME.....: BOE/SCH E DATE/TIME.: 27: 8:02 / 11: 9:19
IMPL.IONS.: IMPL.ENERG.:
IMPL.FLNCE: ANALYSIS...: RBS
ANAL.IONS.: 4HE ALPHA.....: 15 DEG
ANAL.DOSE.: 20E-6 C ANAL.ENERG.: 2 MEV
THETA.....: 165 DEG MATERIAL...: EU-S/SR-S/SI
TARGETPOS.: 39 MM LOGBOOK...: RBS V1/175
NOTE1.....: H.V.GAIN=256X NOTE2.....: 10000 CH/100 V

# 392 2102 1912 1707 1497 1439 1423 1326 1197
1161 1016 1079 977 964 890 893 846 878 839
814 768 753 790 788 733 715 702 708 681
725 624 660 622 644 615 582 584 583 598
590 582 595 586 544 567 553 554 588 544
579 533 561 512 520 529 512 554 506 517
488 495 513 503 525 505 508 480 497 504
513 506 480 474 488 469 496 477 470 440
470 452 452 459 492 472 472 434 478 421
420 450 456 461 420 451 467 483 439 471
449 474 436 412 432 450 477 444 458 400
473 407 436 401 426 443 404 412 417 408
389 409 436 373 402 391 399 379 386 408
449 400 396 372 397 397 419 400 390 373
393 403 415 416 413 363 400 380 362 393
414 392 402 369 350 373 366 295 190 106
57 38 25 16 20 11 9 9 18
41 77 139 136 158 151 134 118 126 97
110 120 95 76 38 11 9 13 6 4
5 2 5 1 3 0 3 0 3 3
0 3 6 3 1 4 1 2 3 13
3 1 1 1 6 3 3 6 3 0
5 9 12 8 6 5 2 4 6 0
7 9 8 13 21 15 29 31 47 106
222 462 704 744 757 621 377 158 53 23
28 22 28 31 53 35 35 23 34 30
39 76 114 170 261 450 879 1432 1775 1744
1861 1749 1733 1647 1418 764 204 19 2 0
1 0 0 0 0 0 0 1 1 0
0 0 0 0 0 0 0 0 0 0

```

On the output we find, after a list of the input, a table of the stoichiometric coefficients vs. depth (see also previous example).

We see that taking the surface channels to be no. ~ 185 for S, no. ~ 276 for Eu and no. ~ 255 for Sr the surface stoichiometry is evaluated as $S_{0.413} Eu_{0.51} Sr_{0.076}$ within the estimated uncertainties. Assuming the stoichiometry to remain constant within the first depthstep, we then find the stoichiometry $S_{0.434} Eu_{0.535} Sr_{0.031}$ at depth $3.77 \cdot 10^{16}$ atoms/cm² by evaluating channels no. ~ 184 for S, no. ~ 275 for Eu and no. ~ 254 for Sr.

The targetcomposition was first only evaluated up to a depth of $1.14 \cdot 10^{17}$ atoms/cm².

We note that the eigenvalue Q varies significantly within the first channels/depthsteps, reflecting the effect of experimental resolution. However, the presence of $\sim 8\%$ Sr on the surface is at least approximately correct, indicating a partial 'cancellation of errors' /1/.

SCATTERING ANGLE = 165.8 , INC.ANGLE = 15.8 AND EXIT-ANGLE = 21.1 DEGREES
 INCIDENT ENERGY = 2888. KEV, 6.391 KEV/CHANNEL, AND ENERGY = 41.172 IN CHANNEL #
 STOP EVALUATION WHEN EBEAM< 1888. KEV, OR WHEN CHANNELS BELOW CH. 181 ARE REQUESTED
 1 SPECTRA ARE EVALUATED WITH THIS INPUT
 PROJECTILE HAS MASS = 4.002, AND Z = 2
 ENERGY-SCALING FACTOR 1.000

TARGET-ELEMENTS

NAME	MASS	Z	COEFFICIENTS				
S	32.068	16	8.1482D+81	8.6791D+88	8.5898D+82	8.3528D+81	8.3211D+81
EU	152.088	63	8.1422D+82	8.3638D+88	8.2284D+83	8.7824D+81	8.1816D+81
SR	87.638	38	8.7126D+81	8.4884D+88	8.1193D+83	8.5784D+81	8.2454D+81

c. Still another experimental spectrum was obtained using 2 MeV ${}^4\text{He}^+$ -ions and $\theta = 165^\circ$. This time the depthresolution was improved by tilting the target an angle $\alpha = 60^\circ$ perpendicular to the scattering plane (Fig. 10). Thus the detectorangle $\beta \simeq 61.1^\circ$.

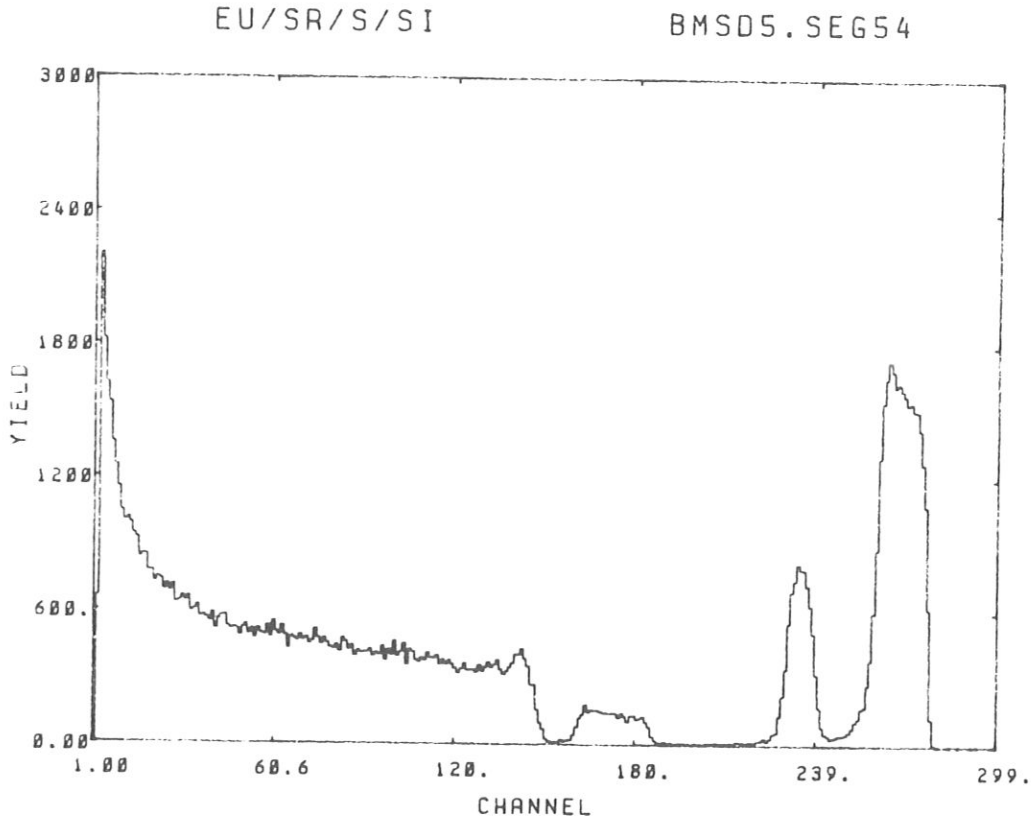


Fig. 10: RBS-spectrum for 2 MeV ${}^4\text{He}$ -ions scattered from 1080 Å EuS/
680 Å SrS/Si
 $\theta = 165^\circ$, $\alpha = 60^\circ$, $\beta = 61.1^\circ$.

Unfortunately the tilting made the small Sr-peak from the surface (see Figs. 8 and 9) disappear in the 'tail' of the Eu-peak, so we may now not correctly evaluate the surface layer from this spectrum. Instead we read in the results from the previous run (residing on segment PRB: B.EUS55,

(see above), and only evaluate the present spectrum for depths larger than $1.14 \cdot 10^{17}$ atoms/cm². We thus remember to link the segment

PRB: B.EU55 to the data in the inputstream (see example 2, sect.6.2), and define a new outputsegment PRB: B.EU355.

We are still considering quite shallow depths from which a Si-signal would be superposed on the S-signal (see above). We therefore still only look for the three targetelements S, Eu and Sr up to such depths, from which the S-signal falls in channels below 166.

The necessary input was:

```

165.#      6.#      61.1
2000.#    6.39#9  +41.172
1000.#    166     # 2 1
3
1      299
4.0016   2      1.#
32.06    16     S
1.402    E+# 6.791 EU E-1 5.898 E+1 3.528 E+# 3.211 E+#
152.0    E+1 3.63  EU E-1 2.284 E+2 7.024 E+# 1.016 E+#
1.4.12   38     S#
97.63    E+# 4.804 E-1 1.193 E+2 5.784 E+# 2.454 E+#
7.125

```

```

299      1      299      #      2206      #      #      1
AMOS-FI-SG: BMSD5.SEG54      EXPERIMENT: EU/SR/S/SI
NAME.....: BOE/SCH      DATE/TIME.: 27: 8:02 / 10:45:55
IMPL.IONS.:      IMPL.ENERG:
IMPL.FLNCE:      ANALYSIS...: RBS
ANAL.IONS.: 4HE      ALPHA.....: 6#
ANAL.DOSE.: 2#E-6 C      ANAL.ENERG: 2 MEV
THETA.....: 165 DEG      MATERIAL...: EU-S/SR-S/SI
TARGETPOS.: 39 MM      LOGBOOK...: RBS VI/175
NOTE1.....: H.V.GAIN=256X      NOTE2.....: 1000 CH/1# V
#      #      #      #      #      #      #      #      #      #
1000 1014 990 1820 1620 1533 1356 1251 1151 1045
730 750 739 941 921 836 851 851 775 775
643 665 596 692 719 687 717 636 643 663
518 565 577 687 624 573 579 568 552 592
538 494 519 476 520 497 493 516 488 526
506 492 533 490 433 486 475 465 492 468
478 453 465 517 476 450 478 454 435 429
440 418 478 460 426 446 399 424 413 415
415 430 397 414 402 443 379 427 404 466
399 416 453 359 429 415 380 372 389 379
414 390 387 400 362 381 360 380 362 342
323 343 367 336 334 339 326 359 329 351
372 349 361 382 338 316 333 351 370 409
400 434 388 354 270 271 159 100 73 28
10 13 14 14 25 16 23 26 47 05
123 140 100 147 157 155 156 151 146 145
143 144 145 125 146 129 105 134 134 117
121 120 102 02 39 19 11 7 10 5
11 7 7 0 10 9 7 9 0 10
6 5 0 10 11 11 16 15 12 22
11 7 17 16 14 12 135 226 348 554
26 34 23 36 55 62 630 505 321 173
694 745 819 794 792 42 47 47 53 65
85 53 46 168 176 275 388 602 886 1301
83 112 126 32 39 42 47 47 53 65
1550 1657 1736 1691 1619 1634 1601 1576 1540 1545
1510 1507 1425 1272 1078 617 125 9 2 0
# # # # # # # # # # # # # # # # #
# # # # # # # # # # # # # # # # #

```

```

299      2001      2299      17      2102      #      #      #      1
AMOS-FI-SG: BMSD5.SEG55      EXPERIMENT: EU/SR/S/SI
NAME.....: BOE/SCH      DATE/TIME.: 27: 8:02 / 11: 9:19
IMPL.IONS.:      IMPL.ENERG:
IMPL.FLNCE:      ANALYSIS...: RBS
ANAL.IONS.: 4HE      ALPHA.....: 15 DEG
ANAL.DOSE.: 2#E-6 C      ANAL.ENERG: 2 MEV
THETA.....: 165 DEG      MATERIAL...: EU-S/SR-S/SI
TARGETPOS.: 39 MM      LOGBOOK...: PES VI/175
NOTE1.....: H.V.GAIN=256X      NOTE2.....: 1000 CH/1# V
#      #      #      #      #      #      #      #      #      #
#      S      EU      SR
#      #      #      #      #      #      #      #      #      #
# 0.3770+17 # 0.413 # 0.510 # 0.076 # 0.0 # 0.0 # 0.0
# 0.7560+17 # 0.434 # 0.535 # 0.031 # 0.0 # 0.0 # 0.0
# 0.1140+18 # 0.459 # 0.517 # 0.023 # 0.0 # 0.0 # 0.0
# # # # # # # # # # # # # # # # #

```


d. Finally we have now evaluated the spectrum to such depths, that we may soon expect the presence of Si (see above). We therefore look for all 4 elements (S, Eu, Sr, and Si) at depths larger than $3.85 \cdot 10^{17}$ atoms/cm². The targetcomposition for depths up to $3.85 \cdot 10^{17}$ atoms/cm² is read in from the segment PRB: B.EU355, see above.

The rest of the input remains the same, except that we now evaluate the spectrum up to such depths, from which the Si-signal falls in channels below 130:

```

165.#      6#.#      61.1
1000.#     6.39#9   +41.172
1000.#     13#     # 2 i
4
1      299
4.#16     2      1.#
32.#6     16     S
1.4#2     E+# 6.791 E-1 5.890 E+1 3.520 E+# 3.211 E+#
152.#     63     EU
1.422     E+1 3.63  E-1 2.284 E+2 7.#24 E+# 1.#16 E+#
87.63     38     SR
7.126     E+# 4.8#4 E-1 1.193 E+2 5.784 E+# 2.454 E+#
28.#6     14     SI
2.1       E+# 6.5  E-1 4.934 E+1 1.788 E+# 4.133 E+#

```

```

299      1      299      #      22#6      #      #      1
AMOS-FI-SG: BMSD5.SEG54      EXPERIMENT: EU/SR/S/SI
NAME: BOE/SCHE      DATE/TIME.: 27: 8:02 / 10:45:55
IMPL. IONS.:      IMPL.ENERG:
IMPL.FLNCE:      ANALYSIS...: RBS
ANAL. IONS.: 4HE      ALPHA.....: 6#
ANAL. DOSE.: 2#E-6 C      ANAL.ENERG: 2 MEV
THETA.....: 165 DEG      MATERIAL...: EU-S/SR-S/SI
TARGETPOS.: 39 MM      LOGBOOK...: RBS VI/175
NOTE1.....: H.V.GAIN=256X      NOTE2.....: 100# CH/1# V
#      #      #      #      #      #      #      #      #      #
100#4 1014 990 182# 162# 1533 1356 1251 1151 1045
73# 75# 739 941 921 836 851 851 775 775
643 665 596 607 719 687 717 636 643 663
518 565 577 581 624 573 579 568 552 592
538 494 519 476 527 518 522 516 488 526
506 492 533 490 433 486 475 465 492 468
478 453 465 517 476 45# 478 454 435 429
448 418 478 46# 426 446 399 424 413 415
415 43# 397 414 4#2 443 379 427 4#4 466
399 416 453 359 429 415 38# 372 389 379
414 34# 387 4#0 362 381 36# 38# 362 342
323 343 367 336 334 339 326 359 329 351
372 349 361 382 338 316 333 351 37# 4#9
4#8 434 388 354 27# 271 159 1#0 73 28
18 13 14 14 25 16 23 26 47 85
123 14# 1#0 147 157 156 151 146 145
143 144 145 125 146 129 1#5 134 134 117
121 12# 1#2 82 39 9 7 3 1# 8
11 5 7 1# 1# 11 7 9 1# 1#
6 7 17 16 14 12 16 16 12 22
11 34 23 36 55 62 136 226 348 554
2# 745 819 794 792 721 63# 5#5 321 173
85 53 46 32 39 42 47 47 53 65
83 112 126 168 176 275 388 6#2 886 13#1
155# 1657 1736 1691 1619 1634 16#1 1576 154# 1545
151# 15#7 1425 1272 1#78 617 125 9 2 #
# 1 1 # # # # # # # # # #
# # # # # # # # # # # # # # # #

```

```

299      1      299      #      22#6      #      #      #      1
AMOS-FI-SG: BMSD5.SEG54      EXPERIMENT: EU/SR/S/SI
NAME: BOE/SCHE      DATE/TIME.: 27: 8:02 / 10:45:55
IMPL. IONS.:      IMPL.ENERG:
IMPL.FLNCE:      ANALYSIS...: RBS
ANAL. IONS.: 4HE      ALPHA.....: 6#
ANAL. DOSE.: 2#E-6 C      ANAL.ENERG: 2 MEV
THETA.....: 165 DEG      MATERIAL...: EU-S/SR-S/SI
TARGETPOS.: 39 MM      LOGBOOK...: RBS VI/175
NOTE1.....: H.V.GAIN=256X      NOTE2.....: 100# CH/1# V
#      #      #      #      #      #      #      #      #      #
#      S      EU      SR      #      #      #      #      #
#.#377D+17 #.413 #.51# #.#76 #.# #.# #.# #.#
#.#756D+17 #.434 #.535 #.#31 #.# #.# #.# #.#
#.#114D+18 #.459 #.517 #.#23 #.# #.# #.# #.#
#.#152D+18 #.491 #.492 #.#17 #.# #.# #.# #.#
#.#173D+18 #.5#0 #.462 #.#37 #.# #.# #.# #.#
#.#193D+18 #.5#2 #.464 #.#34 #.# #.# #.# #.#
#.#214D+18 #.53# #.434 #.#29 #.# #.# #.# #.#
#.#235D+18 #.53# #.43# #.#25 #.# #.# #.# #.#
#.#256D+18 #.519 #.451 #.#3# #.# #.# #.# #.#
#.#277D+18 #.534 #.431 #.#35 #.# #.# #.# #.#
#.#298D+18 #.536 #.412 #.#52 #.# #.# #.# #.#
#.#319D+18 #.53# #.369 #.1#2 #.# #.# #.# #.#
#.#341D+18 #.527 #.284 #.189 #.# #.# #.# #.#
#.#363D+18 #.518 #.185 #.297 #.# #.# #.# #.#
#.#385D+18 #.513 #.117 #.37# #.# #.# #.# #.#
#.#385D+18 #.5#9 #.#74 #.417 #.# #.# #.# #.#

```

The output this time includes two warnings: The spectrum has now been evaluated to such depths from which the S-signal may now be superposed on Si-signals from shallower depths, and the Eu-signal may be superposed on the Sr-signal.

Although this has partly been avoided by evaluating the surface layer from another spectrum (see b. above), and slightly larger depths with the independent knowledge that Si is only found even deeper (see c. above), the evaluation of S-signals from channel 153 and below is not possible (these channels were already evaluated as Si-signals). Correspondingly, signals from channels 223-243 clearly originate from scattering on Sr, and thus may not be evaluated as Eu-signals.

In conclusion we may only believe in the derived targetcomposition up to a depth of $\sim 7.24 \cdot 10^{17}$ atoms/cm². Figures 11a-11d show the results.

3 consecutive runs like these of course require relatively long CPU-time, in the present case a total of ~ 8 seconds.

SCATTERING ANGLE = 165.8 , INC.ANGLE = 68.8 AND EXIT-ANGLE = 61.1 DEGREES
INCIDENT ENERGY = 2888. KEV, 6.391 KEV/CHANNEL, AND ENERGY = 41.172 IN CHANNEL #
STOP EVALUATION WHEN EBEAM< 1888. KEV, OR WHEN CHANNELS BELOW CH. 138 ARE REQUESTED
1 SPECTRA ARE EVALUATED WITH THIS INPUT
PROJECTILE HAS MASS = 4.002, AND Z = 2
ENERGY-SCALING FACTOR 1.000

TARGET-ELEMENTS

NAME	MASS	Z	COEFFICIENTS					
S	32.068	16	0.1482D+01	0.6791D+00	0.5898D+02	0.3528D+01	0.3211D+01	
EU	152.000	63	0.1422D+02	0.3630D+00	0.2284D+03	0.7824D+01	0.1816D+01	
SR	87.638	38	0.7126D+01	0.4884D+00	0.1193D+03	0.5784D+01	0.2454D+01	
SI	28.086	14	0.2180D+01	0.6580D+00	0.4934D+02	0.1788D+01	0.4133D+01	

SPECTRUM NO. 1

299	1	299	2286	8	8	1
AMOS-FI-SG:	BMSD5	SEG54	EXPERIMENT:	EU/SR/S/SI		
NAME.....:	BOE/SCH		DATE/TIME..:	27: 8:82 / 18:45:55		
IMPL.IONS..:			IMPL.ENERG:			
IMPL.FLNCE:			ANALYSIS..:	RBS		
ANAL.IONS..:	4HE		ALPHA.....:	68		
ANAL.DOSE..:	28E-6 C		ANAL.ENERG:	2 MEV		
THETA.....:	165 DEG		MATERIAL...:	EU-S/SR-S/SI		
TARGETPOS.:	39 MM		LOGBOOK...:	RBS VI/175		
NOTE1.....:	H.V.GAIN=256X		NOTE2.....:	1888 CH/18 V		

Ø.	663.	2286.	182Ø.	162Ø.	1533.	1356.	1251.	1151.	1Ø45.
1ØØ4.	1Ø14.	99Ø.	941.	921.	836.	851.	851.	775.	775.
73Ø.	75Ø.	73Ø.	692.	719.	687.	717.	636.	643.	663.
643.	665.	596.	6Ø7.	624.	573.	579.	568.	552.	592.
518.	565.	577.	5Ø1.	527.	518.	522.	516.	488.	526.
538.	494.	519.	476.	5ØØ.	497.	493.	533.	481.	554.
5Ø6.	492.	533.	49Ø.	433.	486.	475.	465.	492.	468.
478.	453.	465.	517.	476.	458.	478.	454.	435.	429.
448.	418.	478.	46Ø.	426.	446.	399.	424.	413.	415.
415.	43Ø.	397.	414.	4Ø2.	443.	379.	427.	4Ø4.	466.
399.	416.	453.	359.	429.	415.	38Ø.	372.	389.	379.
414.	39Ø.	387.	4ØØ.	362.	381.	366.	38Ø.	362.	342.
323.	343.	367.	336.	334.	339.	326.	359.	329.	351.
372.	349.	361.	382.	338.	316.	333.	351.	37Ø.	4Ø9.
4Ø8.	434.	388.	354.	27Ø.	271.	159.	1ØØ.	73.	28.
18.	13.	14.	14.	25.	16.	23.	26.	47.	85.
123.	14Ø.	18Ø.	147.	157.	155.	156.	151.	146.	145.
143.	144.	145.	125.	146.	129.	1Ø5.	134.	134.	117.
121.	128.	1Ø2.	82.	39.	19.	11.	7.	17.	8.
11.	7.	7.	8.	1Ø.	9.	7.	3.	1Ø.	5.
6.	5.	8.	1Ø.	1Ø.	11.	7.	9.	8.	1Ø.
11.	7.	17.	16.	14.	12.	16.	15.	12.	22.
26.	34.	23.	36.	55.	62.	136.	226.	348.	554.
694.	745.	819.	794.	792.	721.	63Ø.	5Ø5.	321.	173.
85.	53.	46.	32.	39.	42.	47.	47.	53.	65.
83.	112.	126.	168.	176.	275.	388.	6Ø2.	886.	13Ø1.
155Ø.	1657.	1736.	1691.	1619.	1634.	16Ø1.	1576.	154Ø.	1545.
151Ø.	15Ø7.	1425.	1272.	1Ø78.	617.	125.	9.	2.	Ø.
Ø.	1.	Ø.	Ø.	Ø.	Ø.	Ø.	Ø.	Ø.	1.
Ø.	1.	Ø.	Ø.	Ø.	Ø.	Ø.	Ø.	1.	Ø.

DEPTH ATOMS/CM2	STOICHIOMETRIC COEFFICIENTS, UNCERTAINTIES				CHANNELS				Q
	S	EU	SR	SI	S	EU	SR	SI	
Ø.Ø	.413	.51Ø	.Ø76	.Ø	.Ø	.Ø	.Ø	.Ø	
Ø.377D+17	.434	.535	.Ø31	.Ø	.Ø	.Ø	.Ø	.Ø	
Ø.756D+17	.459	.517	.Ø23	.Ø	.Ø	.Ø	.Ø	.Ø	
Ø.114D+18	.491	.492	.Ø17	.Ø	.Ø	.Ø	.Ø	.Ø	
Ø.152D+18	.5ØØ	.462	.Ø37	.Ø	.Ø	.Ø	.Ø	.Ø	
Ø.173D+18	.5Ø2	.464	.Ø34	.Ø	.Ø	.Ø	.Ø	.Ø	
Ø.193D+18	.538	.434	.Ø29	.Ø	.Ø	.Ø	.Ø	.Ø	
Ø.214D+18	.538	.438	.Ø25	.Ø	.Ø	.Ø	.Ø	.Ø	
Ø.235D+18	.519	.451	.Ø3Ø	.Ø	.Ø	.Ø	.Ø	.Ø	
Ø.256D+18	.534	.431	.Ø35	.Ø	.Ø	.Ø	.Ø	.Ø	
Ø.277D+18	.536	.412	.Ø52	.Ø	.Ø	.Ø	.Ø	.Ø	
Ø.298D+18	.53Ø	.369	.1Ø2	.Ø	.Ø	.Ø	.Ø	.Ø	
Ø.319D+18	.527	.284	.189	.Ø	.Ø	.Ø	.Ø	.Ø	
Ø.341D+18	.518	.185	.297	.Ø	.Ø	.Ø	.Ø	.Ø	
Ø.363D+18	.513	.117	.37Ø	.Ø	.Ø	.Ø	.Ø	.Ø	
Ø.385D+18	.5Ø9	.Ø74	.417	.Ø	.Ø	.Ø	.Ø	.Ø	
Ø.4Ø7D+18	.47Ø, .Ø4	.Ø47, .ØØØ	.427, .Ø2	.Ø55, .Ø1	.Ø	.Ø	.Ø	.Ø	166. 256. 235. 153. Ø. Ø. Ø.194D+11
Ø.431D+18	.476, .Ø4	.Ø35, .ØØØ	.437, .Ø2	.Ø52, .Ø1	.Ø	.Ø	.Ø	.Ø	165. 254. 234. 152. Ø. Ø. Ø.193D+11
Ø.456D+18	.452, .Ø4	.Ø29, .ØØØ	.449, .Ø2	.Ø7Ø, .Ø2	.Ø	.Ø	.Ø	.Ø	164. 253. 233. 151. Ø. Ø. Ø.193D+11
Ø.48ØD+18	.497, .Ø4	.Ø22, .ØØØ	.38Ø, .Ø1	.1Ø1, .Ø2	.Ø	.Ø	.Ø	.Ø	163. 252. 232. 15Ø. Ø. Ø. Ø.199D+11
Ø.5Ø6D+18	.381, .Ø3	.Ø16, .ØØØ	.342, .Ø1	.26Ø, .Ø3	.Ø	.Ø	.Ø	.Ø	162. 251. 231. 149. Ø. Ø. Ø.195D+11
Ø.532D+18	.339, .Ø3	.Ø13, .ØØØ	.273, .Ø1	.376, .Ø4	.Ø	.Ø	.Ø	.Ø	161. 25Ø. 23Ø. 148. Ø. Ø. Ø.178D+11
Ø.56ØD+18	.224, .Ø3	.Ø1Ø, .ØØØ	.165, .Ø1	.6ØØ, .Ø5	.Ø	.Ø	.Ø	.Ø	16Ø. 249. 229. 147. Ø. Ø. Ø.165D+11
Ø.59ØD+18	.Ø98, .Ø1	.ØØ7, .ØØØ	.Ø82, .Ø1	.813, .Ø5	.Ø	.Ø	.Ø	.Ø	159. 248. 228. 146. Ø. Ø. Ø.191D+11
Ø.623D+18	.Ø62, .Ø1	.ØØ8, .ØØØ	.Ø48, .ØØØ	.883, .Ø5	.Ø	.Ø	.Ø	.Ø	158. 247. 227. 145. Ø. Ø. Ø.173D+11
Ø.656D+18	.Ø42, .Ø1	.ØØ5, .ØØØ	.Ø21, .ØØØ	.931, .Ø5	.Ø	.Ø	.Ø	.Ø	157. 246. 226. 144. Ø. Ø. Ø.2Ø7D+11
Ø.69ØD+18	.Ø34, .Ø1	.ØØ4, .ØØØ	.Ø15, .ØØØ	.946, .Ø5	.Ø	.Ø	.Ø	.Ø	156. 245. 224. 143. Ø. Ø. Ø.222D+11
Ø.724D+18	.Ø36, .Ø1	.ØØ4, .ØØØ	.ØØ9, .ØØØ	.951, .Ø5	.Ø	.Ø	.Ø	.Ø	155. 244. 223. 142. Ø. Ø. Ø.241D+11
Ø.758D+18	.Ø25, .Ø1	.ØØ6, .ØØØ	.Ø1Ø, .ØØØ	.959, .Ø5	.Ø	.Ø	.Ø	.Ø	154. 242. 222. 141. Ø. Ø. Ø.227D+11
Ø.793D+18	.Ø25, .Ø1	.ØØ9, .ØØØ	.ØØ9, .ØØØ	.957, .Ø5	.Ø	.Ø	.Ø	.Ø	153. 241. 221. 14Ø. Ø. Ø. Ø.224D+11
Ø.827D+18	.Ø3Ø, .Ø1	.Ø19, .ØØØ	.ØØØ, .ØØØ	.943, .Ø5	.Ø	.Ø	.Ø	.Ø	152. 24Ø. 22Ø. 139. Ø. Ø. Ø.2Ø9D+11
Ø.861D+18	.Ø46, .Ø1	.Ø39, .ØØØ	.ØØ5, .ØØØ	.91Ø, .Ø5	.Ø	.Ø	.Ø	.Ø	151. 239. 219. 138. Ø. Ø. Ø.2Ø9D+11
Ø.894D+18	.Ø99, .Ø1	.Ø64, .ØØØ	.ØØ5, .ØØØ	.832, .Ø5	.Ø	.Ø	.Ø	.Ø	149. 238. 218. 137. Ø. Ø. Ø.222D+11
Ø.926D+18	.158, .Ø2	.Ø76, .ØØØ	.ØØ5, .ØØØ	.76Ø, .Ø4	.Ø	.Ø	.Ø	.Ø	148. 237. 217. 136. Ø. Ø. Ø.243D+11
Ø.957D+18	.2Ø9, .Ø2	.Ø75, .ØØØ	.ØØ3, .ØØØ	.712, .Ø4	.Ø	.Ø	.Ø	.Ø	147. 236. 216. 135. Ø. Ø. Ø.2Ø3D+11
Ø.989D+18	.298, .Ø2	.Ø68, .ØØØ	.ØØ3, .ØØØ	.631, .Ø3	.Ø	.Ø	.Ø	.Ø	146. 235. 215. 134. Ø. Ø. Ø.338D+11
Ø.1Ø2D+19	.341, .Ø2	.Ø68, .ØØØ	.ØØ4, .ØØØ	.587, .Ø3	.Ø	.Ø	.Ø	.Ø	145. 234. 214. 133. Ø. Ø. Ø.346D+11
Ø.1Ø5D+19	.388, .Ø2	.Ø61, .ØØØ	.ØØ3, .ØØØ	.549, .Ø3	.Ø	.Ø	.Ø	.Ø	144. 233. 213. 132. Ø. Ø. Ø.371D+11
Ø.1Ø8D+19	.422, .Ø2	.Ø53, .ØØØ	.ØØ2, .ØØØ	.523, .Ø3	.Ø	.Ø	.Ø	.Ø	143. 231. 211. 131. Ø. Ø. Ø.388D+11

NGI S-SIGNAL EVALUATED SO DEEP THAT IT MAY RUN INTO SI-SIGNAL!!

NGI EU-SIGNAL EVALUATED SO DEEP THAT IT MAY RUN INTO SR-SIGNAL!!

EUS/SRS/SI

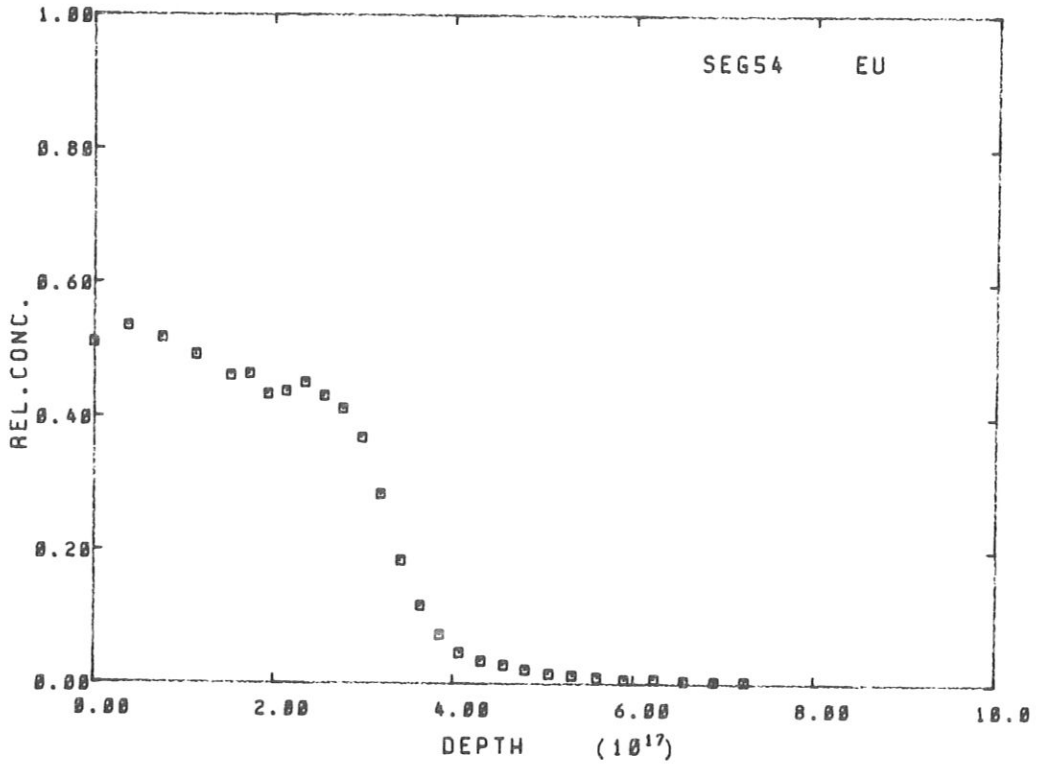


Fig. 11a: Plot of SQUEAKIE - output resulting from evaluation of the spectra in Figs. 9 and 10. Original SQUEAKIE-version. Relative concentration vs. depth of Eu.

EUS/SRS/SI

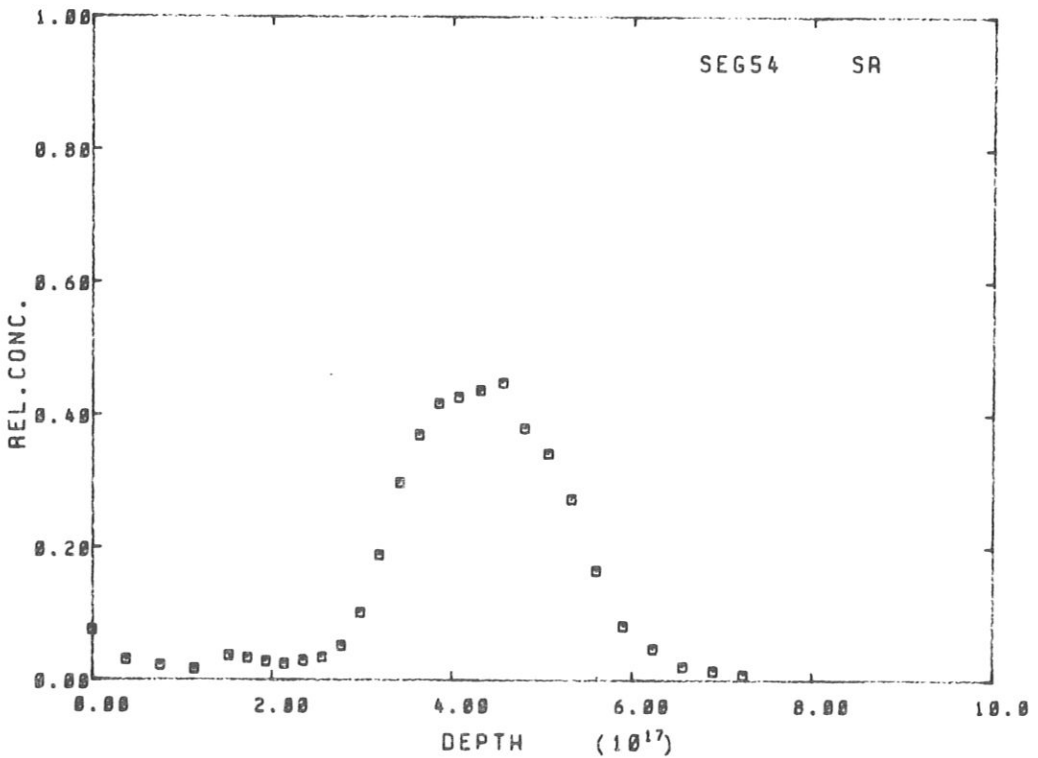


Fig. 11b: Relative concentration vs. depth of Sr

EUS/SRS/SI

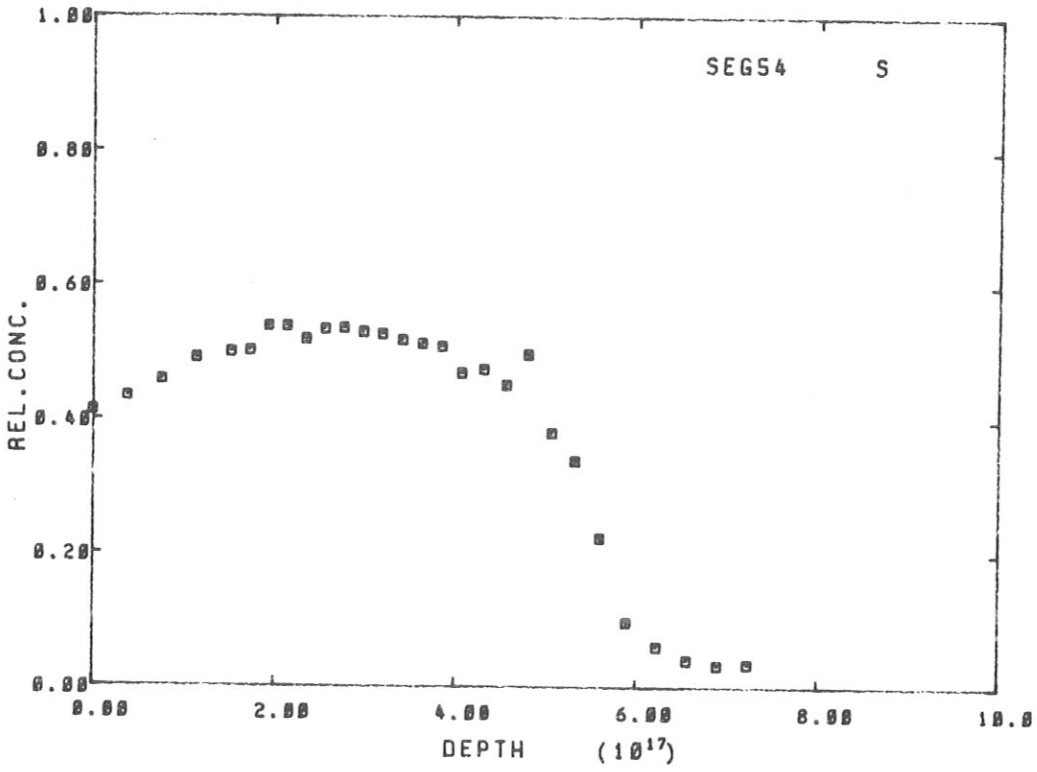


Fig. 11c: Relative concentration vs. depth of S.

EUS/SRS/SI

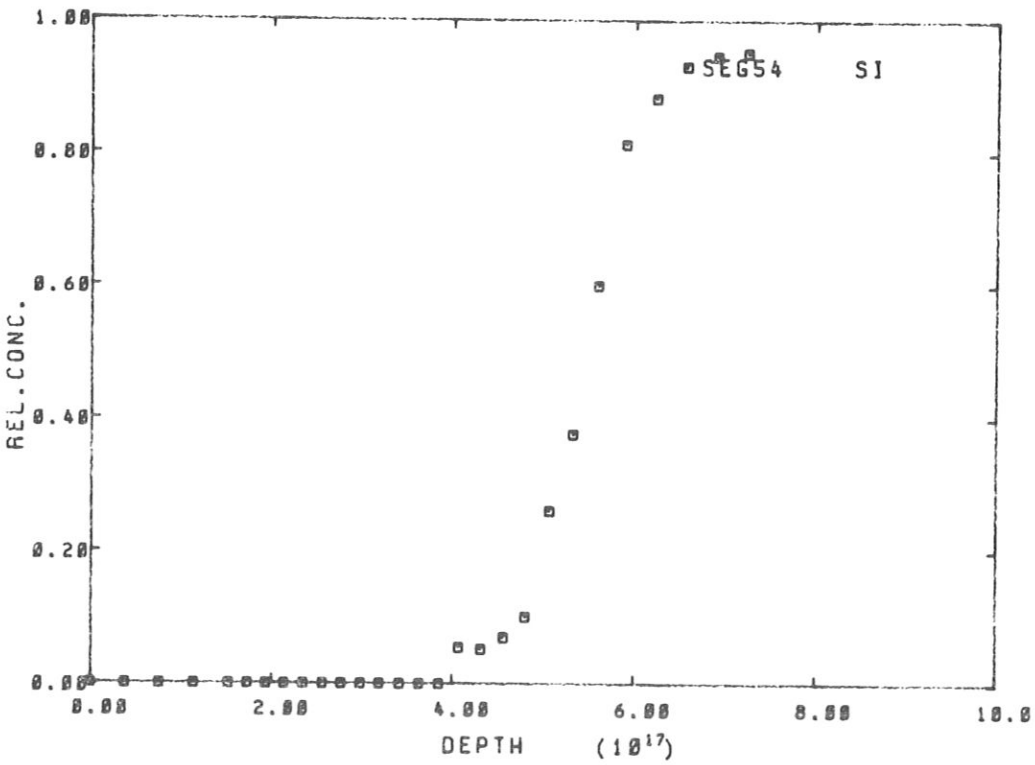


Fig. 11d: Relative concentration vs. depth of Si.

3. The final example demonstrates the use of the alternative version of the program:

The spectrum is the same as used in the first example, but this time we include all three target elements (Eu, S, and Si) in the evaluation. We can therefore also go to much larger depths, but we have to assume that no Eu- or S-signals are superposed on the Si-signal. After a study of the spectrum we then specify the Eu-signals to be confined to the interval between $ch1(Eu) = 199$ and $ch2(Eu) = 230$. Correspondingly we let $ch1(S) = 128$ and $ch2(S) = 161$, and assume that all Si-signals fall in or below channel number 127. The evaluation in the present case is terminated when the Si-signal falls below channel 90.

The necessary input was of course the spectrum (as above), preceded by the set of parameters:

```

178.8      68.8      68.5
2888.      7.6838  +55.8888
              1 2 8
3
1          289
4.8816    2      1.8
32.886    16     S
1.482     E+8 6.791 E-1 5.898      161      E+8 3.211      E+8
152.8     63    EU  E-1 2.284      238      E+8 1.816      E+8
1.422     E+1 3.63  E-1 2.284      127      E+8 4.133      E+8
28.886    14    SI  98
2.1       E+8 6.5   E-1 4.934      E+1 1.788
    
```

The output is on the same form as before, except that also the element markers are given.

```

SCATTERING ANGLE = 178.8 , INC.ANGLE = 68.8 AND EXIT-ANGLE = 68.5 DEGREES
INCIDENT ENERGY = 2888. KEV, 7.683 KEV/CHANNEL, AND ENERGY = 55.8888 IN CHANNEL 8
1 SPECTRA ARE EVALUATED WITH THIS INPUT
PROJECTILE HAS MASS = 4.882, AND Z = 2
ENERGY-SCALING FACTOR 1.888
    
```

TARGET-ELEMENTS

NAME	MASS	Z	INTERVAL	COEFFICIENTS				
S	32.886	16	128 161	8.1482D+81	8.6791D+88	8.5898D+82	8.3528D+81	8.321
EU	152.888	63	199 238	8.1422D+82	8.3638D+88	8.2284D+83	8.7874D+81	8.181
SI	28.886	14	98 127	8.2188D+81	8.6588D+88	8.4934D+82	8.1788D+81	8.413

In the tabulation of the stoichiometric coefficients vs. depth we see that the choice of these markers excludes the presence of S at depths larger than $7 \cdot 10^{17}$ atoms/cm², of Eu at depths larger than $8 \cdot 10^{17}$ atoms/cm², and of Si at depths smaller than $\sim 3.4 \cdot 10^{17}$ atoms/cm². We have no direct check of the validity of this, and correspondingly the table is followed by a warning.

Because of the element markers the calculated coefficient for Si must equal one at depths larger than $8 \cdot 10^{17}$ atoms/cm². On the printed output this appears as **** because of the corresponding FORMAT-statement (line no. 35500 in "STEP"), but on the output-segment it is written correctly. Figure 12 shows plots from this segment.

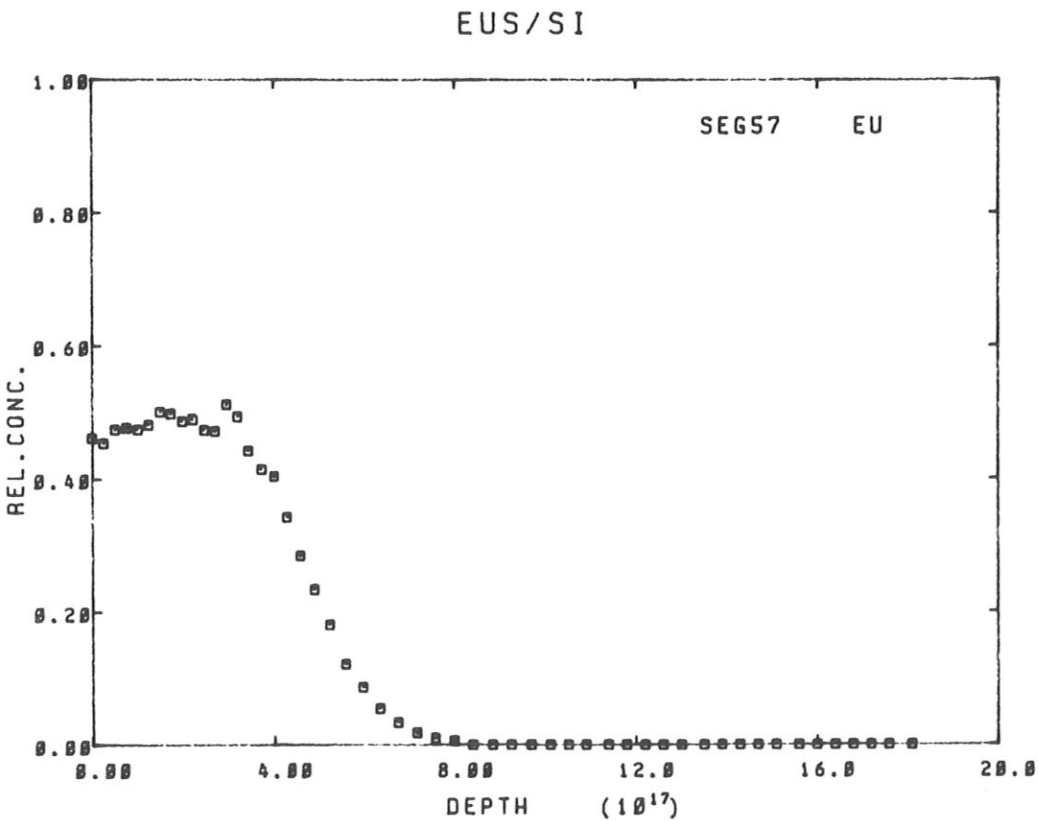


Fig. 12a: Plot of SQUEAKIE-output resulting from evaluation of spectrum in Fig.6. Alternative SQUEAKIE-version. Relative concentration vs. depth of Eu.

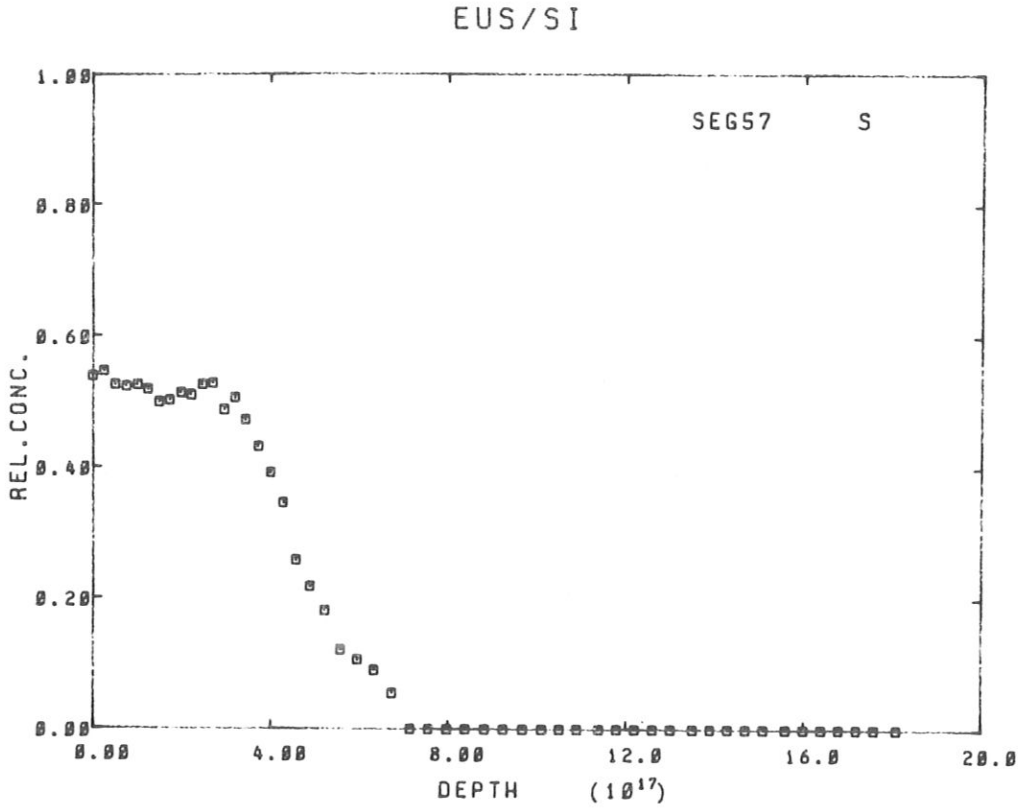


Fig. 12b: Relative concentration vs. depth of S.

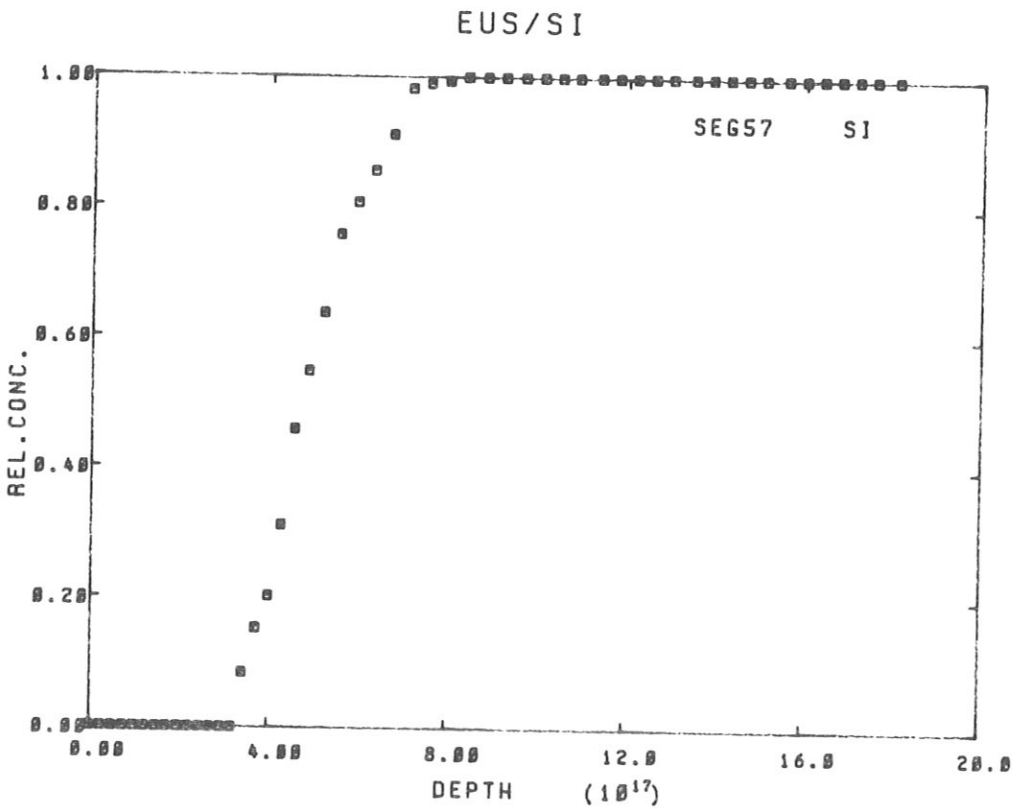


Fig. 12c: Relative concentration vs. depth of Si.

At those depths, where only one element is present, no inverse iteration and improved estimate of Q (Sect. 4.4) was performed. Instead the value Q was simply calculated from the experimental signal, i.e. from eqs. 2.1-2.4. It is seen that Q remains approximately constant up to more than $1.75 \cdot 10^{18}$ atoms/cm², and in good agreement with the 'iterated' values from shallower depths. S- or Eu-signals superposed on the Si-signal would result in larger Q -values than estimated from the inverse iteration, so we may conclude that such signals contribute less than $\sim 5\%$ of the evaluated Si-signal.

Using an average value of $3.8 \cdot 10^{10}$ for $N_{\text{prim}} \Delta\Omega$ we may again estimate the integrated contents from the scattering yields: The values $2.5 \cdot 10^{17}$ S-atoms/cm² and $2.35 \cdot 10^{17}$ Eu-atoms/cm² are in very good agreement with the results determined from the stoichiometry vs. depth.

6.6 Warnings

- i) The present program should not be used by anyone who is not familiar at least with Sect. 2.1 and Chapter 3. Furthermore a study of Sect. 6.5 is recommended.
- ii) The program may not always distinguish between signals from a light element near the surface or a heavy element at larger depth. After each run one should therefore check the printed output vs. the spectrum in order to ascertain that the various channels have been ascribed to the appropriate elements.

- iii) If some target element (e.g. the substrate under a film) is not taken into account, one may at some depth evaluate only noise level signals (background). If none of the elemental signals are significant the resulting faulty stoichiometry may not be obvious. Besides from an inspection of the channel numbers (see above) also a study of the listed eigenvalues Q will reveal this: When Q falls by an order of magnitude or more, something is wrong.

- iv) One should never accept negative stoichiometric coefficients, even if they are very small. The appearance of a negative coefficient indicates that the wrong eigenvector was found; i.e. the stoichiometry at this depth is probably very wrong. Such an error influences all results at larger depths, although perhaps weakly.
This error was never encountered yet, except when deliberately provoked.

- v) The most common input error has been the specification of the wrong number of channels in the spectrum. This usually causes a program interrupt (certainly if the results of previous spectra are included).

- vi) Another common input error is the specification of target element data for fewer or more target elements than given in Record # 4 (Sect. 6.3). This is also a terminal error.

7. TESTS

Two quite different types of tests are described below. One type is designed to ensure that the program functions correctly, i.e. that there are no programming errors. This of course is relevant when implementing the program on another computer, and may even partly be applied to other versions of the program.

The second type of tests has been performed by the authors in order to investigate precision, stability, speed etc. of the program. This is thus also partly a documentation of the applicability of the approach, as already described in Ref. 1.

7.1 Test of programming

Implementing the listed program on another computer, one is bound to experience malfunctions due to language modifications, available libraries, simple typing errors, etc. Most of these are easily identified, but errors may still remain which call for a closer examination. Below is listed a simple test-program, which may help to localize errors in the functions/subroutines.

The MAIN program as well as the subroutine STEP are best tested by repeating one of the examples listed in Section 6.5 (preferably examples 1 or 3).

```

C      *****
C      PROGRAM TEST
C      *****
C      TEST OF SUBROUTINES
C
      IMPLICIT REAL*8(A-H,O-S),INTEGER(I-N)
      COMMON/CALIB/THETA,ALFA,BETA,OFFS,DE1
      COMMON/COLL/A1,A(6),IZ1,IZ(6)
      DIMENSION AM(6,6),S(6),CF(5)
      N=4
      S(1)=4.8
      S(2)=2.8
      S(3)=2.5
      S(4)=3.8
      AM(1,1)=1.
      AM(1,2)=1.
      AM(1,3)=1.
      AM(1,4)=8.25
      AM(2,1)=2.
      AM(2,2)=8.5
      AM(2,3)=1.
      AM(2,4)=2.
      AM(3,1)=1.
      AM(3,2)=1.
      AM(3,3)=2.
      AM(3,4)=3.
      AM(4,1)=4.
      AM(4,2)=1.5
      AM(4,3)=1.
      AM(4,4)=4.5
      QB=6.8
      CALL ITER(AM,S,QB,N)
      WRITE(6,188)(S(I),I=1,N),QB
188  FORMAT(2X,7E12.3)
      EN=1.803
      IT=1
      A(IT)=152
      IZ(IT)=63
      THETA=165*3.14159/188.
      A1=4.
      IZ1=2
      CR=CRSEC(EN,IT)
      WRITE(6,189)CR
189  FORMAT(3X,'CROSS SECTION =',E12.4,' CM2',/)
      XK1=XK(IT)
      WRITE(6,182)XK1
182  FORMAT(3X,'KINEMATIC FACTOR = ',E12.4,/)
      CF(1)=8.1422D+82
      CF(2)=8.3638D+88
      CF(3)=8.2284D+83
      CF(4)=8.7824D+81
      CF(5)=8.1816D+81
      FE=1.8
      STP=STPA(CF,FE,EN)
      WRITE(6,183)STP
183  FORMAT(3X,'STOPPING POWER =',E12.4,' *18**(-15) EV*CM2/ATOM',/)
      STOP
      END

```

Submission of this program together with the subroutine ITER and the functions XK, CRSEC and STPA should provide you with the result of an inverse iteration, as well as with the scattering cross-section ($d\sigma/d\Omega$), the kinematic factor K, and the stopping power S for 1 MeV $^4\text{He}^+$ -ions incident on Eu and a scattering angle $\theta = 165^\circ$. The correct output is:

```

      8.258D+88  8.588D+88  8.749D+88  8.188D+81  8.788D+81
CROSS SECTION = 8.2114D-22 CM2
KINEMATIC FACTOR= 8.9817D+88
STOPPING POWER= 8.1296D+83 *18**(-15) EV*CM2/ATOM

```

Most difficult to find are errors in the subroutine ITER. If the output above shows a malfunction of ITER, or if the testprogram runs for longer than a few seconds (indicating a lack of convergence in ITER), you may therefore still need help to localize the error(s). In that case you simply run the testprogram again, but this time insert a few statements to print out various parameters at different stages in ITER:

Consider the listing of ITER in Sect. 5.7. Immediately before the statement labeled 300 the array AGEM should hold the values

-5	$7.452 \cdot 10^{28}$	$-1.636 \cdot 10^{78}$	$5.334 \cdot 10^{-21}$
2	-2.55	$1.987 \cdot 10^{28}$	$1.027 \cdot 10^{38}$
1	1.2	-2.892	$8.182 \cdot 10^{-79}$
4	0.575	1.057	0.876

If this is so, the error occurs in the iteration itself (below 300). During the first step of the iteration, the array S must contain (0.8, 0.7059, 1.195, -5.037) immediately after the statement labeled 200, and the array T should hold (0.7321, 2.452, 3.949, 5.037) after 210.

7.2 Test of program

- i. The power of the present program depends largely on the swift convergence of the inverse iteration at each depth step (see Sect. 3.2). Let us therefore first test this:

The eigenvector problem

$$\begin{pmatrix} 1. & 1. & 1. & 0.25 \\ 2. & 0.5 & 1. & 2. \\ 1. & 1. & 2. & 3. \\ 4. & 1.5 & 1. & 4.5 \end{pmatrix} \underline{s}_r = Q \underline{s}_r \quad (7.1)$$

has the solution $\underline{s}_r = (0.25, 0.5, 0.75, 1.)$ and the eigenvalue $Q = 7$. A very crude 'initial guess' is here $\underline{s}_{in} = (4, 2, 2.5, 3)$ and $Q_0 = 6$ (this was used as a test in the previous section).

Following the algorithm of Sect. 4.4, the iteration ran as indicated in the table below, leading to an excellent approximation $\underline{y}_k = (y_1, y_2, y_3, y_4)$ of \underline{s}_r in 3-4 steps:

Iterated vector	y_1	y_2	y_3	y_4	'Iterated' Q
\underline{y}_0	1.33	0.667	0.833	1.	6.0
\underline{y}_1	0.1453	0.4868	0.784	1.	6.199
\underline{y}_2	0.2667	0.5011	0.7354	1.	7.054
\underline{y}_3	0.2478	0.5002	0.754	1.	6.995
\underline{y}_4	0.2502	0.4999	0.7491	1.	7.000

Table 1

This is only a 'mathematical' test of the subroutine ITER (Sect. 5.6); the present parameters will probably never occur in a physically relevant situation. Unlike for experimental spectra /1/ we may not even be sure that Eq. 7.1 does not have more eigenvectors with only positive, real coordinates. Nevertheless, in spite of an unusually

bad 'initial guess' we see a very swift convergence of the iteration, adjusting 'concentrations' by up to a factor of 4, and the eigenvalue by 17 %. Actually, even with the guess $Q_0 = 4.0$ the iteration would converge to the same y_k within ~ 40 steps, at the expense of only ~ 0.07 seconds extra CPU-time.

- ii. Quite thorough tests of the program itself were already described in Ref. 1. Further tests have now been performed, showing the individual effects of isotopes, system resolution, energy straggling and counting statistics.

The only way to fully determine the influence of the individual parameters is to test the program on synthesized spectra. For this purpose energy spectra were calculated /21, 8/, corresponding to Rutherford backscattering of $^4\text{He}^+$ -ions from a target composed of 4 layers, each of constant stoichiometry:

1. layer : $\text{C}_{0.55} \text{Mg}_{0.25} \text{Ti}_{0.15} \text{Bi}_{0.05}$, $1 \cdot 10^{18}$ atoms/cm²
2. layer : $\text{C}_{0.2} \text{Mg}_{0.1} \text{Ti}_{0.4} \text{Bi}_{0.3}$, $7.5 \cdot 10^{17}$ "
3. layer : $\text{C}_{0.05} \text{Mg}_{0.1} \text{Ti}_{0.7} \text{Bi}_{0.15}$, $7.5 \cdot 10^{17}$ "
4. layer : $\text{C}_{0.8} \text{Ti}_{0.2}$, $1 \cdot 10^{18}$ "

The "experimental" parameters were taken as $E_0 = 2$ MeV, $N_{\text{prim}} \Delta\Omega = 10^{11}$ ions • sterad, $\theta = 161^\circ$, $\alpha = 19^\circ$, $\beta = 0^\circ$, $\Delta E_1 = 3.3$ keV/channel, and an offset of 230 keV corresponding to channel 0. The spectra were calculated in depthsteps of $1.1 \cdot 10^{16}$ atoms/cm².

a) As already seen previously /1/, the program yields the correct target composition quite accurately, unless the spectrum is somehow perturbed by isotope effects, resolution, statistics, etc.

Figure 13 shows the logarithmic plot of the ideal, synthesized spectrum.

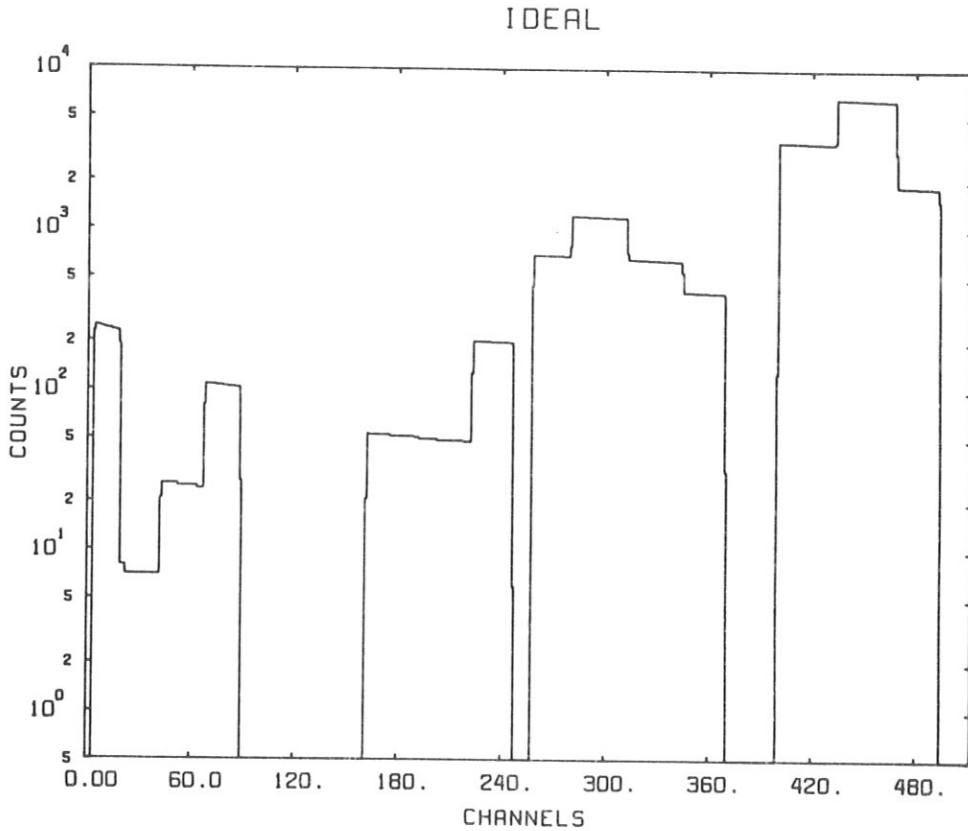


Fig. 13: Synthesized RBS-spectrum, ideal case (see text).
Note logarithmic axis!

With this as input in SQUEAKIE we find the correct target composition vs. depth, except at the interfaces (see Fig. 14a). At surface/interfaces errors arise, both in the generated spectrum and in the evaluation with SQUEAKIE, because of the finite depthsteps used in both programs. These errors are reflected in a plot of the eigenvalue Q vs. depth (Fig. 14b).

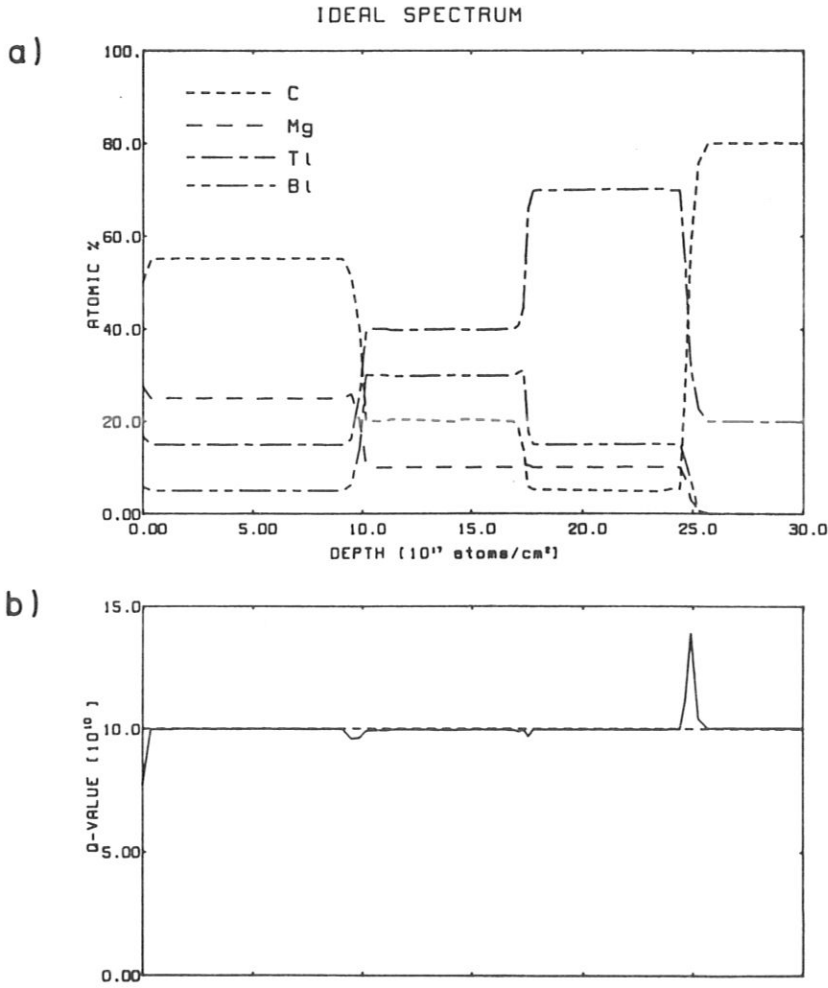


Fig. 14: Plot of SQUEAKIE-output resulting from evaluation of spectrum in Fig. 13. Aarhus-version.

- a) Relative concentrations vs. depth of C (---), Mg(— — —), Ti (- - - -) and Bi (-- — --).
- b) Eigenvalue Q vs. depth.

b) When the various isotopes of the target elements are included, even the ideal spectrum (particularly at surface/interfaces) is perturbed because of the isotopic mass differences. Figure 15 shows the ideal spectrum calculated assuming the natural isotopic ratios, and SQUEAKIE yields a target composition which is correspondingly perturbed (Fig. 16a). As also illustrated by the variation of Q with depth (Fig. 16b), the perturbation is quite small.

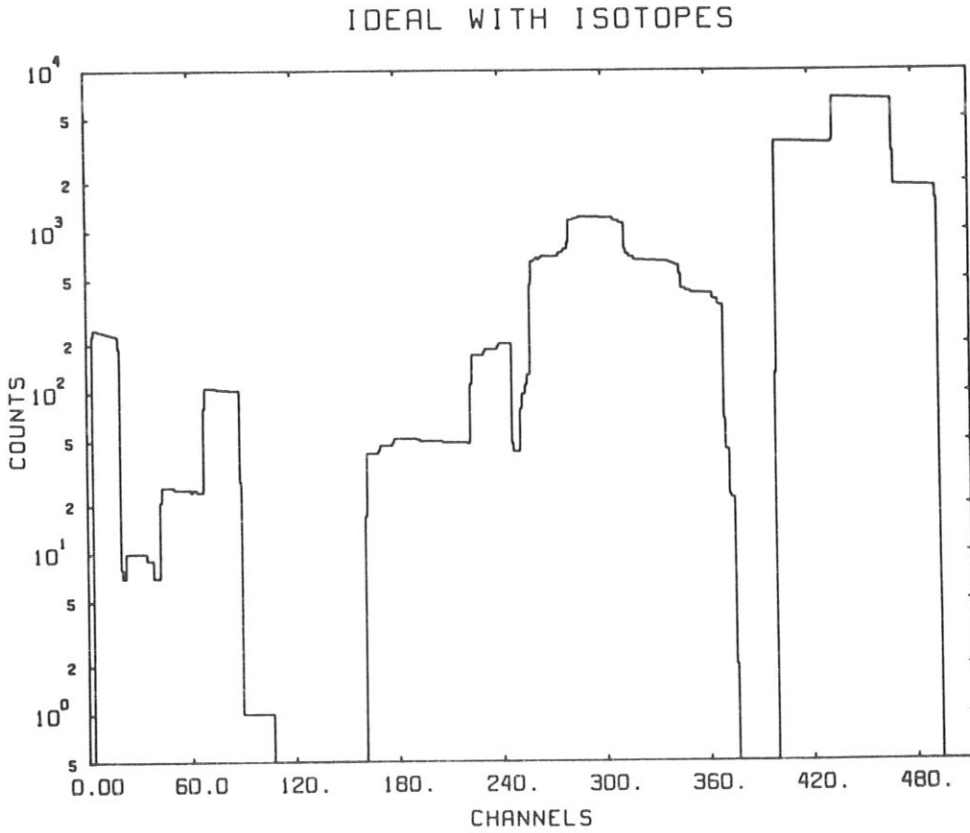


Fig. 15: Synthesized RBS-spectrum, ideal case but including isotopes.
Compare Fig. 13.

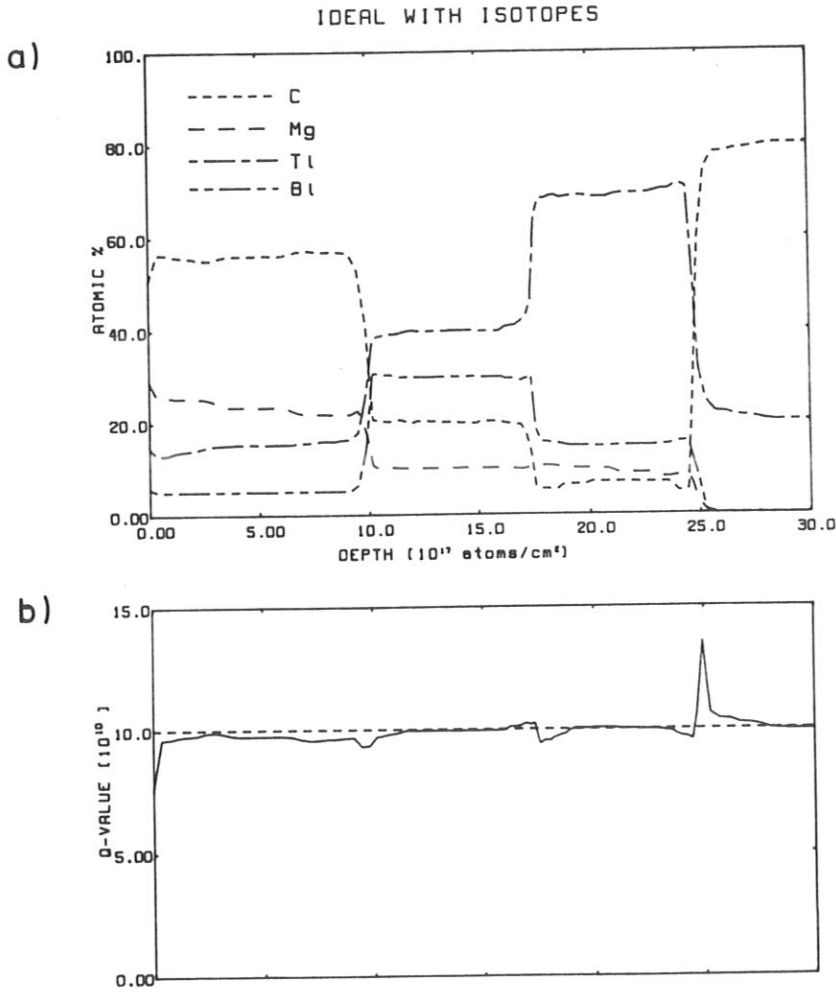


Fig. 16: Plot of SQUEAKIE-output resulting from evaluation of spectrum in Fig. 15. Aarhus-version.

- a) Relative concentrations vs. depth of C (---), Mg(— —), Ti (- — - —) and Bi (-- — --).
- b) Eigenvalue Q vs. depth.

c) For RBS analysis of reasonably thin targets with MeV-beams the effect of energy straggling on the ions is usually rather small. As we see in Fig. 17, the resulting smearing of the edges in the spectrum is in our case less than that caused by the isotopic mass differences. Correspondingly also the derived targetcomposition remains quite accurate (Fig. 18a).

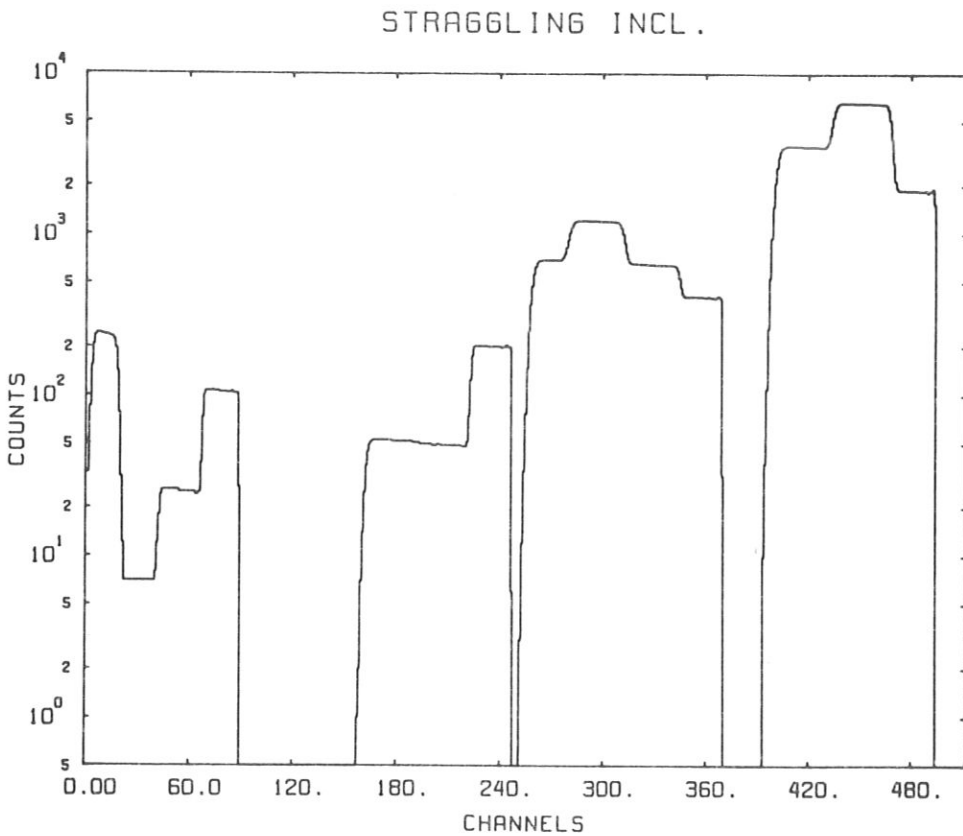


Fig. 17; Synthesized RBS-spectrum, including energy loss straggling. Compare Fig. 13.

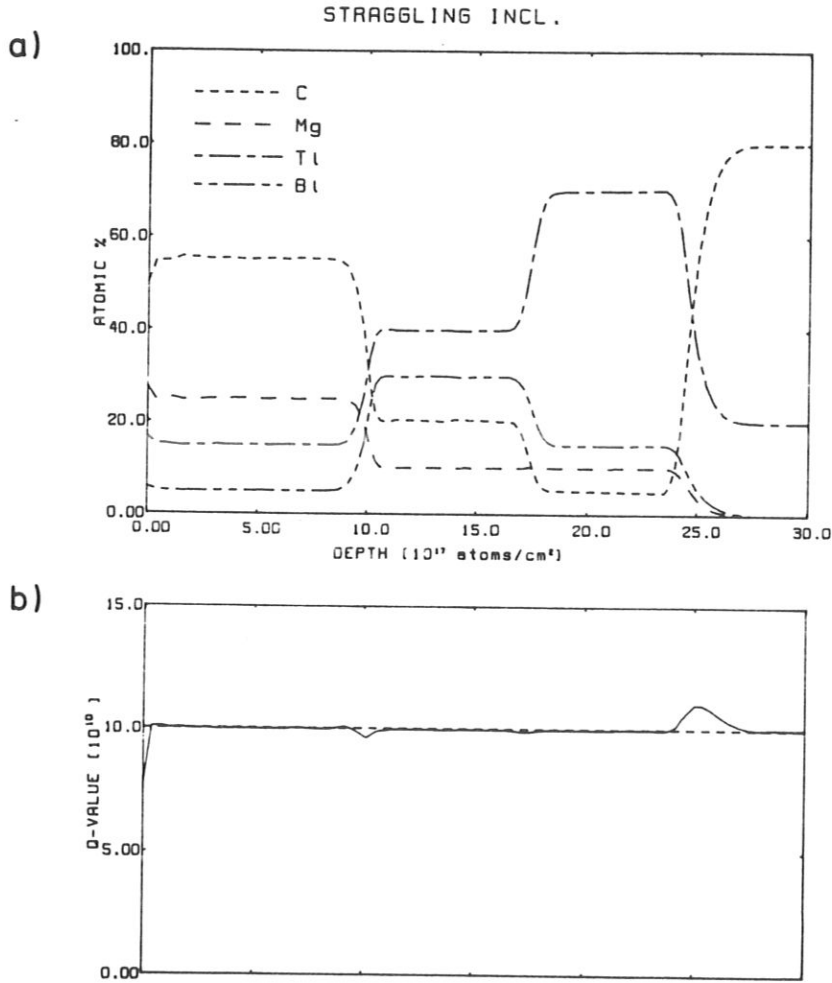


Fig. 18; Plot of SQUEAKIE-output resulting from evaluation of spectrum in Fig. 17. Aarhus-version.

- a) Relative concentrations vs. depth of C (---), Mg (— —), Ti (- — - —) and Bi (-- — --).
- b) Eigenvalue Q vs. depth.

d) If we include an energy resolution of ~ 16 keV of the experimental system, the features are of course all somewhat more smeared (Fig. 19), and so is the resulting targetcomposition (Fig. 20a). However, even with all the above effects combined (also isotopes), the spectrum (Fig. 21) yields a reasonable description of the true targetcomposition (Fig. 22a).

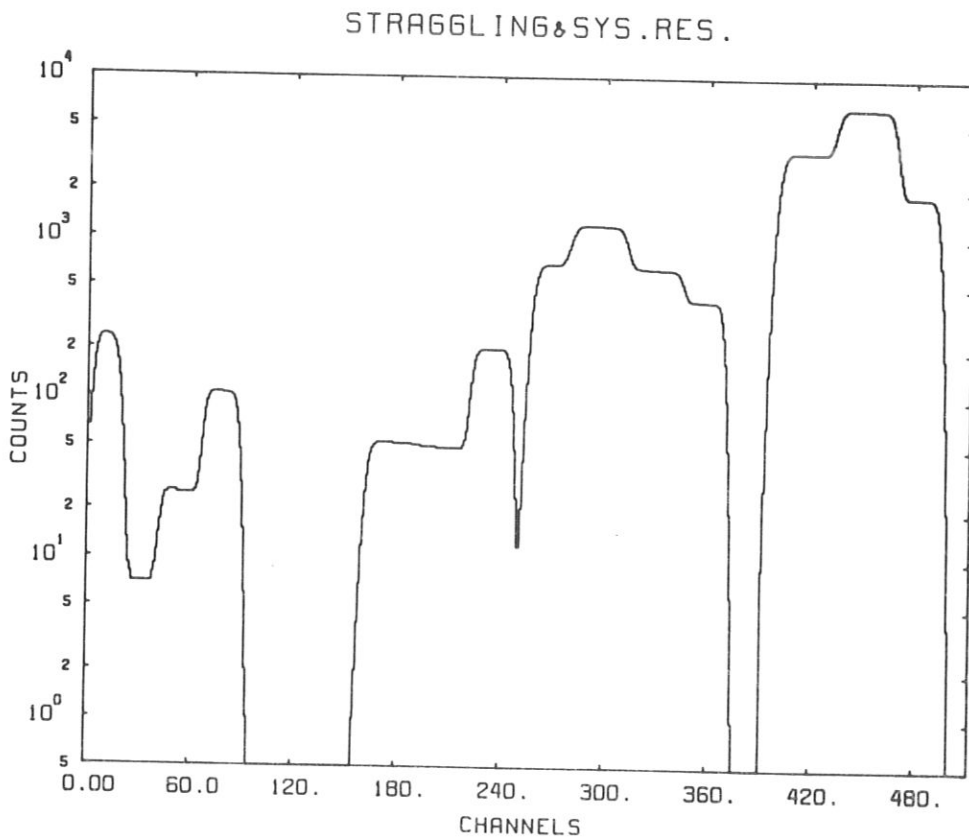


Fig. 19: Synthesized RBS-spectrum, including energy loss straggling and system resolution.

Compare Fig. 17.

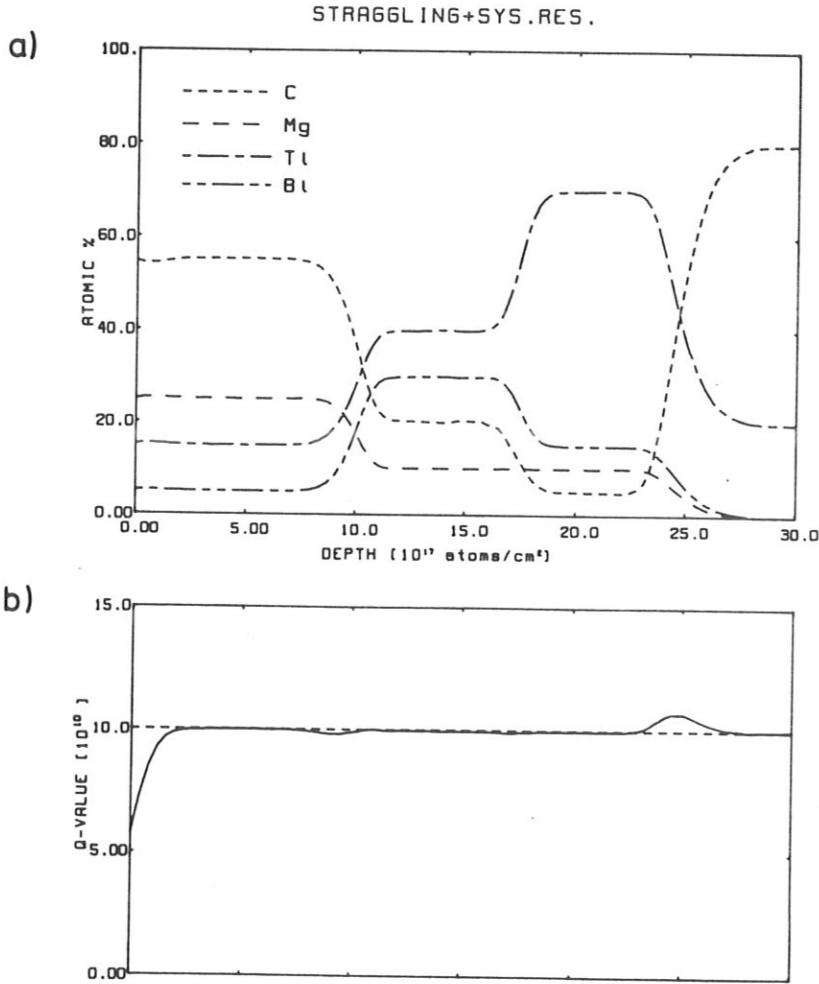


Fig. 20: Plot of SQUEAKIE-output resulting from evaluation of spectrum in Fig. 19. Aarhus-version.

- a) Relative concentrations vs. depth of C(---), Mg(— —), Ti (- — - —) and Bi (-- — --).
- b) Eigenvalue Q vs. depth.

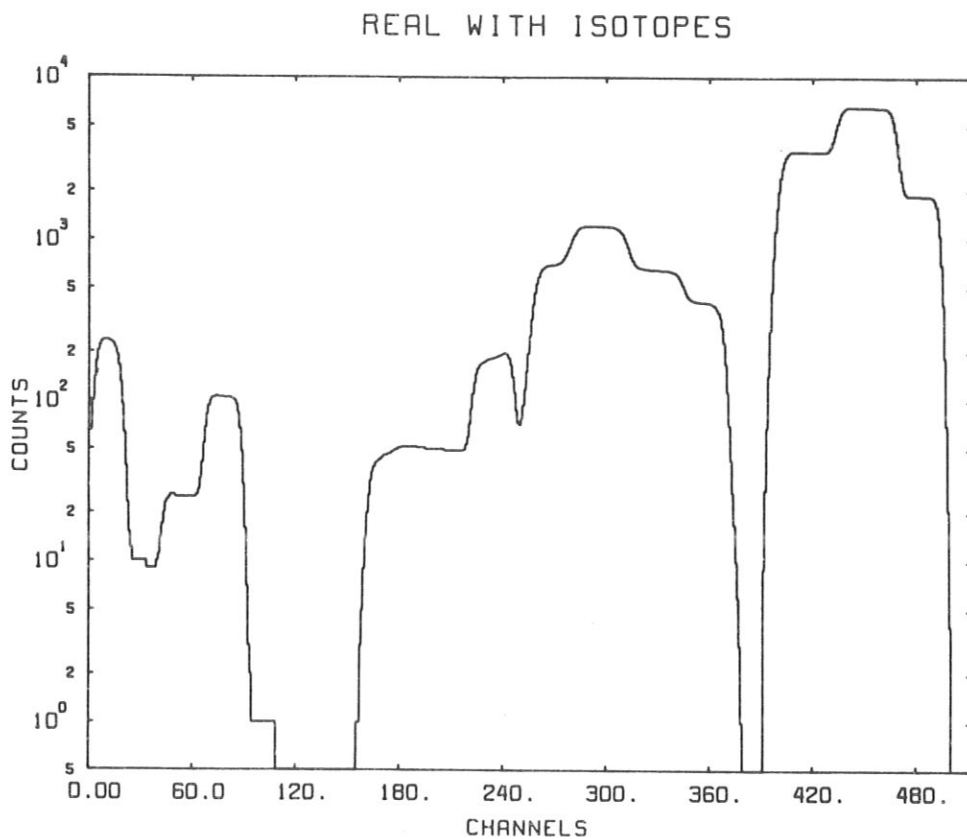


Fig. 21: Synthesized RBS-spectrum, including energy loss straggling, system resolution and isotopes.

Compare Fig. 19.

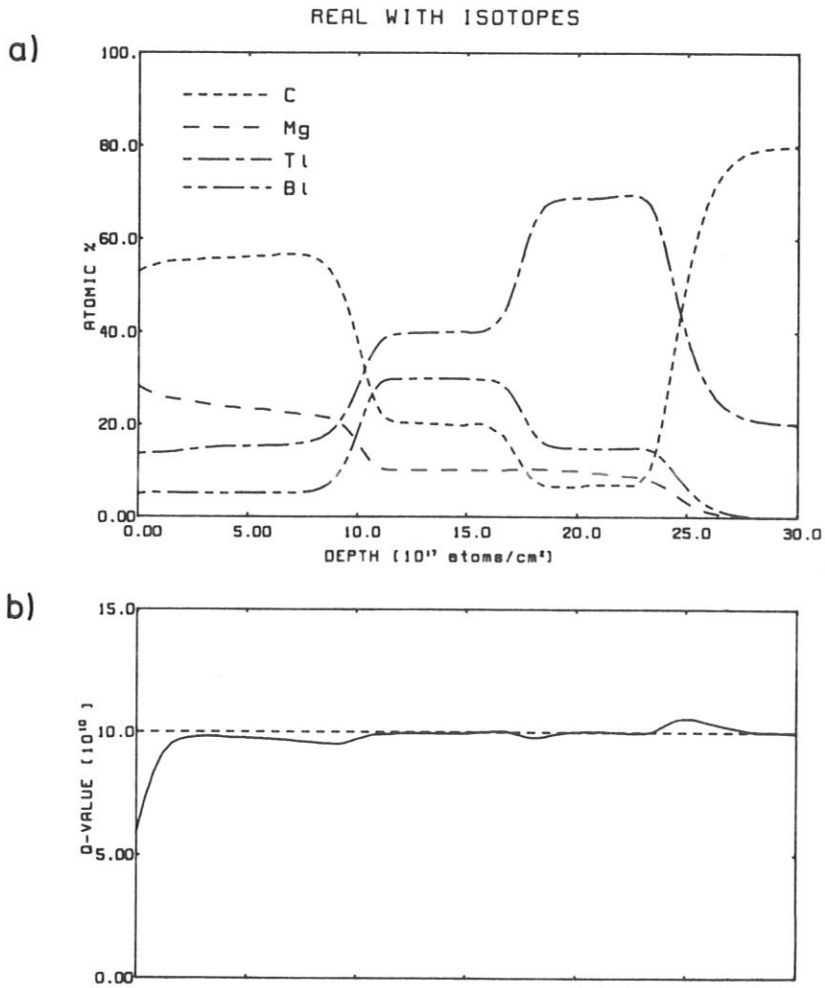


Fig. 22: Plot of SQUEAKIE-output resulting from evaluation of spectrum in Fig. 21. Aarhus-version.

a) Relative concentrations vs. depth of C(---), Mg(— —), Ti (- — - —) and Bi (-- — --).

b) Eigenvalue Q vs. depth.

e) We may conclude that in this quite representative case, energy loss straggling is of minor importance, system resolution simply causes the expected smearing of depth distributions, whereas isotopic mass differences may also result in perturbations of the stoichiometric coefficients in general.

In a realistic experiment, however, we shall expect the statistical errors in the experimental countrates to be a more serious problem. This question was already discussed somewhat in Ref. 1, but not sufficiently tested. The spectrum of Fig. 21 was therefore calculated again using a particular facility of the computerprogram /8/: In the individual channels the countrate H_j was superposed with a statistical error obtained from a random generator. The spectrum (Fig. 23) therefore exhibits the statistical fluctuations which one would expect to find experimentally.

STATISTIC INCL.

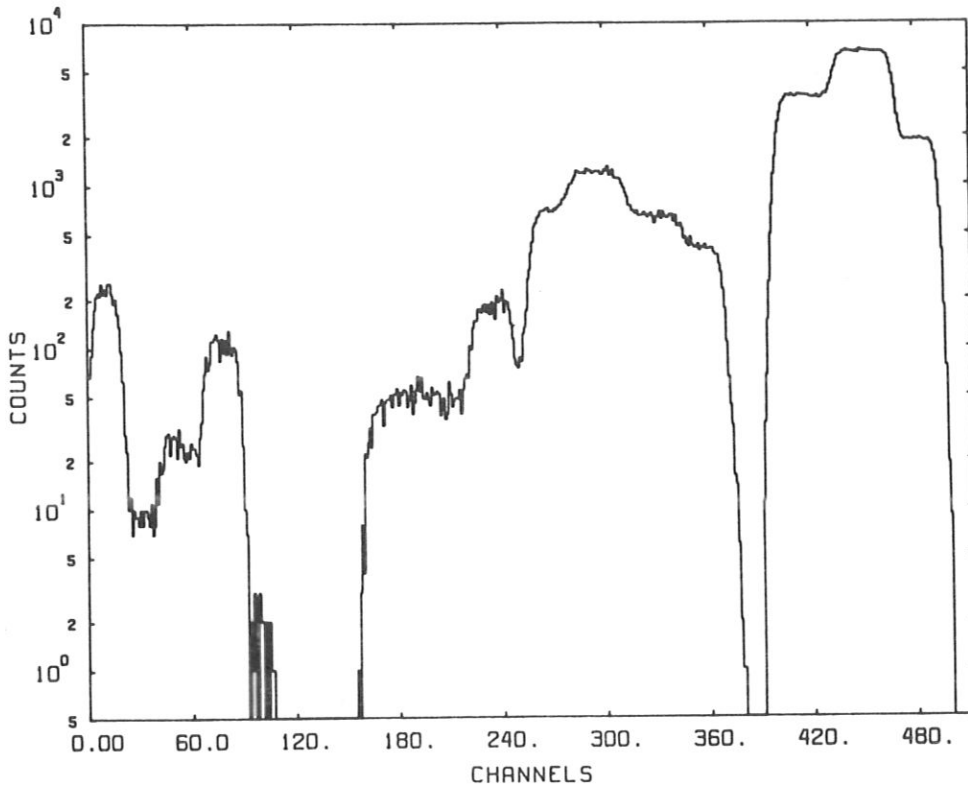


Fig. 23: Synthesized RBS-spectrum, including energy loss straggling, system resolution, isotopes and counting statistics.

Compare Fig. 21.

The resulting targetcomposition (Fig. 24a) of course reflects these fluctuations, but only to the degree expected (Ref. 1); i.e. we may still extract a reasonable estimate of the targetcomposition. Of course, the result may be improved by measuring to larger countrates, if possible.

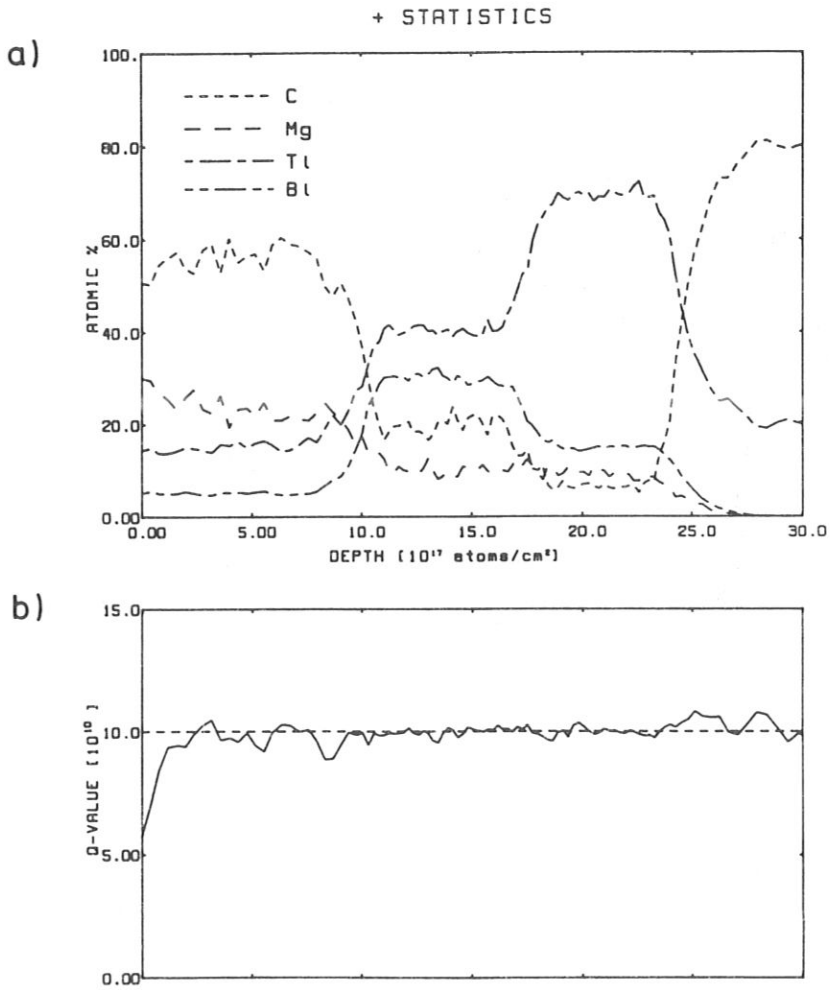


Fig. 24: Plot of SQUEAKIE-output resulting from evaluation of spectrum in Fig. 23. Aarhus version.

- a) Relative concentrations vs. depth of C(---), Mg (— —), Ti (- — - —) and Bi (-- — --).
- b) Eigenvalue Q vs. depth.

iii. The main purpose of the program is the evaluation of depth-distributions, and as discussed in Ref. 1 this is limited towards very thin films by the total experimental resolution. The program does have a facility for deriving the total contents of elements concentrated within the depth resolution (see Sect. 3.3), but if such contents are the only ones in question much simpler programs are available.

The evaluation of thin-film spectra was tested with synthesized RBS-spectra from a target consisting of a $\text{Al}_{0.7} \text{Co}_{0.2} \text{Au}_{0.1}$ -film on a C-substrate. Spectra were calculated for the filmthicknesses 10^{18} , $2 \cdot 10^{17}$ and $1 \cdot 10^{17}$ atoms/cm² (Figs. 25-27), assuming the same resolution-effects and experimental parameters as above.

As expected, the thickest film allows a good evaluation of the targetcomposition (Fig. 28), but also a rather thin film leads to a reasonable estimate of the surface-stoichiometry (Fig. 29). The latter result benefits from a partial 'cancellation of errors' /1/, which is possible until the film is so thin that the substrate-signal (due to resolution-broadening) seems to indicate larger amounts of C on the surface (Fig. 30). However, even for the $1 \cdot 10^{17}$ atoms/cm²-film the ratio $n_{\text{Al}}:n_{\text{Co}}:n_{\text{Au}}$ between the concentrations (ignoring n_{C}) remains essentially correct also in depth. The depthscale, of course, is strongly perturbed by the resolution.

THIN FILMS

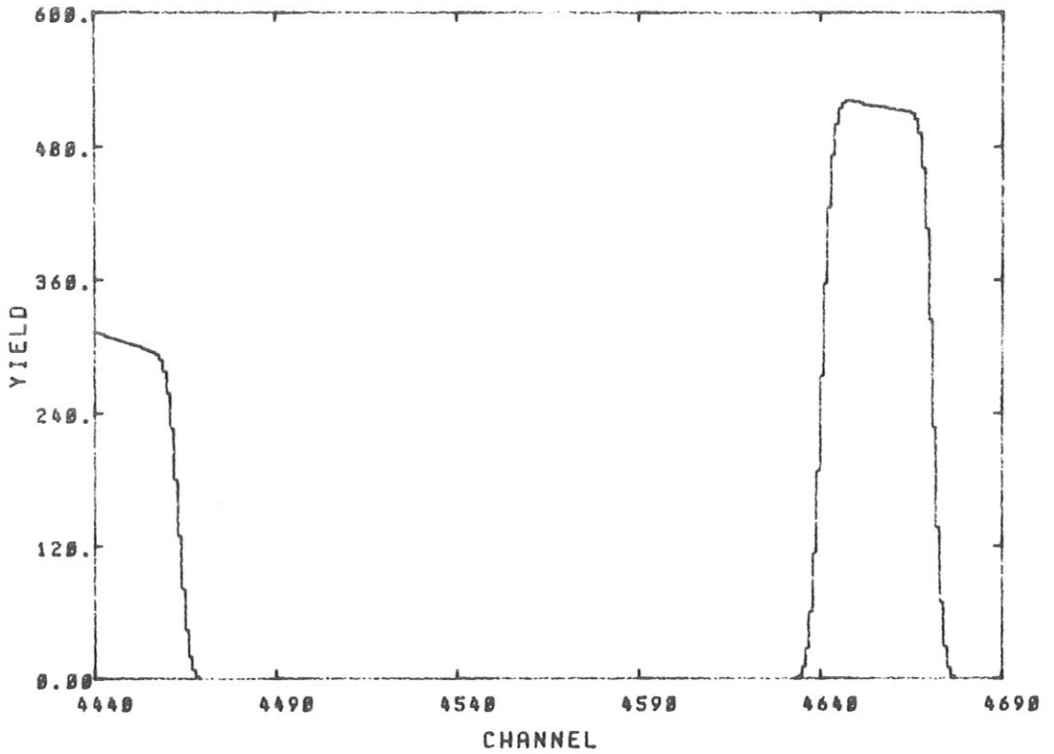


Fig. 25: Synthesized RBS-spectrum for 2 MeV ${}^4\text{He}^+$ -ions incident on 10^{18} atoms/cm 2 of $\text{Al}_{0.7}\text{Co}_{0.2}\text{Au}_{0.1}$ on a carbon-substrate. $N_{\text{prim}} \Delta\Omega = 10^{11}$, $\theta = 161^\circ$, $\alpha = 19^\circ$, $\beta = 0^\circ$, $\Delta E_1 = 3.3$ keV/channel and 230 keV in channel \emptyset .

Energy resolution ~ 16 keV.

THIN FILMS

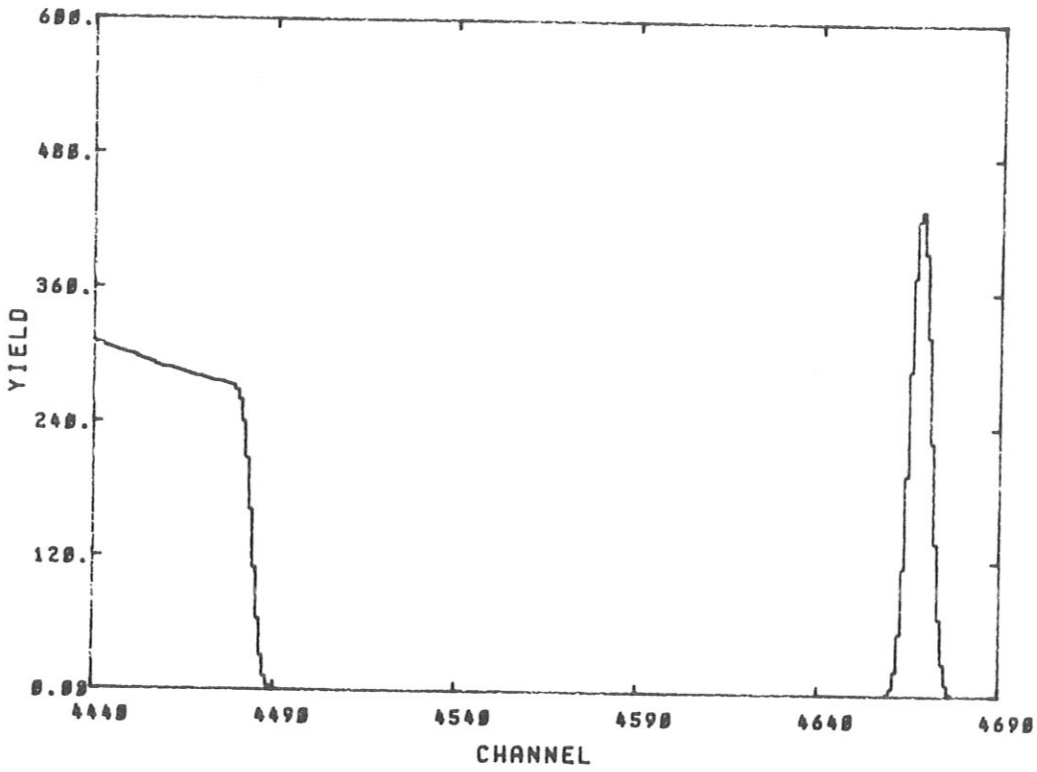


Fig. 26: As Fig. 25, but filmthickness now $2 \cdot 10^{17}$ atoms/cm²

THIN FILMS

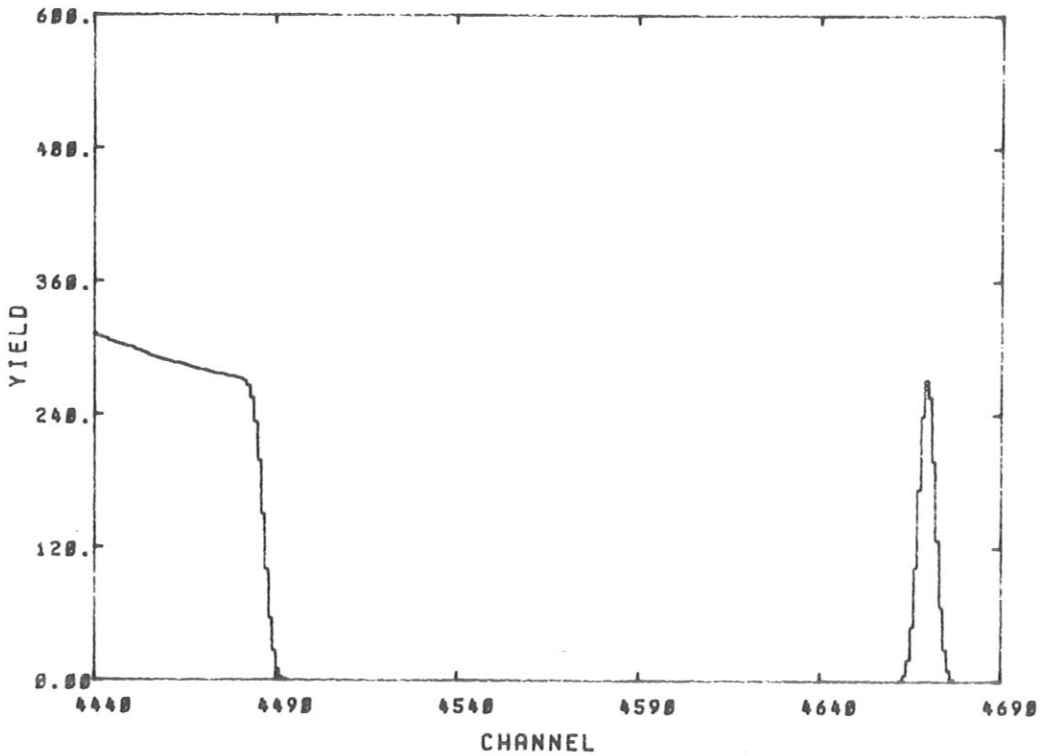


Fig. 27: As Fig. 25, but filmthickness now $1 \cdot 10^{17}$ atoms/cm².

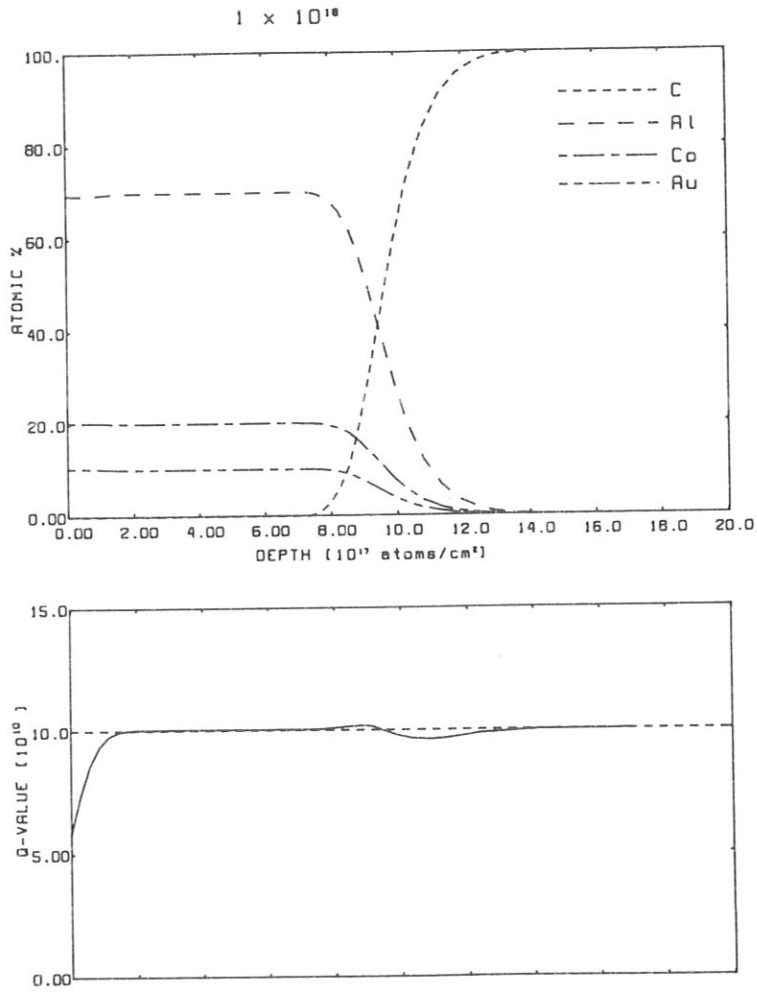


Fig. 28: Plot of SQUEAKIE-output resulting from evaluation of spectrum in Fig. 25.

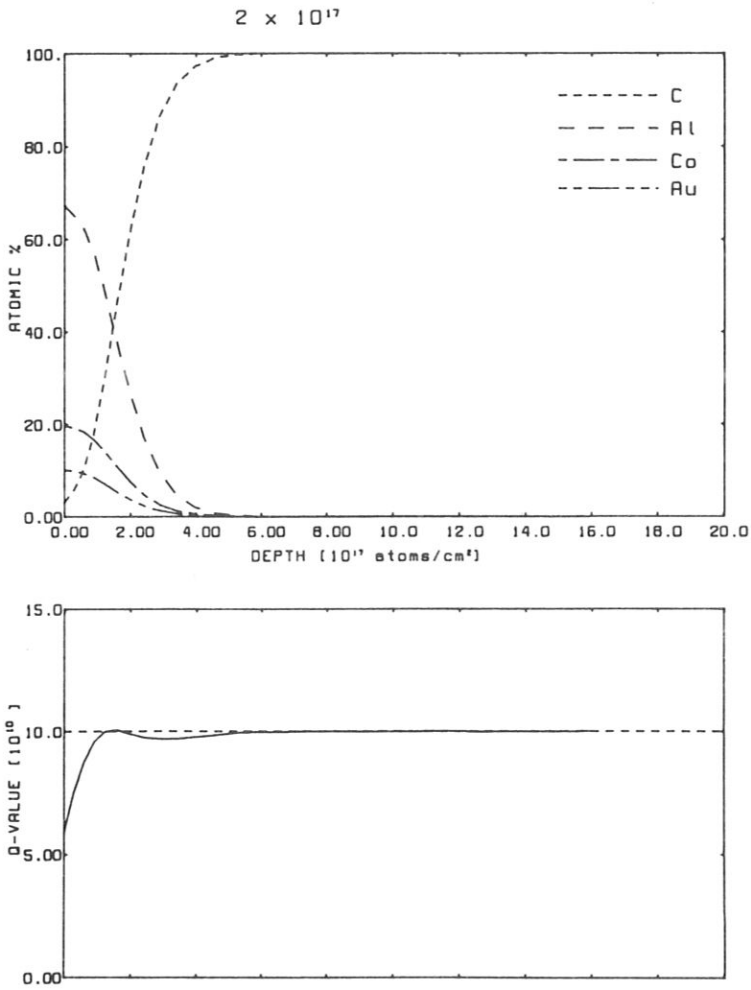


Fig. 29: Plot of SQUEAKIE-output resulting from evaluation of spectrum in Fig. 26

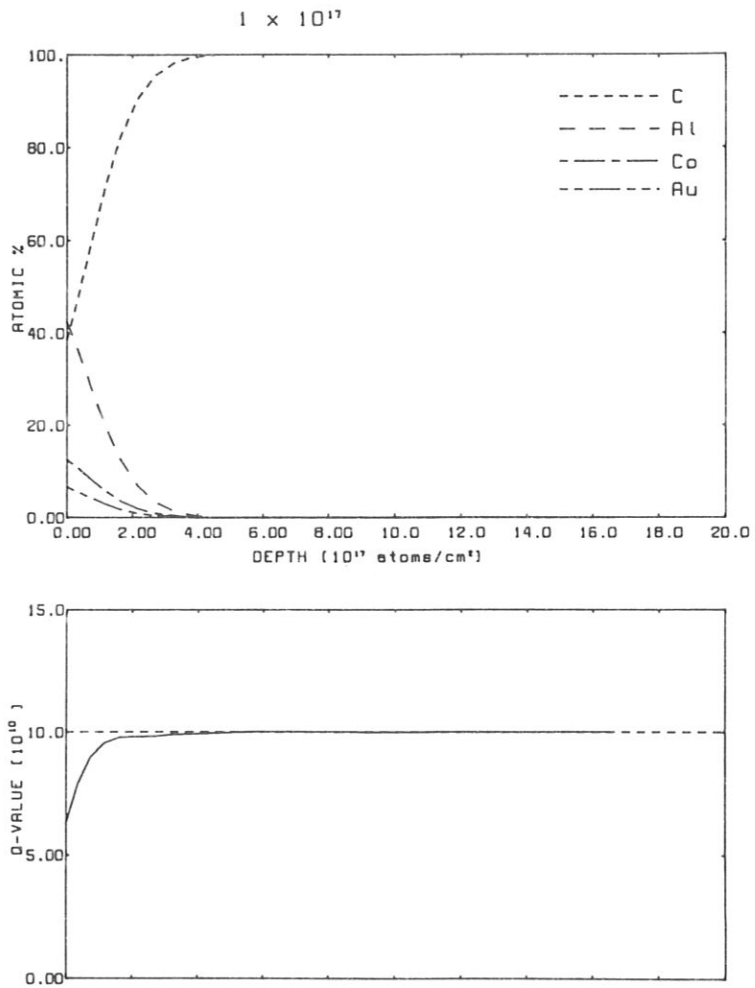


Fig. 30: Plot of SQUEAKIE output resulting from evaluation of spectrum in Fig. 27.

For all three filmthicknesses the total amounts of each element in the film (and thus the filmthickness) are estimated from the total scattering yields (Sect. 3.3) to within $\sim 5\%$. In contrast, of course, the summation of stoichiometric coefficients (Eq. 3.1) works best for the thick film: For the $1 \cdot 10^{18}$ atoms/cm² the total amounts are correct within less than 1 %, whereas for $2 \cdot 10^{17}$ atoms/cm² the errors increase to $\sim 15\%$, and for $1 \cdot 10^{17}$ atoms/cm² the total amounts are underestimated by 30 - 35 %.

8. RESUMÉ

The present computerprogram is capable of evaluating RBS-spectra in which the individual signals from the targetcomponents may be distinguished. A spectrum, in which each signal is clearly separated from the others (Fig. 31a), may therefore be directly evaluated without previous analysis. If, however, a signal is superposed on another (Fig. 31b), some kind of separation or background subtraction is necessary. The Aarhus-version of the program has facilities for a simple background subtraction, whereas in Garching this must be performed by a separate program. In any case such problems require a certain insight from the user, and are often too complicated for a simple treatment (Fig. 31c).

The program is primarily intended for the purpose of extracting the depth distributions of the targetelements. For rapidly varying targetcompositions the results will of course be smeared by resolution effects, and for very thin targets the total amounts may be evaluated by means of much simpler programs.

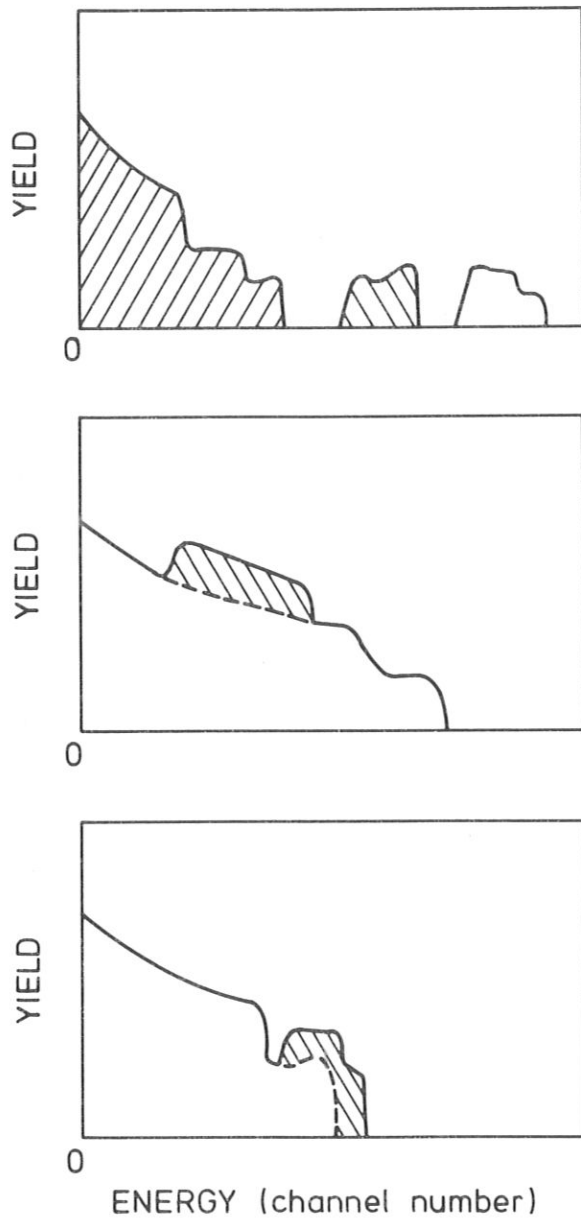


Fig. 31: Examples of RBS-spectra, principle.

- a) Directly applicable as input: Separate signals from each element (here 3).
- b) Applicable after simple background subtraction: Signals from two different elements overlap.
- c) Only applicable after previous (advanced) analysis: Overlapping signals of varying structure.

References

- /1/ P. Børgesen, R. Behrisch, and B.M.U. Scherzer, Appl.Phys. A27 (1982) 183
- /2/ "New Uses of Ion Accelerators", ed. J.F. Ziegler, (Plenum Press, N.Y., 1975)
- /3/ W.-K. Chu, J.W. Mayer, and M.-A. Nicolet: "Backscattering Spectrometry" (Academic Press, N.Y. 1978)
- /4/ J. Bøttiger, J.Nucl.Mat. 78 (1978) 161
- /5/ B.M.U. Scherzer, H.L. Bay, R. Behrisch, P. Børgesen, and J. Roth, Nucl.Instrum.Meth. 157 (1978) 75
- /6/ P. Børgesen, R. Behrisch, and B.M.U. Scherzer, in Proc. EPS Nucl. Phys. 7th Div. Conf. on "Nuclear Physics Methods in Material Research", Darmstadt (1980) p. 363
- /7/ L.G. Svendsen and P. Børgesen, Nucl.Instr.Meth. 191 (1981) 141
- /8/ S.S. Eskildsen, in "Ion Implantation into Metals", (eds. V. Ashworth, W.A. Grant, and R.P.M. Procter), Proc. Conf. on "Modification of the Surface Properties of Metals by Ion Implantation", Manchester, U.K., 1981 (Pergamon, Oxford 1982), p. 315
- /9/ L.G. Svendsen, Ph.D.-thesis, Univ. of Aarhus (1982)
- /10/ J.S. Williams, W. Möller, Nucl.Instr.Meth. 157 (1978) 213
- /11/ J.F. Ziegler, "Helium Stopping Powers and Ranges in All Elemental Matter", Pergamon Press 1977
- /12/ H.H. Andersen and J.F. Ziegler, "Hydrogen Stopping Powers and Ranges in All Elements", Pergamon Press 1977
- /13/ L.G. Svendsen, S.S. Eskildsen, and P.Børgesen, to be published
- /14/ P.Børgesen, S.S. Eskildsen, and L.G. Svendsen, in preparation
- /15/ H.H. Andersen, F. Besenbacher, P.Loftager, and W.Möller, Phys. Rev. A21 (1980) 1891
- /16/ W.Möller and F. Besenbacher, Nucl.Instr. Meth. 168 (1980) 111

- /17/ E. Lägsgaard, "Stopping and range routines", Internal Publ.,
Institute of Physics, University of Aarhus, 1980
- /18/ J.H. Wilkinson, "The Algebraic Eigenvalue Problem" (1965,
Oxford Univ. Press, London)
- /19/ J.H. Wilkinson, "Rounding Errors in Algebraic Processes"
(1963, H.M. Stationary Office, London) N.P.L. Notes on Applied
Science 32
- /20/ K.Ertl, Ph.D-Thesis, Techn. Univ. München (1981),
Report IPP 9/39, 1982.
- /21/ P.Børgesen, J.M. Harris, B.M.U.Scherzer: RADC-TR-76-182
Interim Technical Report, National Techn.Inform.Serv., USA